

**Democratic Republic of Algeria**  
**Ministry of Higher Education and Scientific Research**  
**University of Ahmed Draïa – Adrar**  
**Faculty: Science and Technology**  
**Department: Electrical Engineering**



Thesis presented to obtain the diploma of ACADEMIC Master :

**Domaine:** Electrical Engineering

**Option:** Electrical control

**Entitled:**

***Performance assessment of an  
acquisition system for PV simulators***

**Presented by:**

Barka Khalil  
Guerrout Abdelhadi

**In front of the jury, composed of:**

Dr. Hassani Islame	President	MAB	<b>University Ahmad Draia – Adrar Algeria</b>
Dr. HARTANI Mohamed Amine	Supervisor	MCB	
Dr. LAIDI Abdallah	Co-Supervisor	MAA	
Dr. Laribi Slimane	Examiner	MCA	

**Academic year: 2022/2023**

الجمهورية الجزائرية الديمقراطية الشعبية  
وزارة التعليم العالي والبحث العلمي



جامعة أحمد درايعة - أدرار  
كلية العلوم والتكنولوجيا

قسم الهندسة الكهربائية

الرقم: ..... / 2023

شهادة الترخيص بالإيداع

نحن الأستاذ (ة): ..... حرطاني محمد أمين و ..... العايدى عبد الله  
مشرف على مذكرة الماستر الموسومة: .....

.....  
Performance assessment of an acquisition system  
for P.V simulators

.....  
من انجاز الطالب (ة): ..... بركة خليل  
و الطالب (ة): ..... قسروط عبد المجادى  
Guerrout Abdelhach

.....  
التخصص: ..... بحكم كمر باي  
Commande électrique  
تاريخ تقييم / مناقشة: ..... 2023 / 06 / 18

أشهد أن الطلبة قد قاموا بالتعديلات و تصحيحات المطلوبة من طرف لجنة التقييم / المناقشة ،  
و أن المطابقة بين النسخة الورقية و الإلكترونية استوفت جميع شروطها.

و بإمكانهم إيداع النسخ الورقية و لإلكترونية (PDF)

رئيس القسم

اسم و لقب و توقيع مشرفا

Harani Mohamed Amine



LAI DE Abdallah

# **Dedication**

*I dedicate this modest work*

*To my mother my reason for being, my reason for living, the lantern that illuminates my path, and illuminates me with sweetness and love.*

*To my father, as a sign of love, gratitude, and gratitude for all the support and sacrifices he showed to me.*

*To my dear brothers **ABDELKADER** and my sisters and all the **Guerrou** family and the **KHOUZ** family*

*No words can describe your dedication and sacrifice.*

*To my Supervisors **Dr.HARTANI MOHAMMED AMINE** and **Dr. LAIDI ABDALLAH***

*To my best friend **BARKA KHALIL** and all the comrades and family of the **GENIE ELECTRIQUE** department.*

*To all the friends and testimony of the sincere friendship that bound us and the good times spent together*

**GUERROUT Abdelhadi**

# *Dedication*

*I dedicate this modest work*

*My dear parents made me what I am today and who made sure to guide my steps throughout my life with their help, their great emotions, their sacrifices, and their support and encouragement during the realization of the .graduation project*

*To My dearest brother: Abdelwahid, Faysal, and Mohamed*

*To Our supervisors : Dr.HARTANI MOHAMMED AMINE , Dr.LAIDI*

*ABDALLAH*

*To my friends: Abdelhadi, Souleymane, and Ghiles*

*TO All the promotion of ELECTRIC CONTROL 2023*

*BARKA Khalil*

## **Acknowledgment**

*First and foremost, I express my gratitude to God for granting me the will, motivation, and most importantly, good health throughout my master's studies. I would like to warmly thank Dr. HARTANI Mohamed Amine and Dr. LAIDI Abdallah to whom we are immensely grateful for their encouragement and support in completing our master's program.*

*Additionally, we would like to express our sincere gratitude to our parents, who are the dearest people in the world to us, for their sacrifices and guidance, without which we would not have achieved this level of success. May God bless them.*

*Furthermore, we would like to thank all our friends and colleagues for the unforgettable moments and memories we shared.*

*Without forgetting to thank our examiners Dr. LARIBI Slimane and Dr. Hssani Islame for their precious remarks and comments to improve our Master thesis content.*

*Finally, we would like to express our gratitude to everyone who has contributed, directly or indirectly, to the development and deepening of this work.*

# Table of Content

<i>Dedication</i> .....	I
<i>Dedication</i> .....	II
<i>Acknowledgment</i> .....	III
<i>Table of Content</i> .....	IV
<i>List of Figures</i> .....	VII
<i>List of Tables</i> .....	IX
<i>Table of Abbreviations</i> .....	X
<i>Table of Symbols</i> .....	XI
GENERAL INTRODUCTION .....	2
<b>Chapter 01: Literature Review</b>	
I.1 INTRODUCTION.....	5
I.2 PV systems and emulator.....	6
I.2.1 PV-Emulators .....	8
I.2.2 Types of PV emulators.....	9
I.2.2.A Single Panel Emulators:.....	9
I.2.2.B PV Array Emulators: .....	10
I.2.2.C Diode Model Approximation-Based Emulators: .....	10
I.2.3 Control Strategies for PV Emulators .....	11
I.2.4 Real-time applications.....	12
I.2.4.A Examples of Real-time applications.....	12
I.3 Hardware implementation of PV-Emulators.....	14
I.3.1 Power Electronic-based PV Emulators .....	14
I.3.2 FPGA-based PV Emulators.....	14
I.3.3 Hardware implementation Requirements.....	15
I.4 Sensitiveness to environmental conditions .....	16
I.5 PV emulator brands in markets.....	16
I.6 Data acquisition systems .....	19
I.6.1 Standalone DAS.....	19
I.6.2 PC-Based DAS.....	19
I.6.3 Distributed DAS .....	20
I.6.4 Wireless DAS .....	20

I.6.5	Remote DAS.....	21
I.6.6	Web-Based DAS .....	21
I.7	Previous research on solar emulator acquisition systems.....	21
I.8	Conclusion.....	22

### Chapter 02: Modeling and Design of the PV-Conversion Chain

II.1	Introduction .....	24
II.2	Modeling of the PV-Source.....	25
II.2.1	PV curves in the PV-Emulator .....	28
II.2.2	Closed-loop control of the standalone PV-System.....	28
II.2.3	MPPT control methods .....	29
II.2.3.A	Perturb and Observe (P&O) .....	29
II.2.3.B	Incremental Conductance (INC).....	30
II.2.4	FPPT control methods .....	31
II.3	Modeling of the DC-DC Boost Converter .....	32
II.3.1	The protection system of DC-DC Converters .....	35
II.3.2	Sizing of the standalone PV-System.....	36
II.3.2.A	Sizing of the DC Load .....	36
II.3.2.B	Sizing of the PV source .....	37
II.3.2.C	Sizing the DC/DC converters.....	37
II.3.2.D	Sizing the Current/Voltage Sensors .....	41
II.3.2.D	Sizing of the Gate-drive (GD).....	44
II.3.3	Description of realized acquisition boards .....	45
II.3.3.F	Generate Gerber file .....	50
II.3.4	Description of the experimental setup .....	50
II.3.5	Selection of acquisition components .....	52
II.3.5.A	DSpace 1104 .....	52
II.3.5.B	MicroLabBox.....	52
II.3.5.C	DSP-TMS 28379D .....	53
II.4	Conclusion.....	53

### Chapter 03: Simulation results and discussion

III.1	Introduction .....	55
III.2	Simulation results of the Standalone PV system- under study .....	55
III.2.1	PV diagram identification.....	58
III.2.2	The impact of variable weather conditions on the PV system.....	59
III.2.2.A	The impact of variable irradiation .....	60
III.2.2.B	The impact of variable temperature.....	62

<b>III.2.3</b>	<b>Impact of variable load demand.....</b>	<b>65</b>
<b>III.2.4</b>	<b>Impact of variable MPPT simple time (Ts).....</b>	<b>66</b>
<b>III.2.5</b>	<b>Impact of Duty cycle variation or Delta-duty (Dd).....</b>	<b>68</b>
<b>III.2.6</b>	<b>Impact of Variable PV control methods.....</b>	<b>70</b>
<b>III.2.6. A</b>	<b>Impact of switching between MPPT and FPPT control methods .....</b>	<b>70</b>
<b>III.3</b>	<b>Conclusion.....</b>	<b>73</b>
	<b>GENERAL CONCLUSION.....</b>	<b>75</b>
	<b>REFERENCES.....</b>	<b>76</b>
	<b>APPENDIX.....</b>	<b>80</b>



# List of Figures

## Chapter I

<b>Figure III. 1:</b> Presentation of the PV conversion chain components: A- Simulink model, B-DC/DC Boost, C-DC variable load with its control profile, and D-Direct P&O-MPPT schema. ....	56
<b>Figure III. 2:</b> Schema of the PV conversion chain using MATLAB Simulink. ....	58
<b>Figure III. 3:</b> VI and VP characteristics of the PV Panel using Ramp Signal test. ....	59
<b>Figure III. 4:</b> Variations of the PV outputs in the IV/VP curves: A- Initialization of MPPT search, B- Step change in solar irradianations from 1000 to 500 (w/m2), and C- A step change in solar irradianations from 100 to 1000 (w/m2). ....	61
<b>Figure III. 5:</b> Simulation result of the impact of variable irradiation levels. ....	62
<b>Figure III. 6:</b> Variations of the PV outputs in the IV/VP curves: A- Initializing the search for the proposed point, B- A step change in temperature from 60 to 40 (°C), and C- A step change in temperature from 40 to 25 (°C). ....	63
<b>Figure III. 7:</b> Simulation result of the impact of variable temperatures. ....	64
<b>Figure III. 8:</b> Variations of SPV outputs in the IV/VP curves: A- Initializing the search for MPPs, B- A step change in load: 9.78 to 4.89 ( $\Omega$ ), and C- A step change in load: 4.89 to 3.423( $\Omega$ ). ....	65
<b>Figure III. 9:</b> Simulation result of the impact of variable Load resistance. ....	66
<b>Figure III. 10:</b> Variations of PV outputs in IV/VP curves: A- $T_s=1e-4$ (s) and B- $T_s=1e-2$ (s). ....	67
<b>Figure III. 11:</b> Variations of PV outputs in IV/VP curves: A- $\Delta d=1e-2$ (PU) and B- $d =1e-4$ (PU). ....	68
<b>Figure III. 12:</b> Impact of Variable Delta-duty cycle on the PV output power. ....	69
<b>Figure III. 13:</b> Impact of Variable Delta-duty on the DC-DC converter efficiency. ....	69
<b>Figure III. 14:</b> (A) Variable profiles of the FPT setpoint, (B) power and load schedule ....	70
<b>Figure III. 15:</b> Variations of PV outputs in IV/VP curves: A- Initializing the search for MPPs, B- switching from MPPT to FPPT: [0.5-1](s), and C- switching from FPPT to MPPT: [0.5-1](s). ....	71
<b>Figure III. 16:</b> Impact of switching control between MPPT and FPPT modes. ....	72

## Chapter II

<b>Figure II. 1:</b> The block diagram of the PV system under study. ....	25
<b>Figure II. 2:</b> A diagram showing the photovoltaic effect [53]. ....	25
<b>Figure II.3:</b> Solar cell single-diode model. ....	26
<b>Figure II. 4:</b> PV module characteristic (VI Curve). ....	27
<b>Figure II.5:</b> PV module characteristic (VP Curve). ....	27
<b>Figure II. 6:</b> VI and VP curves using the PV emulator Chroma 62020H-150S. ....	28
<b>Figure II. 7:</b> Tracking regions of MPPT control using a DC/DC boost converter. ....	29
<b>Figure II.8:</b> P&O-based MPPT technique. ....	30
<b>Figure II.9:</b> INC-based MPPT technique. ....	31
<b>Figure II.10:</b> Principles of PV control-based FPPT technique. ....	32
<b>Figure II.11:</b> DC-DC Boost converter circuit [63]. ....	33
<b>Figure II. 12:</b> Boost converter circuit when switch S is <b>ON</b> . ....	33
<b>Figure II. 13:</b> Boost converter circuit when switch S is <b>OFF</b> . ....	33

<b>Figure II. 14:</b> Supply current, diode current, inductor current, and inductor voltage.....	34
<b>Figure II. 15:</b> DC/DC Boost circuit using protective devices (Fuse and Circuit Breaker).....	35
<b>Figure II. 16:</b> Main Window of Power Stage Designer Displaying Topologies. ....	37
<b>Figure II. 17:</b> Topology Window for the DC-DC Converters Design Demo Application. ....	41
<b>Figure II. 18:</b> The LEM LV 25-P voltage transducer schematic[73]. ....	42
<b>Figure II. 19:</b> The LEM-LA25 voltage transducer schematic[74].....	43
<b>Figure II. 20:</b> The LEM-LA25 voltage transducer schematic[74].....	44
<b>Figure II. 21:</b> Circuit Diagram of the optocoupler HCPL-3120 .....	45
<b>Figure II. 22:</b> Gate drive(HCPL-3120): a-Circuit Schematic PCB. b- PCB layout design diagram and c- 3D visualizer for HCPL-3120.....	46
<b>Figure II. 23:</b> Chopper Circuit with Fusible Protection Schematic PCB.....	47
<b>Figure II. 24:</b> (a) PCB layout design diagram and (b) design 3D visualizer. ....	49

### Chapter III

<b>Figure III. 1:</b> Presentation of the PV conversion chain components: A- Simulink model, B-DC/DC Boost, C-DC variable load with its control profile, and D-Direct P&O-MPPT schema. ....	56
<b>Figure III. 2:</b> Schema of the PV conversion chain using MATLAB Simulink. ....	58
<b>Figure III. 3:</b> VI and VP characteristics of the PV Panel using Ramp Signal test. ....	59
<b>Figure III. 4:</b> Variations of the PV outputs in the IV/VP curves: A- Initialization of MPPT search, B- Step change in solar irradiations from 1000 to 500 (w/m2), and C- A step change in solar irradiations from 100 to 1000 (w/m2).....	61
<b>Figure III. 5:</b> Simulation result of the impact of variable irradiation levels.....	62
<b>Figure III. 6:</b> Variations of the PV outputs in the IV/VP curves: A- Initializing the search for the proposed point, B- A step change in temperature from 60 to 40 (°C), and C- A step change in temperature from 40 to 25 (°C).....	63
<b>Figure III. 7:</b> Simulation result of the impact of variable temperatures. ....	64
<b>Figure III. 8:</b> Variations of SPV outputs in the IV/VP curves: A- Initializing the search for MPPs, B- A step change in load: 9.78 to 4.89 ( $\Omega$ ), and C- A step change in load: 4.89 to 3.423( $\Omega$ ).....	65
<b>Figure III. 9:</b> Simulation result of the impact of variable Load resistance.....	66
<b>Figure III. 10:</b> Variations of PV outputs in IV/VP curves: A- $T_s=1e-4$ (s) and B- $T_s=1e-2$ (s). ....	67
<b>Figure III. 11:</b> Variations of PV outputs in IV/VP curves: A- $\Delta d=1e-2$ (PU) and B- $d =1e-4$ (PU). ....	68
<b>Figure III. 12:</b> Impact of Variable Delta-duty cycle on the PV output power.....	69
<b>Figure III. 13:</b> Impact of Variable Delta-duty on the DC-DC converter efficiency.....	69
<b>Figure III. 14:</b> (A) Variable profiles of the FPT setpoint, (B) power and load schedule .....	70
<b>Figure III. 15:</b> Variations of PV outputs in IV/VP curves: A- Initializing the search for MPPs, B- switching from MPPT to FPPT: [0.5-1](s), and C- switching from FPPT to MPPT: [0.5-1](s).71	
<b>Figure III. 16:</b> Impact of switching control between MPPT and FPPT modes. ....	72

# List of Tables

## Chapter I

**Table I. 1:** Contributions and achievements of recent works in PV systems..... 7

**Table I. 2:** Contributions and achievements of recent works in PV Emulators..... 7

## Chapter II

**Table II. 1:** Parameters and Data of the PV selected Module (**Anji Technology AJP-M660-245**) 27

**Table II. 2:** Sizing results: DC fuse..... 36

**Table II. 3:**DC-DC Boost Converter Design Parameters..... 38

**Table II. 4:**DC-DC Boost Converter Sizing data and results..... 41

**Table II. 5:** Specifications of LEM-LV25..... 42

**Table II. 6:**Sizing results of the LV Voltage sensor..... 42

**Table II. 7:** Specifications of LEM-LA25-NP. .... 43

**Table II. 8:** Primary Turns, Nominal Output Current, and Recommended Connections. .... 43

**Table II. 9:**Sizing LA sensor..... 43

**Table II. 10:** Sizingof the Gate-Driver (HCPL-3120)..... 45

**Table II. 11:** Steps for Manual PCB Fabrication Process. .... 50

## Chapter III

**Table III. 1:** Settings for VI and VP Curve identification. .... 58

**Table III. 2:** Experimental Parameters for Irradiation Variation Analysis. .... 60

**Table III. 3:** Impact of irradiation variation on the PV outputs..... 61

**Table III. 4:** Experimental Parameters for Temperature Variation Analysis..... 62

**Table III. 5:** Impact of temperature variation on the PV outputs..... 63

**Table III. 6:** Experimental Parameters for Load Variations Analysis. .... 65

**Table III. 7:** Parameters for simple time Variation Analysis..... 67

**Table III. 8:** Comparison of Power and Efficiency for  $T_s = 1e-4$  and  $T_s = 1e-2$ . .... 67

**Table III. 9:** Impact of Delta-duty (Dd) Variations using the FPPT control. .... 68

**Table III. 10:** Comparison of Power and Efficiency for  $D_d = 1e^{-2}$ ,  $1e^{-4}$ , and  $1e^{-6}$  (PU)..... 70

**Table III. 11:** Impact of MPPT/FPPT switching under proposed variations..... 70

**Table III. 12:** Statistical results of the switching control between MPPT and FPPT modes..... 72

# *Table of Abbreviations*

Abbreviations	Definition
AC	Alternative Current
DC	Direct Current
FPGA	Field Programmable Gate Array
HIL	HARDWARE-IN-THE-LOOP
RTDS	Real-time digital simulator
PV	Photovoltaïque
PHILS	Power Hardware in the Loop Simulation
FPGA	Field-Programmable Gate Arrays
MPPT	Maximum Power Point Tracker
DAS	Data Acquisition System
GD	Gate Driver
UPS	Uninterrupted Power Supply
PLC	Programmable Logic Controller
P&O	Perturb & Observe MPPT
INC	Incremental Conductance MPPT
V-P	Power-Voltage curve
V-I	Current-Voltage curve
I-O	Input-Output
CP-PV-T	Concentrated Photochemical-Photovoltaic-Thermochemical
RTDS	Real-Time Digital Simulator
CPV	Concentrated PV
DCM	Discontinuous Conduction Mode
CCM	Continuous Conduction Mode
STC	Standar Test Conduction
RMS	Root-Mean-Square
GaN	Gallium Nitride
WBG	Wide-Bandgap
MPC	Model Predictive Control
ANN	Artificial Neural Network
SCADA	Supervisory Control and Data Acquisition
LQR	Linear Quadratic Regulator
RE	renewable energy
ESS	Energy Storage System
IOT	Internet Of Things
EV	Electric Vehicles
EMS	Energy Management System
USB	Universal Serial Bus
PCI	Peripheral Component Interconnect
HTML	Hypertext Markup Language
CSS	Component as a Service
Wp	Watt-peak
FPPT	Flexible power point tracking
STC	Standard Test Conditions
V-S	Volt-Second
PU	Per Unit

## *Table of Symbols*

<b>Symbols</b>	<b>Unit (SI / PU)</b>	<b>Definition</b>
<b>I<sub>PV</sub></b>	Ampe (A)	PV current
<b>I<sub>Battery</sub></b>	Ampe (A)	Battery current
<b>I<sub>PH</sub></b>	Ampe (A)	Photo-current
<b>I<sub>SH</sub></b>	Ampe (A)	Shunt-current
<b>I<sub>D</sub></b>	Ampe (A)	Diode-current
<b>I<sub>sc</sub></b>	Ampe (A)	PV Short-circuit current
<b>V<sub>PV</sub></b>	Volt (V)	PV output voltage
<b>V<sub>OC</sub></b>	Volt (V)	PV Open-circuit voltage
<b>ΔP</b>	Watt (W)	Change in the PV power
<b>ΔV</b>	Volt (V)	Change in the PV voltage
<b>ΔI</b>	Ampe (A)	Change in the PV current
<b>V<sub>MPP</sub></b>	Volt (V)	The PV voltage at the maximum power point
<b>I<sub>MPP</sub></b>	Ampe (A)	The PV current at the maximum power point
<b>P<sub>MPP</sub></b>	Watt (W)	The PV resistor at the maximum power point
<b>V<sub>IN (min)</sub></b>	Volt (V)	The minimum input voltage
<b>V<sub>IN (max)</sub></b>	Volt (V)	The maximum input voltage
<b>V<sub>OUT</sub></b>	Volt (V)	Nominal Output Voltage
<b>I<sub>Out(max)</sub></b>	Ampe (A)	Maximum Output Current
<b>I<sub>C</sub></b>	Ampe (A)	Integrated Circuit
<b>I<sub>PN</sub></b>	Ampe (A)	Primary nominal RMS Current
<b>I<sub>S</sub></b>	Ampe (A)	Secondary nominal RMS current
<b>I<sub>FUSE</sub></b>	Ampe (A)	The fuse current
<b>V<sub>FUSE</sub></b>	Volt (V)	The fuse voltage
<b>T<sub>A</sub></b>	Degree Celsius (°C)	Ambient operating temperature
<b>R<sub>M</sub></b>	Ohm (Ω)	Measuring Resistor of sensors
<b>R<sub>Load</sub></b>	Ohm (Ω)	Load resistor
<b>C</b>	Farad (F)	Capacitor value
<b>L</b>	Henry (H)	Inductor value
<b>P<sub>OUT</sub></b>	Watt (W)	Output power
<b>P<sub>IN</sub></b>	Watt (W)	Input power
<b>I<sub>Sh</sub></b>	Ampe (A)	Shant-Current
<b>I<sub>o</sub></b>	Ampe (A)	Reverse saturation current of the diode

<b>q</b>	Coulombs(C)	Elementary charge
<b>K</b>	Joules per kelvin(J/K)	Boltzmann's constant
<b>T</b>	Kelvin(K)	Temperature
<b>R<sub>se</sub></b>	Ohm ( $\Omega$ )	Series Resistor of the solar cell
<b>R<sub>mpp</sub></b>	Ohm ( $\Omega$ )	The Resistor Maximum Power Point
<b>D</b>	Seconds (S)	Duty Cyle
<b>I<sub>min</sub></b>	Ampe(A)	Minumum Current
<b>I<sub>max</sub></b>	Ampe(A)	Maximum Current
<b>I<sub>L</sub></b>	Ampe(A)	Inductor Current
<b>V<sub>s</sub></b>	Volt (V)	Source Voltage
<b>t</b>	Second(S)	Period
<b>L<sub>f min</sub></b>	Henry (H)	Minumum Inductor for a given frequency
<b>L<sub>min</sub></b>	Henry (H)	Minumum inductor
<b>Q</b>	Coulombs(C)	Charge
<b><math>\Delta Q</math></b>	Coulombs(C)	Change in Charge
<b><math>\Delta V_o</math></b>	Voltage (V)	Change in output voltage

## Abstract

This thesis explores PV emulators, their control strategies, and hardware implementation. It covers the types of emulators, The study discusses real-time applications, hardware options such as power electronic-based and FPGA-based emulators, and the sensitivity of emulators to environmental conditions. Data acquisition systems and previous research on solar emulator acquisition systems are reviewed. The thesis also focuses on modeling and sizing the PV conversion chain, including PV source modeling, DC-DC boost converter modeling, and system sizing considerations. Simulation results investigate the impact of weather conditions, load demand, MPPT control methods, and switching between MPPT and FPPT control. The findings contribute to optimizing PV system performance for practical use.

**Key words:** PV simulator, Real-time application, Data acquisition system, DC-DC Boost converter, MPPT/FPPT control.

## ملخص :

تستكشف هذه الرسالة المحاكيات الكهروضوئية ، واستراتيجيات التحكم الخاصة بها ، وتنفيذ الأجهزة. يغطي أنواع المحاكيات. تناقش الدراسة التطبيقات في الوقت الفعلي ، وخيارات الأجهزة مثل المحاكيات القائمة على الطاقة الإلكترونية والقائمة على FPGA ، وحساسية المحاكيات للظروف البيئية. تتم مراجعة أنظمة الحصول على البيانات والأبحاث السابقة حول أنظمة اقتناء المحاكيات الشمسية. تركز الأطروحة أيضًا على نمذجة وتحجيم سلسلة التحويل الكهروضوئية ، بما في ذلك نمذجة مصدر الكهروضوئية ، ونمذجة محول دفعة DC-DC ، واعتبارات تغيير حجم النظام. تبحث نتائج المحاكاة في تأثير الظروف الجوية ، والطلب على الحمل ، وطرق التحكم في MPPT ، والتبديل بين التحكم في MPPT و FPPT. تساهم النتائج في تحسين أداء النظام الكهروضوئي للاستخدام العملي.

**الكلمات المفتاحية:** محاكي المصدر الطاقة الشمسية ، تطبيق في الوقت الفعلي ، نظام تحصيل على البيانات ، محول رافع للجهد تيار مستمر – تيار مستمر ، تحكم استخراج طاقة المصدر الشمسي MPPT / FPPT.



**General**

**Introduction**



The rapid advancement of technology has brought about transformative changes in various domains, and one such domain is photovoltaic (PV) systems. PV systems have emerged as a promising renewable energy solution, offering clean and sustainable power generation. To ensure their efficient operation and performance, the use of PV emulators has become essential. These emulators simulate the behavior and characteristics of real PV systems, enabling a wide range of applications such as testing, research, development, and training[1].

In recent years, there has been a significant research trend focused on enhancing the efficiency of solar systems through the implementation of new technologies. One such technology gaining prominence is the maximum power point tracking (MPPT) system. This technology ensures that solar panels operate at their highest efficiency levels, even under varying environmental conditions such as shading or temperature fluctuations. By extracting the maximum available power from solar panels, MPPT systems contribute to overall system efficiency and maximize the energy harvested from renewable sources. As a result, research efforts are increasingly directed toward developing more advanced and intelligent MPPT algorithms and control systems to further enhance the performance and cost-effectiveness of solar installations[2].

The main objective of this work is to contribute to the study and simulation of Stand-Alone solar photovoltaic (PV) systems, to monitor the performance of these PV systems by studying and analyzing the impact of variable weather conditions, such as temperature and solar radiation, Additionally, the study seeks to analyze the effects of load fluctuations by implementing different algorithms ( MPPT and FPPT ) to the DC/DC converter used in each system.

To achieve the above-mentioned objectives and facilitate the presentation of the results obtained in this research work, the thesis is organized as follows:

The introduction chapter serves as a starting point, providing a comprehensive overview of the research topic. We begin by defining PV emulators and highlighting their significance in the context of PV systems. We delve into the types of PV emulators, emphasizing their diverse capabilities and applications. Next, we will present the hardware implementation of PV-Emulators and different data acquisition systems. In the end, we will touch on the previous research conducted in the field of solar emulator acquisition systems. Building upon existing knowledge and insights, this research contributes to the body of work surrounding PV systems and emulators, offering new perspectives and solutions.

The second chapter is devoted to the modeling and design aspects of the studied standalone PV system. It begins by addressing the modeling of the PV source, which involves accurately capturing the electrical characteristics and behavior of the PV array. Next, we will present the different control methods (MPPT and FPPT). The modeling of the DC-DC Boost Converter, the sizing of the Current/Voltage Sensors, and the process of realized acquisition boards are discussed in detail. The third chapter is reserved for the simulation and evaluation of the results. Using MATLAB Simulink software, we analyze the impact of variable weather conditions, the impact of variable load demand, and the impact of switching between MPPT and FPPT control methods in cases direct/ indirect on the performance of our PV system.

This manuscript concludes with a general conclusion in which the perspectives of this work are included.



# **C**hapter **1**

*Literature review*

## **I.1 INTRODUCTION**

A brief literature review of standalone PV systems and PV emulators in power electronic applications reveals key insights into these fields of study. These are also referred to as independent solar systems. PV arrays are the primary source of energy for these systems, which supply DC and AC to electrical loads. Independent PV system design, operation, and maintenance have been the focus of recent studies. Research in this field ought to focus on enhancing system design and achieving more efficient operation and maintenance.

Previous studies have shown that to improve the efficiency of PV systems, new designs must be developed and in-depth evaluations of critical system components must be performed. Research into the development of various PV emulator topologies and their implementation in power electronic applications has been carried out in the field of PV emulators. To optimize system performance and spot possible faults, PV simulators are crucial tools for testing and evaluating PV systems in a controlled environment.

Previous literature studies have investigated and described the many types of PV emulators, their setups, and their uses in a wide range of applications. The assessments also provide insights into the challenges, opportunities, and primary research objectives in the area of PV emulators.

Finally, the literature on both freestanding PV systems and PV emulators in power electronic applications highlights the importance of improving system designs, achieving optimal operation and maintenance, and developing and utilizing PV emulators for testing and evaluation. The ongoing studies seek to enhance the functionality of PV emulators in power electronic applications and boost the effectiveness, efficiency, and dependability of standalone PV systems.

**Chapter Objectives:** The focus of this chapter is centered on the comprehensive review of the literature surrounding PV systems and emulators, as well as data acquisition systems (DAS). The objectives of this chapter are to provide a comprehensive overview of PV emulators and their types, explore their real-time applications, and examine the hardware implementation requirements and sensitivity to environmental conditions. Furthermore, this chapter aims to delve into the various types of DAS and their relevance to solar emulator acquisition systems.

**Chapter Outline:** The remainder of this chapter involves a systematic exploration of the different sections. We will introduce the concept of PV systems and simulators, discuss the types of PV simulators, and explore their real-time applications. Furthermore, we will investigate the hardware implementation of PV simulators. We will also delve into the sensitivity of PV simulators

to environmental conditions and highlight prominent PV simulator brands in the market. Shifting our focus to DASs, we will review the various types of DAS and their significance in solar emulator acquisition systems. Lastly, we will review previous studies in the field to identify research gaps and potential avenues for future exploration.

## I.2 PV systems and emulator

PV systems are a rapidly growing source of RE that has the potential to reduce greenhouse gas emissions and dependence on fossil fuels. PV systems are composed of solar panels that convert sunlight into electricity, which can be used directly or stored in batteries for later use [3]. PV systems have various applications, including powering homes and businesses and supplying power to remote areas that are not connected to the electrical grid. PV systems can also be integrated with the grid, allowing excess energy to be sold back to the utility company, making it a cost-effective solution for energy production [4] as shown in Figure I.1.

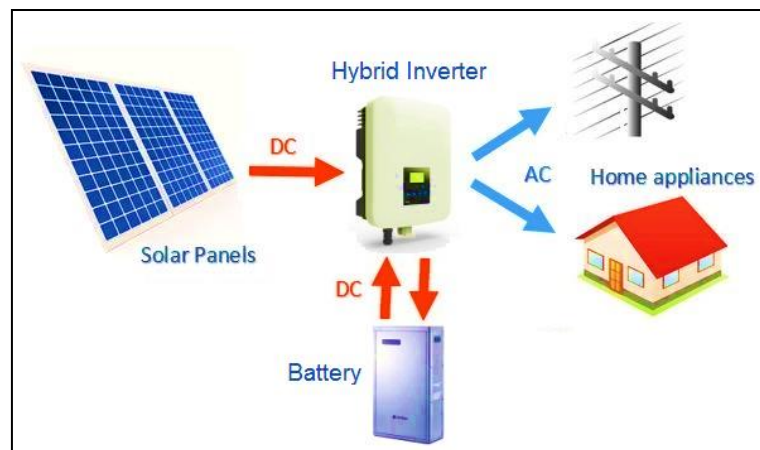


**Figure I. 1:** Simplified layout of a hybrid solar system[5].

As shown in Figure I-2, PV emulators are essential tools for developing and testing the various components of a PV system. An emulator can accurately replicate the output of a PV system, allowing researchers and engineers to simulate different environmental conditions, and evaluate the performance of various system components [6].

Several studies have explored the use of PV systems and emulators, including the evaluation of the economic and environmental benefits of PV systems in various regions.

Tables (I.1 and I.2) present examples of PV systems and PV simulators, with their corresponding application areas, real-time implementation, and contributions/achievements. Table

I.1 includes examples of PV systems such as grid-connected PV systems, and standalone PV systems and our study focuses on this type, each with unique application areas and contributions, such as efficiency improvement or cost-effectiveness.

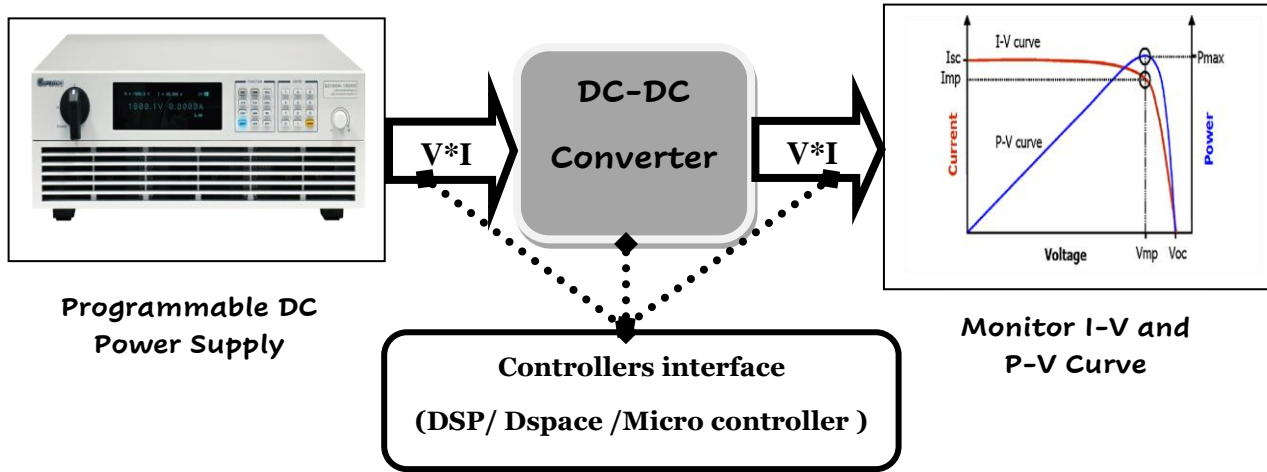


Figure I. 2: Controller implemented PV emulator.

Table I. 1: Contributions and achievements of recent works in PV systems.

Ref	PV systems			Contribution and achievements
	Category	Application	Real-time execution	
[7]	ON-Grid-PV systems	Buildings (Residential)	Smartphone application	Supply homeowners with affordable PV systems, reducing electricity costs, and promoting clean energy.
[8]	Standalone PV system	ANN-P&O MPPT	dSpace 1104	Enhancing accuracy and efficiency of MPPT systems using ANN approaches.
[9]	CPV systems	Hydrogen fuel production.	SCADA Systems	Evaluating <b>CP-PV-T</b> system, achieving enhanced energy utilization.
[10]	Floating PV systems	RE generation of water	Arduino Uno	water conservation: reduced evaporation, inhibited algae.
[11]	Tracking PV systems	PV applications	Arduino card	Design and simulation for enhanced PV performance and optimized sun tracking.
[12]	Water Pumping Systems	Rural water supply and irrigation systems	Microcontroller 16F877	Promoting solar water pumping and Improving water access in rural areas.
[13]	Portable PV Systems	Camping, hiking, and emergencies.	Microcontrollers	Clean energy access in off-grid areas and emergency power supply in disasters.

Table I. 2: Contributions and achievements of recent works in PV Emulators.

Ref	PV emulator system			Contribution and achievements
	Category	Application	Real-time execution	
[14]	PV Emulators	Small Residential/commercial systems.	HIL testing (DSP platform)	Testing, research, and development to improve performance and reliability.
[15]		MPPT algorithm	FPGA platform	Improved power quality and efficiency of PV systems
[16]		PV System Monitoring	Arduino Mega 256	Design and implementation of a low-cost autonomous data logger for monitoring PV systems.
[17]	Emulator using GaN/WBG semiconductor	Solar panel testing, research, and development.	HIL testing (DSP platform)	Improved flexibility and accuracy in testing and evaluation.
[18]	PV emulator-LQR control.	MPPT control of the PV system.	FPGA	Improves MPPT efficiency in PV systems.
[19]	PV Array Emulator	Grid Integration Studies	RTDS	Improved testing and evaluation of PV systems at different irradiances and temperatures.
[20]	Emulators based on Switching Converters	Solar panel testing, research, and development	HIL testing (DSP platform)	Improved testing and evaluation of PV systems.

On the other hand, table I.2 includes examples of PV emulators such as single panel emulators and PV array emulators, which are designed to mimic the behavior of PV panels under different conditions for testing and research purposes. The Real-time Execution column in both tables indicates whether the systems or simulators can be run in real time, and the Contributions/Achievements column highlights significant achievements or developments made by each example. Overall, the tables provided an overview of a set of previous studies of some PV systems and emulators through their applications and contributions to the field of REs.

### I.2.1 PV-Emulators

PV emulators, also known as solar simulators, are devices that simulate the characteristics of a PV cell or panel. They are commonly used in the testing and development of solar energy systems, as they allow researchers, engineers, and manufacturers to simulate the behavior of PV systems under various conditions, without the need for expensive or time-consuming field testing [21].

PV emulators typically consist of a power supply, a control system, and a set of programmable parameters that allow users to simulate different environmental conditions, such as temperature, sunlight intensity, and shading. Some PV emulators also include built-in sensors that allow users to monitor and measure the output of the system in real-time [20].

In addition to their use in testing and development, PV emulators are also used in education and research, as they provide a safe and controlled environment for students and researchers to study and experiment with PV systems. They are also used in certification and compliance testing, as many regulatory agencies require PV systems to be tested and certified before they can install [22].

Global, PV emulators play important roles in the development, testing, and certification of solar systems, and are an essential tool for researchers, engineers, and manufacturers in REs.

### I.2.2 Types of PV emulators

There are three parts to the PV emulator system introduced by the researcher, as shown in Figure I.3. The first part of the PV emulator system is the PV model. The function of the PV model is to produce the I-V characteristics of the PV module signal.

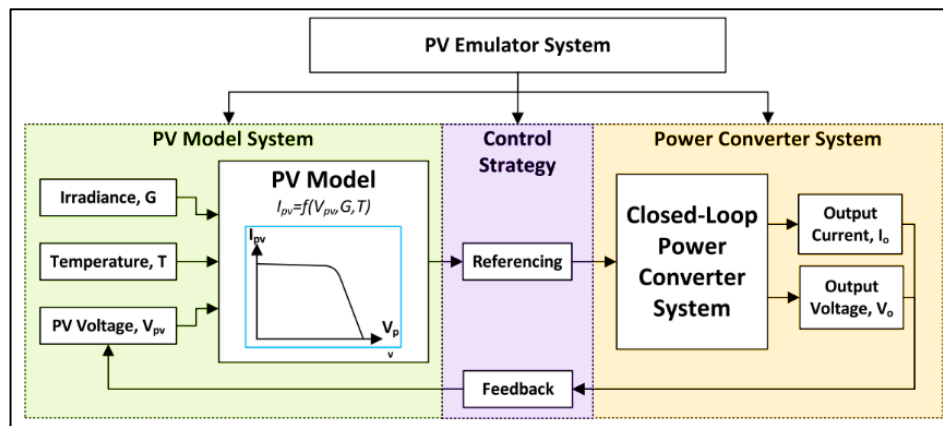


**Figure I. 3:** Three parts of the PV emulator system[23].

This signal is used by the closed-loop power converter system to emulate the characteristic of the PV module. The PV model is highly responsible for the accuracy of the PV emulator; however, the PV emulator requires real-time calculations of the PV model to operate properly.

The control and monitoring system in the PV emulator regulates and monitors the emulator and the overall system. It employs control algorithms, sensors, and feedback loops to adjust the emulator's output. The system also facilitates data acquisition to measure and record parameters for analysis and evaluation[23].

Therefore, the PV model used in the PV emulator application must remain simple without compromising the accuracy of the I-V characteristics produced. They are commonly used to study the behavior and performance of PV systems. We mention three categories of PV emulators:

**I.2.2.A Single Panel Emulators:** These PV emulators are designed to mimic the electrical behavior of a single PV panel. They typically have a power output of around 300 W. Examples of



single panel emulators available in the market include the Elgar ETS60X14C-PVF priced at \$6385 and the Magna Power TSD50050240 priced at \$21,000 [23].

**I.2.2.B PV Array Emulators:** such emulators can emulate the electrical characteristics of larger PV arrays and provide more comprehensive simulations of multiple PV panels. The power output of PV array emulators is typically higher than 300 W. Commercial solutions and market options for PV array emulators have also been mentioned in the literature (Figure I.4) [24].

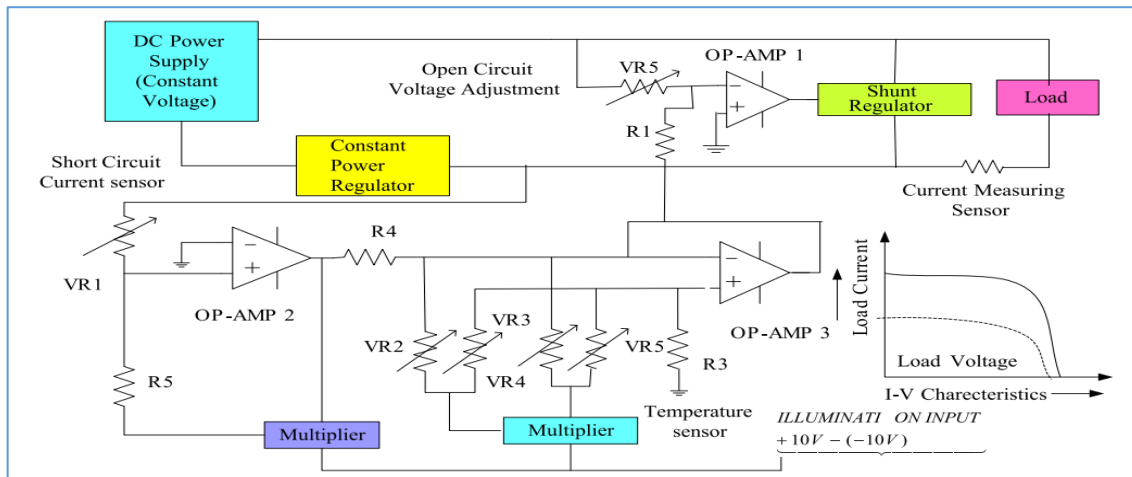


Figure I. 4: Analog PV emulator [1].

**I.2.2.C Diode Model Approximation-Based Emulators:** The types of PV emulators in Figure I.5 approximate the electrical behavior of a PV panel using diode models to provide an accurate representation of PV characteristics and have been widely discussed in the literature [1].

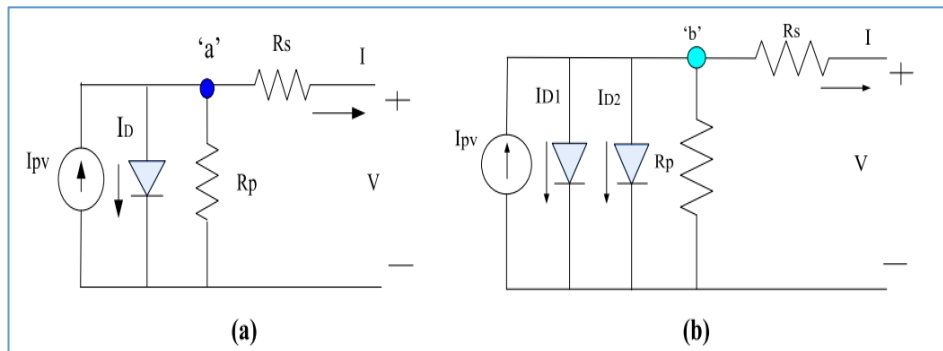
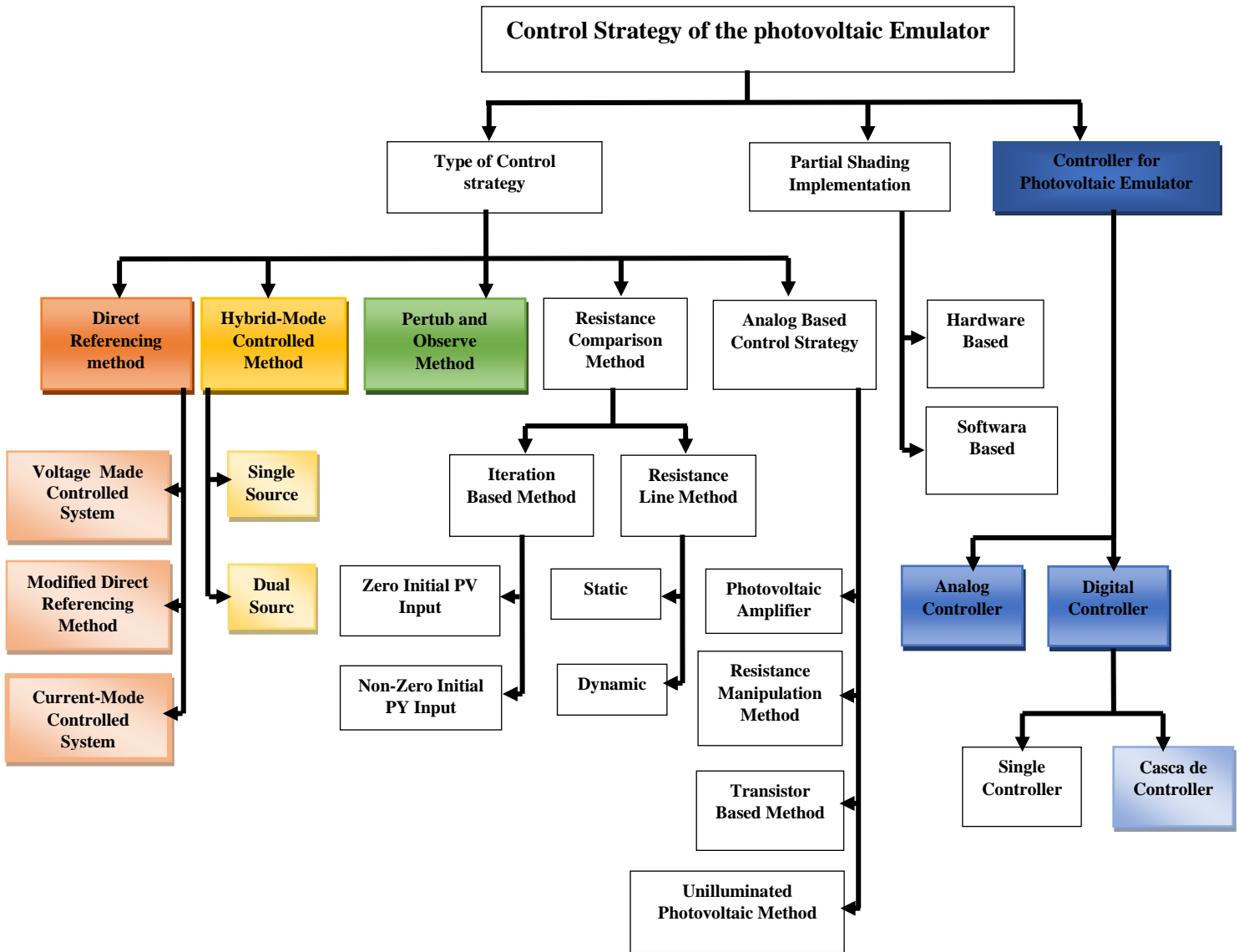


Figure I. 5: PV models with (a) Single diode and (b) Double diode [1].

**I.2.3 Control Strategies for PV Emulators**

Various control strategies have been reported in the literature (see Figure I.6) to regulate the operation of PV emulators. These strategies include the resistance comparison method, hill-climbing method, hybrid-mode controlled method, and direct referencing method [20].



**Figure I. 6:** The control strategy of the PV emulator[20].

### I.2.4 Real-time applications

The real-time applications of PV emulators are significant because they allow researchers, engineers, and technicians to study and test the behavior of PV systems in a controlled environment, and in real time. This is important because PV systems are subject to a wide range of environmental conditions and parameters, including varying levels of sunlight, temperature, shading, and load, and it is difficult to replicate these conditions accurately in a laboratory or testing facility [25].

This can help identify potential issues with these components before they are integrated into a full system, and can lead to more efficient and reliable systems overall.

#### I.2.4.A Examples of Real-time applications

- **PV System Testing**

PV emulators are used to test the performance of entire PV systems, including their response to different levels of sunlight and shading. This allows researchers and engineers to identify potential issues before it is deployed, and to optimize the system's performance for specific environmental conditions [26]. Figure I.7 displays PV systems using PV panels and emulators.

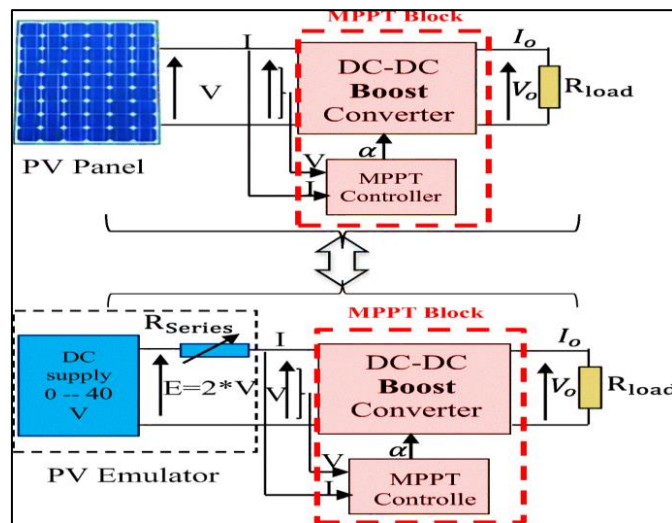
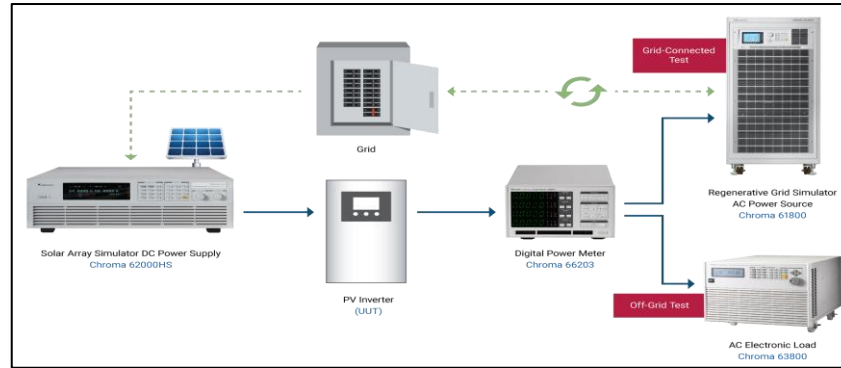


Figure I. 7: A schematic of PV panel and PV emulator systems [27].

- **Inverter Testing**

Inverters are a critical component of PV systems, as they convert the DC power generated by the PV panels into AC power that can be used by users. PV emulators can be used to test the performance of inverters in real-time (see Figure I.8), including their ability to handle changes in voltage and frequency, and their response to grid disturbances such as voltage dips and surges [28].



**Figure I. 8:** PV inverter test equipment-Chroma [29].

- **Research and Development**

PV emulators are widely used in the research and development of new PV technologies, including advanced materials, new cell designs, and improved manufacturing processes as Figure II.6 shows. By simulating different environmental conditions and system parameters, researchers can better understand the PV systems' behaviors and improve their efficiency and performance [1].

- **Education and Training**

PV emulators are commonly used in educational settings to teach students about the principles of solar energy and the behavior of PV systems. They provide a safe and controlled environment for students to learn about PV technology and can be used to demonstrate the effects of different environmental conditions on the performance of a PV system. PV emulators can be used to train technicians and engineers on PV systems operation and maintenance, as seen in Figure I.9 [30].

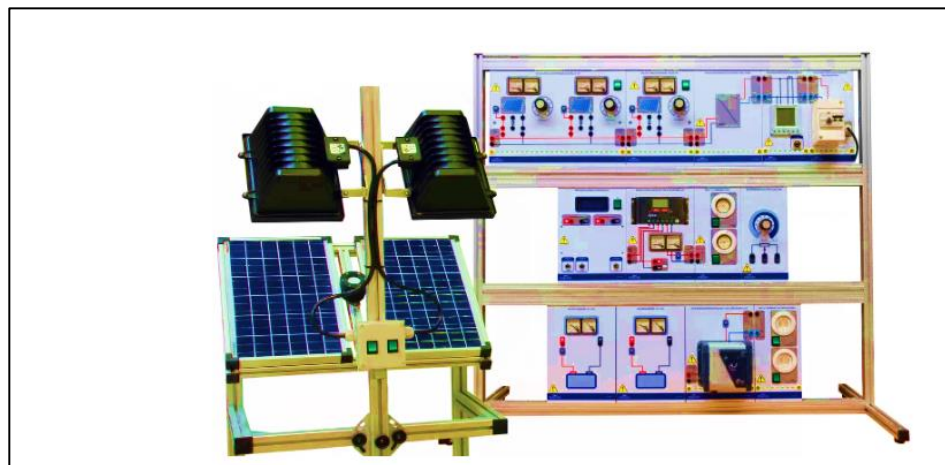


**Figure I. 9:** Solar training equipment [31].

- **Certification and Compliance Testing**

PV emulators are also used in certification and compliance testing, as many regulatory agencies require PV systems to be tested and certified before they can be sold or installed. PV

emulators can be used to perform these tests, ensuring that PV systems meet the required safety and performance standards [32].

Overall, the real-time applications of PV emulators are diverse and widespread and are essential to the continued development and optimization of PV systems. By simulating different environmental conditions and system parameters, PV emulators enable researchers, engineers, and technicians to better understand the behavior of PV systems and to develop new technologies that are more efficient, reliable, and cost-effective.

### I.3 Hardware implementation of PV-Emulators

PV emulators can be implemented in hardware using a variety of different technologies, depending on the specific application and requirements using two common types:

#### I.3.1 Power Electronic-based PV Emulators

Power electronic-based PV emulators use power electronics circuits to simulate the behavior of a typical PV system, and can be programmed to simulate different environmental conditions and system parameters. Power electronic-based PV emulators are commonly used in the research and development of new PV technologies, as well as in the testing and certification of PV systems [33].

#### I.3.2 FPGA-based PV Emulators

Figure I.10 shows the FPGA-based PV emulators using Field-Programmable Gate Arrays (FPGAs) to simulate the behavior of a PV system. FPGAs are highly flexible and can be programmed to simulate a wide range of different scenarios and parameters, making them ideal for the research and development of new PV technologies.

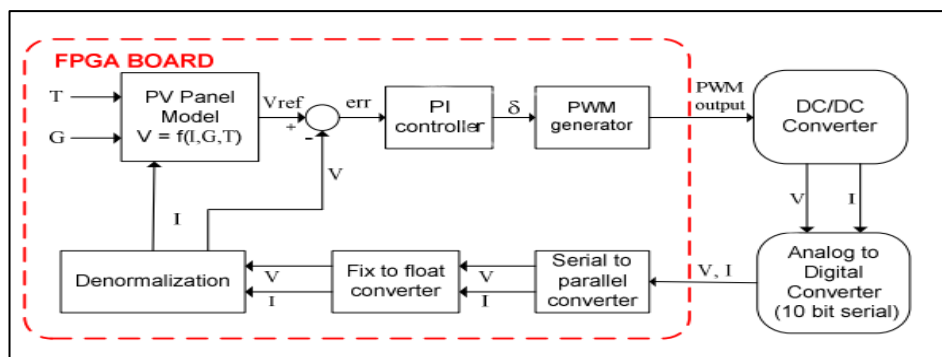


**Figure I. 10:**Control schematic diagram of PV panel emulator system [34].

Additionally, FPGA-based PV emulators are highly accurate and can simulate the behavior of a PV system in real-time, making them ideal for testing and certification of PV systems [35]. Both powers electronic-based and FPGA-based PV emulators have their advantages and disadvantages, and the specific implementation chosen will depend on the specific requirements of the application. However, both technologies have proven to be highly effective in simulating PV systems behavior, and are widely used in research, development, and testing of PV technologies [35].

### **I.3.3 Hardware implementation Requirements**

There are other details to consider when implementing PV emulators in hardware. Some additional details to consider include [26].

- **Voltage and Current Range:** PV emulators must be capable of generating the voltage and current ranges that are typical of a PV system. This requires careful selection of the components used in the emulators, as well as precise control of the voltage and current waveforms.
- **Response Time:** PV emulators must be able to respond quickly to changes in environmental conditions and system parameters. This requires high-speed control systems and components that are capable of responding quickly to changes in voltage and current.
- **Accuracy:** PV emulators must be highly accurate to provide reliable and repeatable results. This requires careful calibration and testing of the emulators, as well as precise control of the voltage and current waveforms.
- **Safety:** PV emulators must be designed with safety in mind, as they are capable of generating high voltages and currents. This requires careful design of the circuits and components used in the emulators, as well as the use of appropriate safety measures and equipment.
- **Cost:** The cost of implementing PV emulators in hardware can vary widely, depending on the specific implementation and requirements. This requires careful consideration of the costs and benefits of different technologies, components, and potential return on investment.

Overall, the hardware implementation of PV emulators requires careful consideration of a wide range of factors, including voltage and current range, response time, accuracy, safety, and cost. By carefully selecting the components and technologies used in the emulators, and by designing them with these factors in mind, researchers and engineers can develop highly effective and reliable PV emulators that are capable of simulating PV behaviors in different scenarios and conditions.

## I.4 Sensitiveness to environmental conditions

PV emulators are sensitive to environmental conditions, as they are designed to simulate the behavior of PV systems under different scenarios and conditions. The performance of PV emulators can be affected by a range of environmental conditions, including **temperature, humidity, light intensity, and shading**.

**Temperature** is one of the most important environmental factors that can affect the performance of PV emulators. The temperature of the PV emulator can affect the performance of the power electronics and the accuracy of the voltage and current measurements. High temperatures can also cause thermal drift, which can affect the accuracy of the voltage and current waveforms.


**Humidity** is another environmental factor that can affect the performance of PV emulators. High humidity can cause corrosion and other issues with the electronics, which can affect the accuracy and reliability of the emulator.

**Light intensity** and **shading** are also important environmental factors that can affect the performance of PV emulators. Changes in light intensity and shading can affect the voltage and current waveforms generated by the emulator, which can affect the accuracy of the simulation.

To minimize the effects of environmental conditions on the performance of PV emulators, it is important to design the emulators with appropriate thermal management systems and to calibrate them carefully under different environmental conditions. It is also important to use appropriate sensors and monitoring systems to ensure that the emulator is performing correctly under different environmental conditions. Overall, sensitivity to environmental conditions is an important consideration when designing and using PV emulators, and careful attention must be paid to minimize the effects of these conditions on the performance of the emulator[16].

## I.5 PV emulator brands in markets

Several brands of PV emulators are commonly used by researchers and engineers in the field of PV. Some of the most famous brands of PV emulators include:

 **Chroma ATE:** Chroma ATE is a global leader in precision test and measurement equipment, including power electronics and PV testing solutions. They offer a range of PV emulators, including the 62000P and 61600 series (see Figure I.11), which are designed to simulate various environmental conditions and system parameters.

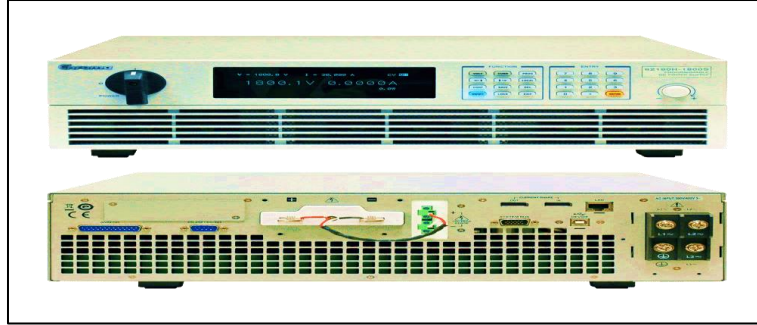


**Figure I. 11:** Solar Array Simulator DC Power Supply from Chroma ATE [36].

These emulators have been used in research studies like Chroma 62050H-600, which has been used to implement and validate experiments of three dynamic test procedures, including stepped operation procedure, day-by-day operation procedure, and EN50530 dynamic test procedure [37].

✚ **Keysight Technologies:** Keysight Technologies is a multinational technology company that specializes in electronic test and measurement equipment. They offer a range of PV emulators, including the E4360 Series (see Figure I.12), which is designed to simulate real-world PV conditions and verify the performance of PV inverters and other components. These emulators have been used in various research studies, such as developing a HIL system to emulate PV behavior including PV panels associated with a DC-DC Boost converter [38].



**Figure I. 12:** E4360 Series Modular Solar Array Simulators, 1.2 kW | Keysight [39].

✚ **NH Research:** NH Research is a leading manufacturer of power electronics test systems, including PV emulators. They offer a range of PV emulators, including the 9430 and 9430A series as shown in Figure II.13, which are designed to simulate various environmental conditions and system parameters.

These emulators have been used in various research studies, as used in [40], where a HIL Test Platform was adopted for a Vehicular Auxiliary Power System with an Onboard PV system.





**Figure I. 13:**NH Research 9430[41]

✚ **Regatron:** Regatron is a Swiss manufacturer of power electronics test systems, including PV emulators. They offer a range of PV emulators, including the RPV series, which is designed to simulate various environmental conditions and system parameters. These emulators have been used in various research studies investigating the energy unbalance in electric vehicles (EV), ESS, and PV arrays with a flexible energy management system (EMS) [42].

✚ **Preen:** a US-based manufacturer of electronic test equipment, including PV emulators, the **Preen** PV Simulator, which is designed to simulate various environmental conditions and system parameters [43]. These emulators have been used in various studies.

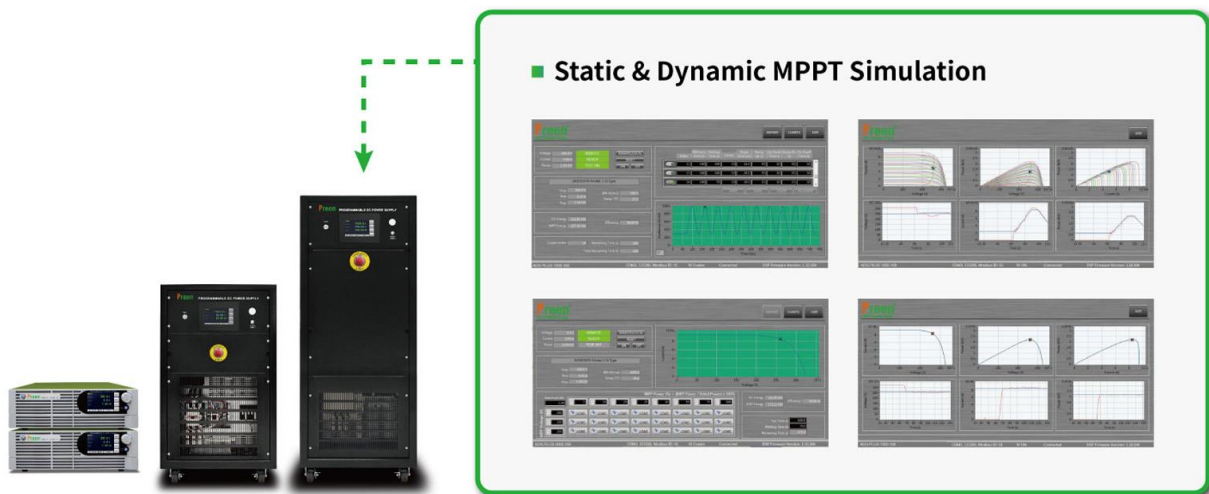


**Figure I. 14:** Preen Modular Solar Array Simulators [43].

**To note,** these are just a few examples of the many brands of PV emulators that are available to researchers and engineers in the field of PV. The specific brand chosen will depend on the specific requirements of the application, as well as the budget and other considerations.

## I.6 Data acquisition systems

A DAS is a system that collects and records data from various sensors or sources in real-time. In the context of a PV system, a DAS system is used to monitor and control the performance of solar panels by measuring parameters such as solar irradiance, panel temperature, and output voltage and current. This data can be used for monitoring, identifying issues or faults, optimizing the system, and remote monitoring and control. DAQ systems are crucial components in PV systems, allowing for real-time monitoring and control to maximize energy production [44].

### I.6.1 Standalone DAS

Standalone DAS are used in PV systems to monitor and control the performance of solar panels. These self-contained devices collect, record, and store data from sensors that measure parameters such as solar irradiance, panel temperature, and output voltage and current as shown in Figure I.15. The data collected by the standalone DAS system is used to optimize the PV system for maximum efficiency and to identify any issues or faults.

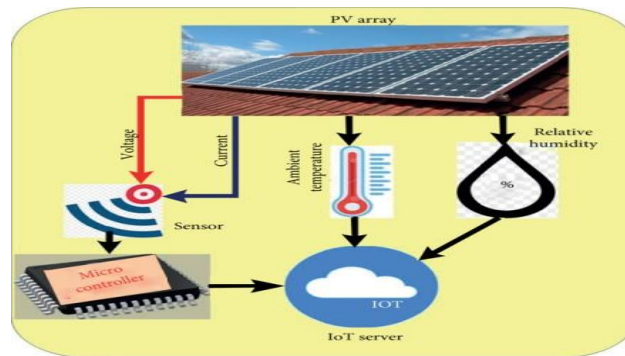


**Figure I. 15:**Data from the PV panel to the IOT server [45].

Standalone DAS systems are particularly useful in remote or harsh environments where a computer may not be practical, and they can be customized for specific PV system applications. Overall, they are essential tools for real-time monitoring and control of PV systems, ensuring maximum energy production [46].

### I.6.2 PC-Based DAS

Systems require a computer to operate and typically consist of a data acquisition card or module that connects to the computer's bus, such as **USB** (Universal Serial Bus) or **PCI** (Peripheral

Component Interconnect) as seen in Figure I.16 providing a high-level of accuracy and control over data analysis. They are critical for real-time monitoring and data control in various applications [47].

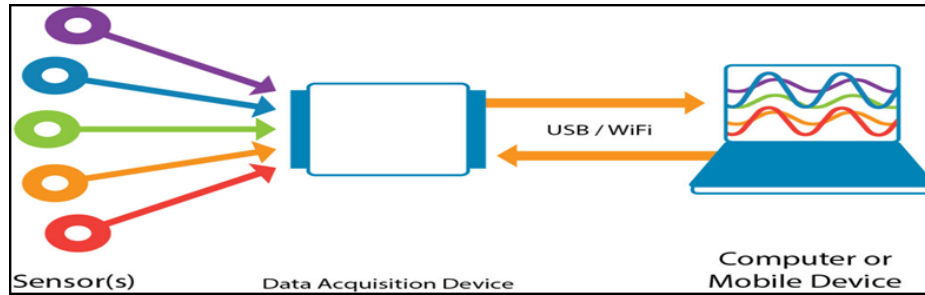


**Figure I. 16:**Data Acquisition From Analog Signals to Digital Data [48].

### I.6.3 Distributed DAS

Distributed data acquisition (DAS) systems collect, record, and analyze data from multiple sources or sensors across a network. They consist of a central unit that communicates with multiple remote units, which are responsible for collecting and processing data from sensors or sources in their respective locations. Distributed DAS systems are commonly used in large-scale applications where sensors are located in multiple locations or where the data needs to be collected from remote or hard-to-reach areas. They are highly customizable, and they provide real-time monitoring and control of data, making them essential tools in various industries.

### I.6.4 Wireless DAS

These systems use wireless communication protocols such as Bluetooth or Wi-Fi to transmit data from sensors to a data acquisition module or a computer [49].

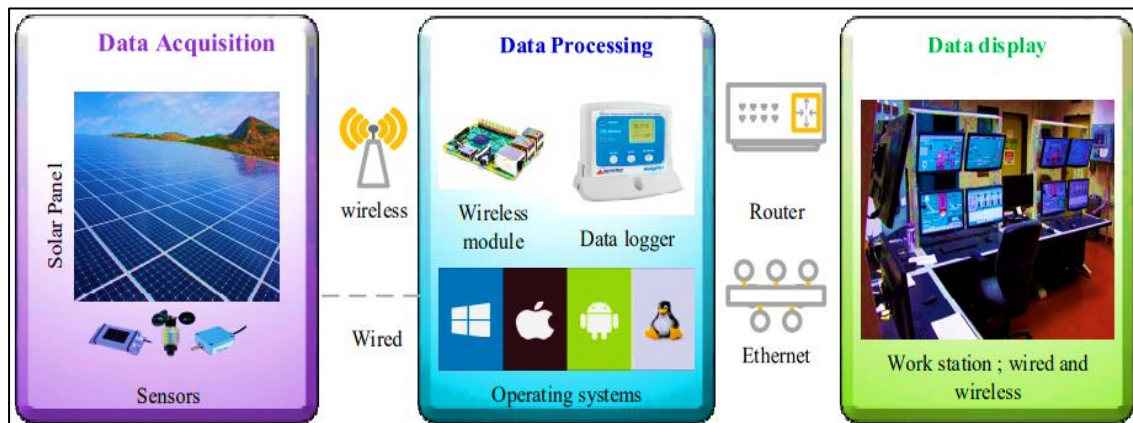


**Figure I. 17:** The basic architecture of a solar PV monitoring system [49].

### I.6.5 Remote DAS

Remote DASs collect, record, and analyze data from remote or hard-to-reach locations using wireless communication methods such as cellular or satellite networks. They are commonly used in environmental monitoring, precision agriculture, and remote infrastructure monitoring, among other applications.

Remote DAS systems are highly customizable and provide real-time monitoring and control of data from remote locations, making them essential tools in many industries. They enable remote monitoring and control of critical systems and infrastructure, making them powerful tools for collecting and analyzing data from remote locations [44].

### I.6.6 Web-Based DAS

Web-based DAS are computer systems that enable remote monitoring and control of data acquisition processes using a web browser interface. They utilize web technologies such as **HTML** (Hypertext Markup Language), JavaScript, and **CSS** (Component as a Service) to provide a user-friendly interface for data acquisition and visualization. Web-based DAS are highly flexible and convenient, accessible from anywhere with an internet connection, and commonly used in industries such as manufacturing, energy, and environmental monitoring. They offer a cost-effective and accessible alternative to traditional DAS, as they eliminate the need for dedicated software or hardware and can be easily integrated with existing infrastructures [50].

### I.7 Previous research on solar emulator acquisition systems

Solar emulator acquisition systems are used to simulate the behavior of solar cells and panels under different conditions. There has been considerable research in this field, and here are some of the previous works:

1. This **paper** [16] presents developed a low-cost autonomous data logger for monitoring PV systems. The system included an indoor solar emulator, which was used to simulate different levels of solar irradiance. The authors tested the system on a 100 **Wp** PV module and found that it was able to accurately measure the PV module's performance.
2. This **paper** presents and evaluated the performance of a solar module with an emulator and DC microgrid. The system included a solar emulator, which was used to simulate different levels of solar irradiance, and a DC microgrid, which was used to store and distribute

energy. The authors tested the system on a 120 **Wp** solar module and found that it was able to improve the overall efficiency of the module [51].

3. This **paper** presents developed a solar module emulator based on a low-cost microcontroller. The system included a solar emulator, which was used to simulate different levels of solar irradiance, and a microcontroller, which was used to control the emulator. The authors tested the system on a 100 **Wp** solar panel and found that it was able to accurately emulate the panel's behavior at different levels of solar irradiance[52].

Overall, the previous research presents various approaches to designing and implementing solar emulator systems for PV module monitoring, load emulation, and performance evaluation. These systems incorporate a range of components, such as field programmable gate arrays, digital signal processors, and microcontrollers, to accurately simulate different levels of solar irradiance and improve the efficiency of solar modules. The findings suggest that these systems are capable of accurately emulating the behavior of solar panels and can improve the overall performance of PV systems. However, further research is needed to optimize these systems for a wider range of PV modules and environmental conditions.

Accordingly, our study contributes to the development of high-flux solar simulators and provides a useful technique for describing their performance. The results should be useful to researchers and practitioners working on designing and testing solar energy systems.

## **I.8 Conclusion**

this literature review chapter has provided a comprehensive understanding of PV systems, emulators, and DAS. It has highlighted the significance of PV emulators in accurately assessing the performance of PV systems and their components. The chapter emphasized the diverse applications of PV emulators and the importance of selecting the appropriate type based on hardware implementation requirements. Additionally, it discussed the sensitivity of PV emulators to environmental conditions and provided an overview of prominent PV emulator brands in the market. Furthermore, the chapter delved into the different types of DAS and their relevance to solar emulator acquisition systems. Finally, the chapter identified research gaps and the need for further studies to enhance the effectiveness and efficiency of PV emulators and DAS, to drive progress in the RE sector.



# Chapter 2

*Modeling design and sizing of the PV  
conversion chain*

## II.1 Introduction

Chapter 2 of this dissertation delves into the detailed analysis of the PV-conversion chain, which is a crucial component in standalone PV systems. Building upon the foundation established in the previous chapter, which provided an overview of PV systems, emulators, and DAS, this chapter focuses on exploring the intricacies of the PV-conversion chain and its associated elements.

The PV-conversion chain acts as a vital link between the PV source and the electrical loads in standalone PV systems. Its performance optimization is essential for efficient energy conversion, system stability, and overall system efficiency maximization.

The primary objective of this chapter is to thoroughly investigate the modeling and design aspects of the studied standalone PV system. It begins by addressing the modeling of the PV source, which involves accurately capturing the electrical characteristics and behavior of the PV array. This precise modeling of the PV source serves as a foundation for subsequent analysis.

Next, the chapter shifts its focus to PV curves in the PV emulator, which is a critical aspect of the closed-loop control system of the standalone PV system. It explores closed-loop control, with particular emphasis on the maximum power point tracking (MPPT) control process. Additionally, the chapter also delves into the Flexible power point tracking (FPPT) control process.

Another crucial component in the PV-conversion chain, the modeling of the DC-DC converter, is thoroughly examined. The investigation also encompasses the protection system of DC-DC converters, as it plays a pivotal role in ensuring system reliability and safeguarding against faults. The sizing of the DC load, an essential aspect of PV system design, is also discussed, emphasizing the importance of accurate sizing calculations based on specified load requirements.

To facilitate the sizing process, this chapter provides insights into the tools and resources available for sizing the PV source, DC/DC converters, current/voltage sensors, and gate drive components. Furthermore, it concludes by describing the realized acquisition boards and outlining the objectives of the experimental validation. The experimental setup, implementation procedures, and methodologies employed for calibration, validation, and data analysis are also discussed.

The analyzed standalone PV system consists of three distinct components: the PV Emulator, which compensates for the solar panel; a chopper that functions as a DC/DC converter, and a variable load, as shown in Figure II-1. Together, these components work in tandem to create an efficient and effective system for converting solar energy into usable power. The PV Emulator

compensates for the solar panel, while the chopper converts the DC power generated by the PV Emulator to the desired voltage level. The variable load allows precise control over the generated power, ensuring optimal system performance. Overall, this system offers a robust and reliable solution for harnessing solar energy sustainably.

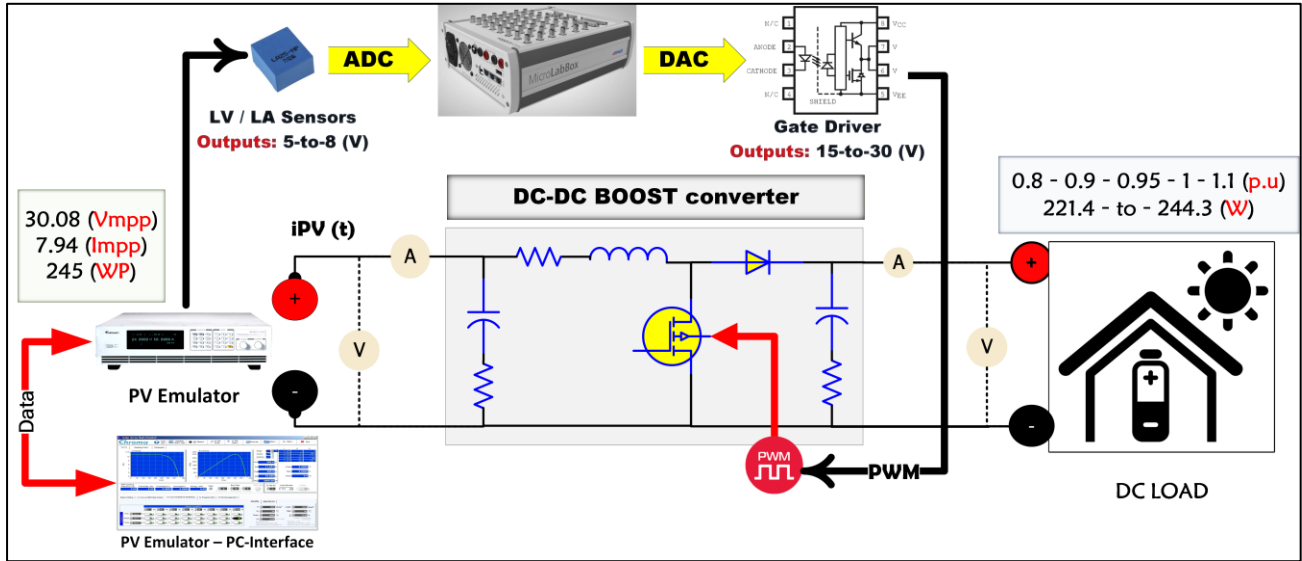


Figure II. 1: The block diagram of the PV system under study.

## II.2 Modeling of the PV-Source

A solar panel is an electronic device that converts sunlight into electricity. It consists of PV cells that absorb photons from sunlight, causing electrons to be released from the atoms in the cells as Figure II.2 shows. These electrons are then captured and converted into DC electrical energy, which can be used to power electronic devices or stored in batteries for later use.

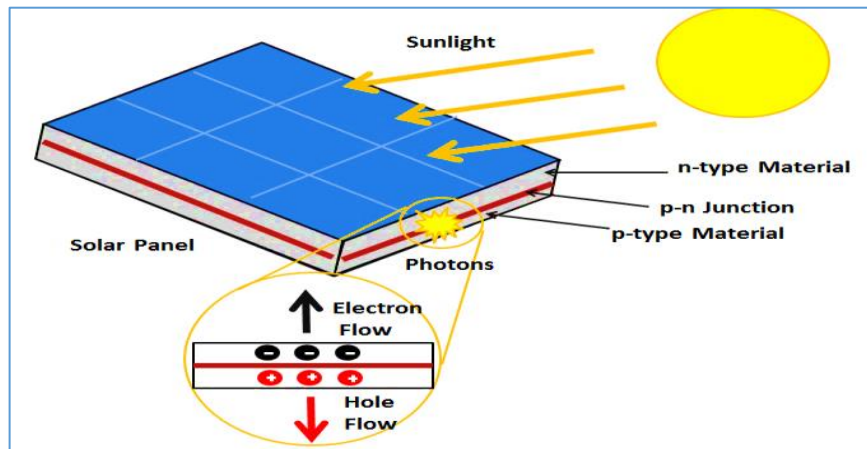


Figure II. 2: A diagram showing the photovoltaic effect [53].



In an ideal representation, a solar cell can be modeled as a parallel combination of a current source and a diode. However, in practical applications, additional elements such as shunt and series resistances are included in the model to account for manufacturing defects and contact resistances [54]. These additional components are essential to accurately depict the behavior of real-world solar cells, as illustrated in Figure II.3.

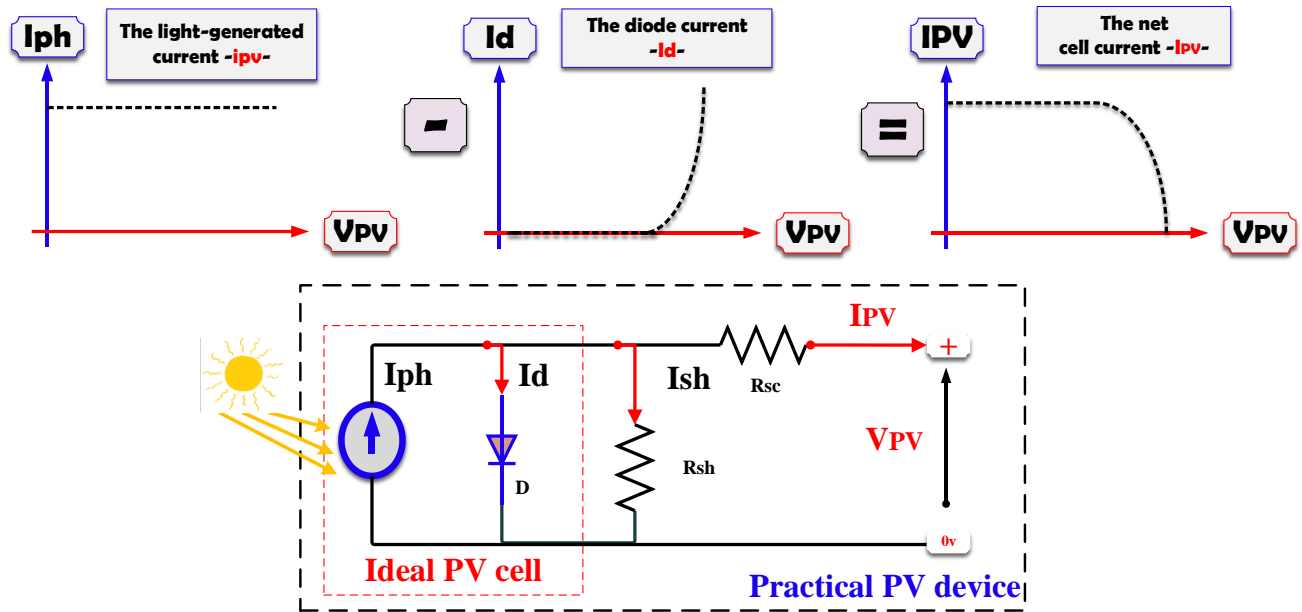


Figure II.3: Solar cell single-diode model.

The current generated by the solar cell  $I_{pv}$  can be computed by Equation (II.1) as follows.

$$I_{pv} = I_{ph} - I_D - I_{sh} \tag{II.1}$$

The equation and Ohm's law can be used to calculate the current through a diode and shunt resistor, as shown in Equations (II.2) and (II.3), respectively:

$$I_D = I_0 \left[ \exp \left( \frac{q}{N_{cs} \cdot k \cdot T} (V_{pv} + I_{pv} \cdot R_{SE}) \right) - 1 \right] \tag{II.2}$$

$$I_{sh} = \frac{V_{pv} + I_{pv} \cdot R_{se}}{R_{sh}} \tag{II.3}$$

Thus, the distinctive Equation of solar cell output current can be written as:

$$I_{pv} = I_{ph} - I_0 \left[ \exp \left( \frac{q}{n \cdot k \cdot T} (V_{pv} + I_{pv} \cdot R_S) \right) - 1 \right] - \frac{V_{pv} + I_{pv} \cdot R_{se}}{R_{sh}} \tag{II.4}$$

A PV module consists of multiple solar cells arranged together to generate usable electrical power when exposed to light. To ensure its suitability for outdoor applications, the module requires

protection. This protection serves two purposes: mechanical safeguarding to protect the fragile cells from damage and corrosion, and shielding against environmental factors such as humidity and temperature variations. These protective measures are essential to maintain the module's performance and durability in various climatic conditions [55].

In this study, the chosen PV source was the module-type **Anji Technology AJP-M660-245** solar panels. The characteristic curves of the PV module, specifically Voltage-Current (VI) and Voltage-Power (VP) curves are presented in Figures II.4 and II.5, respectively.

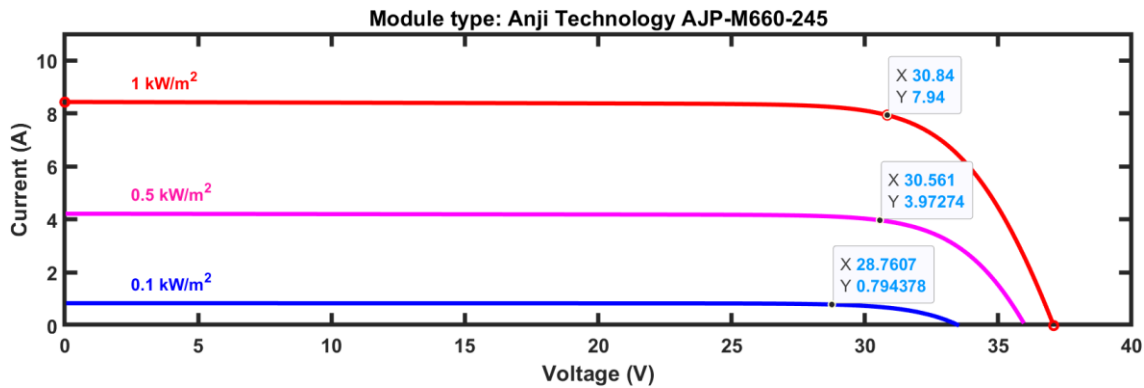


Figure II. 4: PV module characteristic (VI Curve).

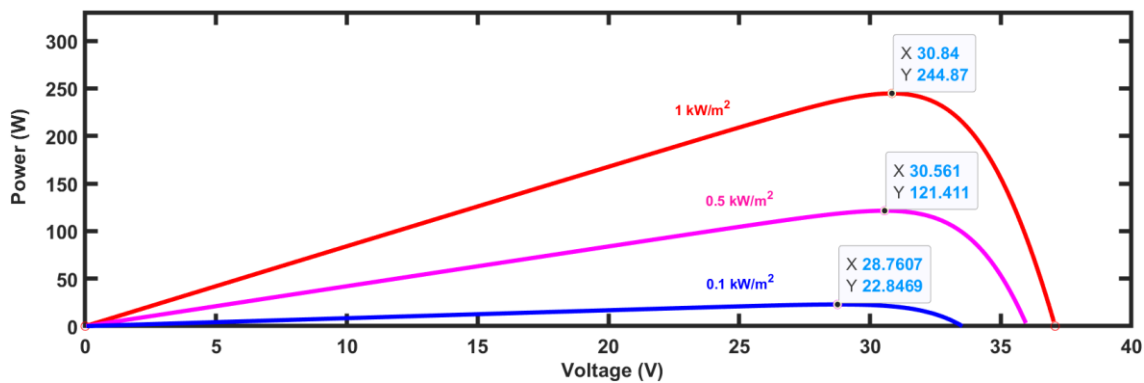


Figure II.5: PV module characteristic (VP Curve).

Table II.1 provides detailed information regarding the module settings and data.

Table II. 1: Parameters and Data of the PV selected Module (Anji Technology AJP-M660-245)

Model data	Values	Model parameters	Values
Maximum or Peak Power (Wp)	244.8696	Light-generated current $I_L$ (A)	8.4405
Cells per module ( $N_{CELL}$ )	60	Diode saturation current $I_0$ (A)	2.9125e-10
Open circuit voltage $V_{OC}$ (V)	37.08	Diode ideality factor	0.99901
Short-circuit current $I_{SC}$ (A)	8.43	Shunt resistance $R_{Sh}$ ( $\Omega$ )	366.2277

The voltage at the MPP $V_{MPP}$ (V)	30.84	Series resistance $R_S$ ( $\Omega$ )	0.20357
The current at MPP $I_{MPP}$ (A)	7.94	Temperature coefficient of $V_{OC}$ (%/deg.C)	-0.359

### II.2.1 PV curves in the PV-Emulator

Figure II.6 illustrates the photovoltaic simulator utilized in our laboratory for conducting the study. We implemented specific settings, including temperature and solar radiation conditions at STC (Standard Test Conditions), as well as the parameters of the solar panel such as  $V_{oc}$ ,  $I_{sc}$ ,  $I_{mpp}$ , and  $V_{mpp}$  mentioned in Table II.1 of our research. V-P and V-I curves extracted in the shape were

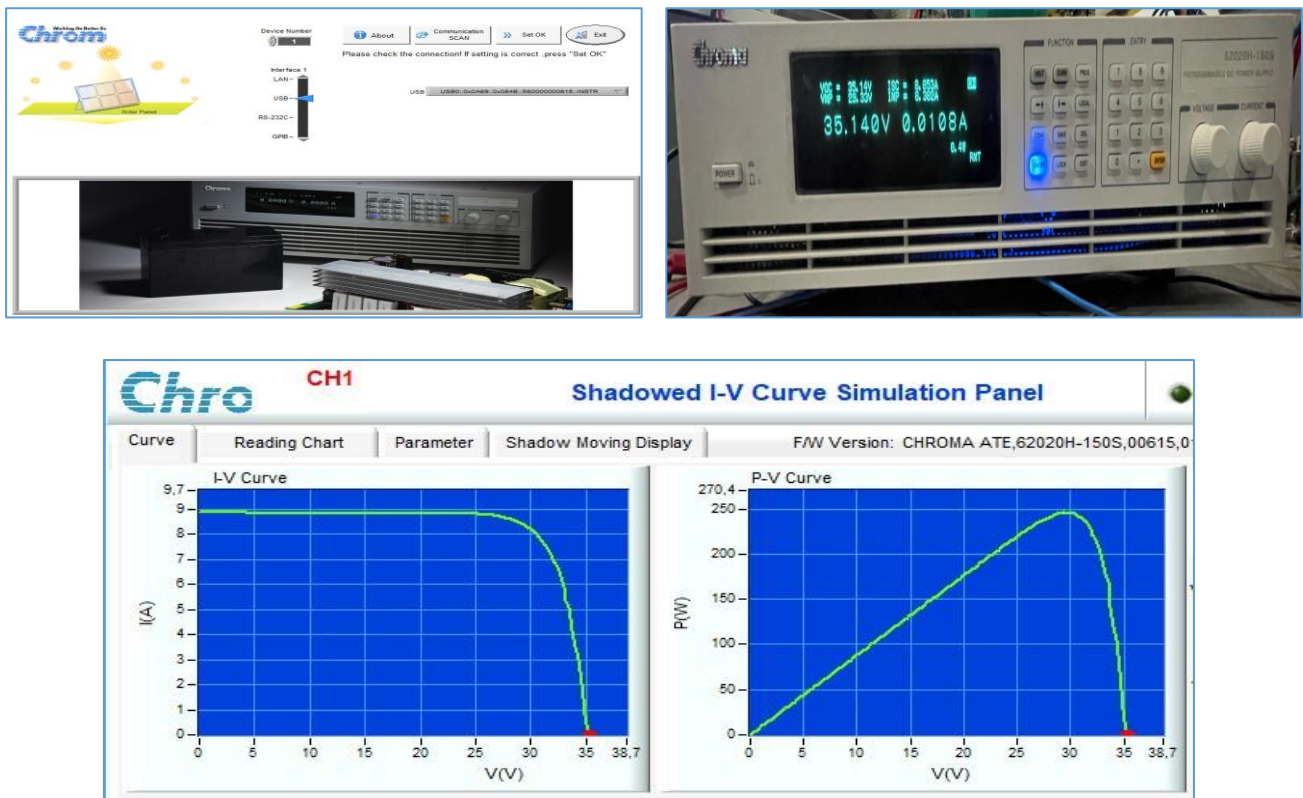


Figure II. 6: VI and VP curves using the PV emulator Chroma 62020H-150S.

### II.2.2 Closed-loop control of the standalone PV-System

A closed-loop control system is a mechanical or electronic system that regulates a process variable automatically without human intervention to maintain it at a desired state or set point [56]. In the context of a PV system, a closed-loop control system typically includes components such as a PV cell array, a DC/DC converter, a low-pass filter, and a closed-loop control circuit.

The control system is used to extract the maximum power from the PV cell while maintaining the desired voltage and current values, so we distinguish numerous Maximum-Power-Point-Tracking (MPPT) and Flexible-Power-Point-Tracking (FPPT) methods.

Our study specifically emphasized the performance of the DC-DC Boost converter, in tracking the MPP. We focused on a specific region where the resistance of the PV panel is either below or equal to the load resistance ( $R \leq R_{MPP}$ ). This region is illustrated in Figure II.6.

$$R_{MPP} = \frac{V_{MPP}}{I_{MPP}} \quad (\text{II.5})$$

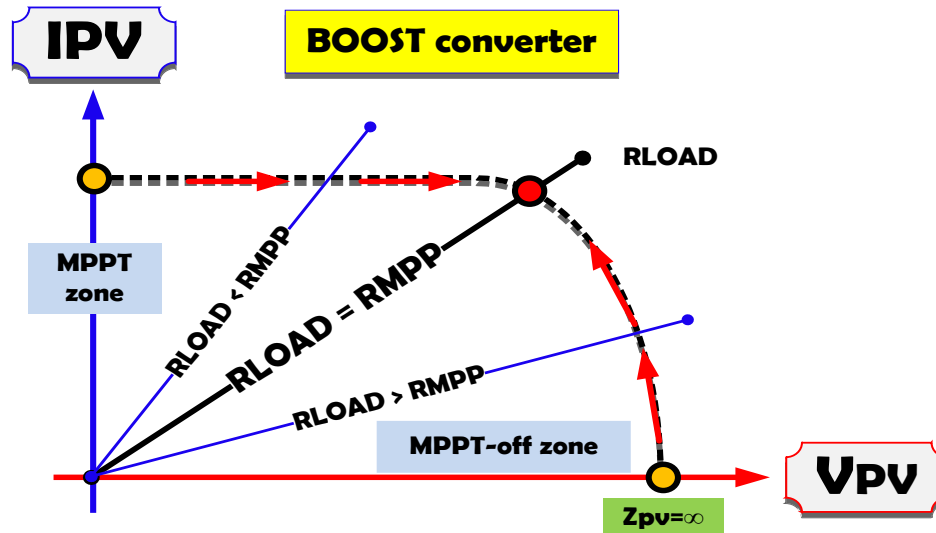


Figure II. 7: Tracking regions of MPPT control using a DC/DC boost converter.

### II.2.3 MPPT control methods

The MPPT technique is a control strategy that enables the efficient operation of a non-linear electrical generator to consistently generate its maximum power output. This technique is commonly applied to photovoltaic generators or wind generators. In the context of a PV system, an MPPT controller is employed to regulate a static converter that connects the load to the PV panel. Its purpose is to optimize power transfer and ensure the maximum power is delivered to the load.

#### II.2.3.A Perturb and Observe (P&O)

The P&O-MPPT technique is widely utilized in various applications due to its simplicity, easy implementation, minimal sensor requirements, and cost-effectiveness [57, 58]. It is an iterative approach that aims to track the MPP of a PV array. The P&O method operates by making small changes to the voltage of the PV array and observing the resulting impact on power output. This is

achieved by adjusting the duty cycle of the DC-DC converter used in the system. By analyzing the changes in power, the optimal operating point can be determined.

If increasing the voltage leads to an increase in power, it indicates that the PV module's operating point is on the left side of the power-voltage (P-V) curve. Conversely, if increasing the voltage results in a decrease in power, the operating point is on the right side of the P-V curve. To track the MPP effectively, the direction of perturbation must be adjusted to converge towards the desired end. The iterative process continues until the MPP is reached. Figure II.8 illustrates the step-by-step procedure for implementing this technique and demonstrates its working principle [54].

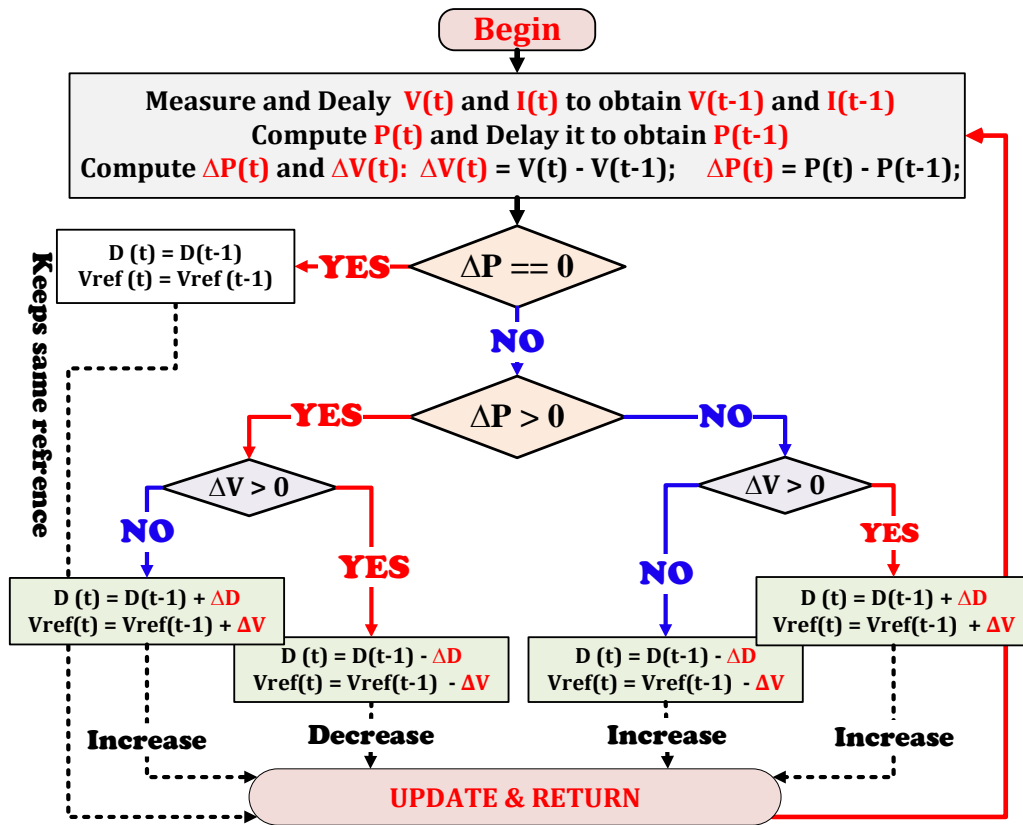


Figure II.8: P&O-based MPPT technique.

### II.2.3.B Incremental Conductance (INC)

Figure II.9 illustrates the flowchart depicting the implementation of the INC approach for MPP tracking. The incremental conductance (INC) technique represents an enhanced version of the P&O method and is capable of efficiently tracking the maximum power point (MPP) even in rapidly changing environmental conditions [54, 59]. This technique relies on computing the slope of the VP curve, denoted as "P". Since instantaneous power is determined by multiplying instantaneous voltage

and current ( $V_{PV} \cdot I_{PV}$ ), the INC approach utilizes the comparison between incremental conductance and instantaneous conductance to track the MPP accurately.

The VP curve slope can be computed as noted in equation II.6:

$$\frac{\partial p}{\partial v} = \frac{\partial(v \cdot i)}{\partial v} = i + v * (\partial i / \partial v) \tag{II.6}$$

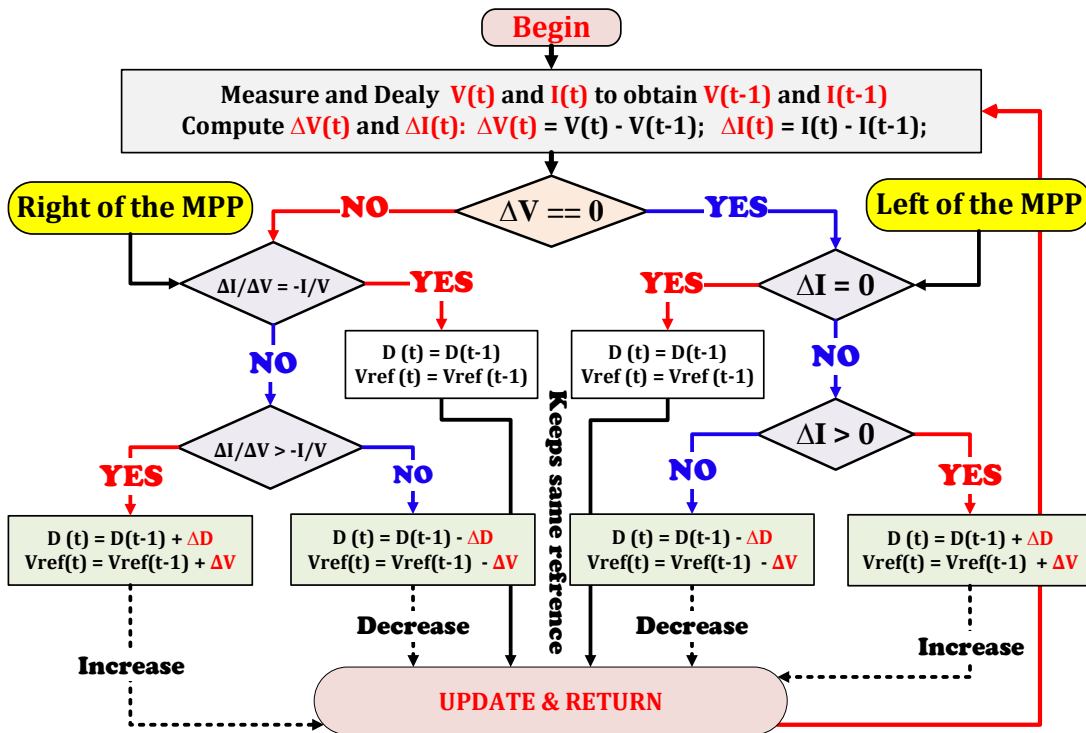


Figure II.9:INC-based MPPT technique.

The following conditions can be drawn from Equation (II.6):

- ✓ If  $\partial i / \partial v = -v/i$   $\partial p / \partial v = 0$  .....On MPP.
- ✓ If  $\partial i / \partial v < -v/i$   $\partial p / \partial v < 0$  .....On the right side of MPP.
- ✓ If  $\partial i / \partial v > -v/i$   $\partial p / \partial v > 0$  .....On the left side of MPP.

While the INC technique can effectively eliminate oscillations in steady-state conditions, it behaves similarly to the P&O method during transitional states.

### II.2.4 FPPT control methods

FPPT is a special method that uses a single or double-stage control system to regulate the voltage and current of the PV system during special scenarios different from regular MPPT circumstances. FPPT uses a feedback loop to adjust the voltage and current based on the difference

between the desired and actual values, which improves the efficiency and reliability of the system [60], as seen in Figure II.10.

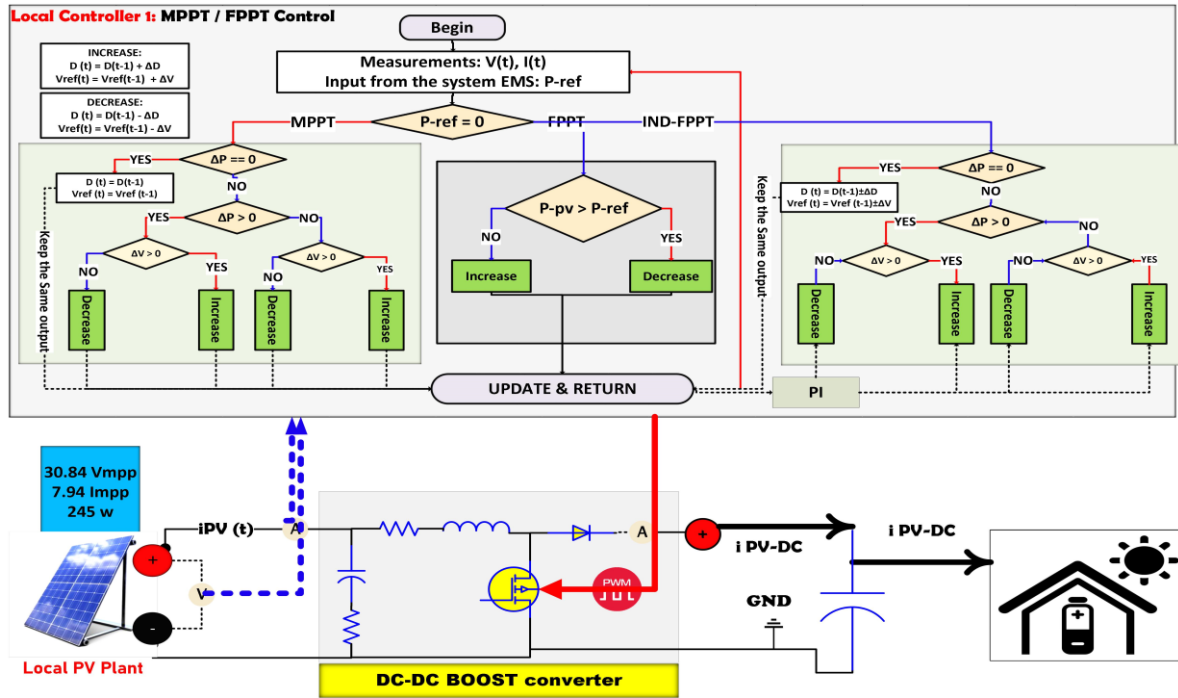
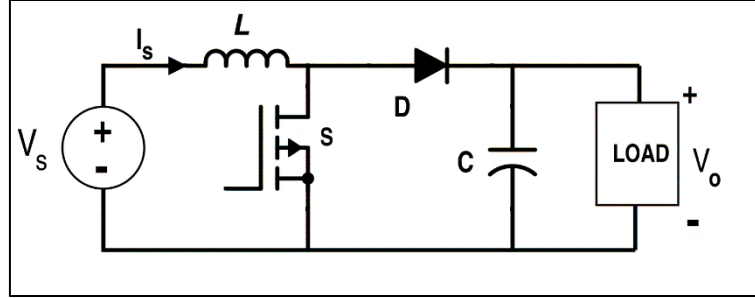


Figure II.10: Principles of PV control-based FPPT technique.

### II.3 Modeling of the DC-DC Boost Converter

A DC-DC converter is an electrical device that transforms direct current (DC) from one voltage level to another. It is sometimes referred to as a voltage converter or a power converter. It is frequently used to regulate and manage the voltage levels in power systems across a variety of applications. Much electrical equipment requires DC-DC converters, particularly when the power supply or load needs a different voltage than what is available. Depending on the design and application, they can boost or buck the voltage, reverse the polarity, or conduct voltage-level transformations [61].

In our study, we have adopted a DC-DC Boost converter as seen in Figure II-11 shows. The focus of our research is on step-up power conversion. The selection of a DC-DC boost converter allows us to investigate and analyze the specific characteristics and challenges associated with boosting the voltage levels in power conversion applications [62].



**Figure II.11:** DC-DC Boost converter circuit [63].

The equivalent circuit during the switch **ON** and **OFF** conditions of switch **S** is shown in Figure **II.12** and Figure **II.13** respectively.

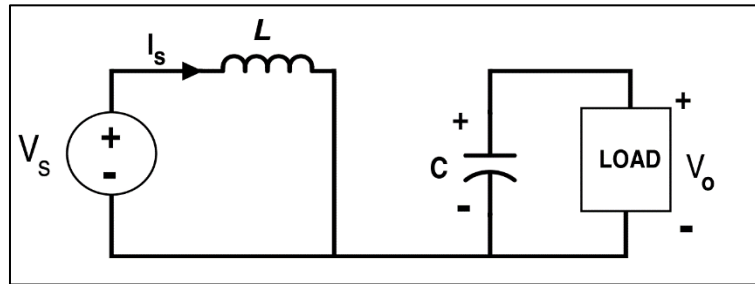


**Figure II. 12:** Boost converter circuit when switch S is **ON**.

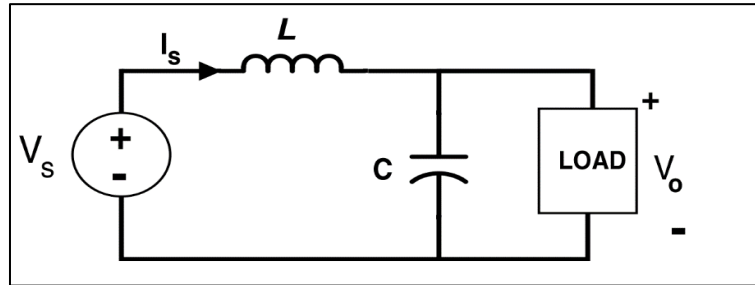


**Figure II. 13:** Boost converter circuit when switch S is **OFF**.

The duty cycle **D** of the switching device **S** is defined as follows:

$$D = 1 - \frac{V_s}{V_o} \tag{II.7}$$

When S is **ON** ‘close’, the inductor current and voltages are expressed by equation **II.8**:

$$\begin{cases} V_L = V_s = L \frac{di_L}{dt} \\ \frac{di_L}{dt} = \frac{V_s}{L} \end{cases} \tag{II.8}$$

The current ripple in the inductance is defined by equation **II.9**:

$$\begin{cases} \frac{di_L}{dt} = \frac{\Delta i_L}{\Delta t} = \frac{\Delta i_L}{DT} = \frac{V_s}{L} \\ (\Delta i_L)_{\text{closed}} = \left(\frac{V_s}{L}\right) \cdot DT \end{cases} \tag{II.9}$$



Instead, when **S** is **OFF** ‘Open’, the inductor current/voltages are stated in equation **II.10**:

$$\begin{cases} V_L = V_S - V_O = L \frac{di_L}{dt} \\ \frac{di_L}{dt} = \frac{V_S - V_O}{L} \end{cases} \quad (\text{II.10})$$

The current ripple (change) in the inductance is defined by equation **II.11**. The current rate of change is constant, so the current change linearly.

$$\begin{cases} \frac{di_L}{dt} = \frac{\Delta i_L}{\Delta t} = \frac{\Delta i_L}{(1-D)T} = \frac{V_S - V_O}{L} \\ (\Delta i_L)_{\text{open}} = \left( \frac{V_S - V_O}{L} \right) \cdot (1 - D)T \end{cases} \quad (\text{II.11})$$

Waveforms of the voltage and current during the one-cycle period are shown in Figure **II-14**.

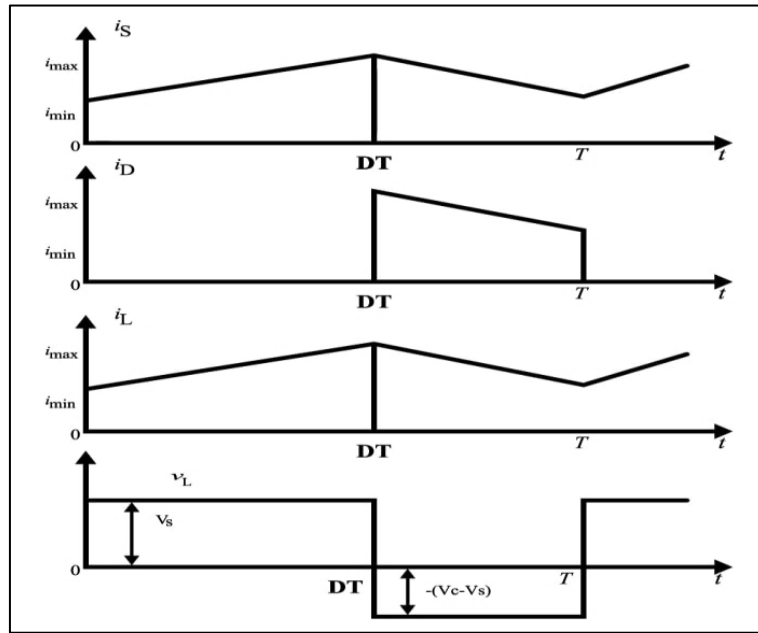


**Figure II. 14:** Supply current, diode current, inductor current, and inductor voltage.

According to the inductor **V-S** balance, steady-state the net change in inductor current over one period is zero using Equation (**II.8**).

$$\begin{cases} (\Delta i_L)_{\text{closed}} + (\Delta i_L)_{\text{open}} = 0 \\ \left( \frac{V_S}{L} \right) DT + \left( \frac{V_S - V_O}{L} \right) (1 - D)T = 0 \\ V_O = \frac{V_S}{1-D} \end{cases} \quad (\text{II-12})$$

The average current in the inductor is determined by recognizing that the average power supplied by the source must be the same as the average power absorbed by the load resistor.

$$\begin{cases} P_{out} = \frac{V_o^2}{R} = V_o \cdot I_o \\ P_{in} = V_o \cdot I_o \end{cases} \quad (II.13)$$

Using Equation (II.12):

$$I_L = \frac{V_s}{(1-D)^2 R} = \frac{V_o^2}{V_s R} = \frac{V_o I_o}{V_s} \quad (II.14)$$

The maximum and minimum inductor current using average and change in current is defined in Equation (II.9). From a design perspective, it is useful to express ‘L’ in terms of desired  $\Delta i_L$  using Equation (II.9).

$$\begin{cases} I_{max} = I_L + \frac{\Delta i_L}{2} = \frac{V_s}{(1-D)^2 R} + \frac{V_s D T}{2L} \\ I_{min} = I_L - \frac{\Delta i_L}{2} = \frac{V_s}{(1-D)^2 R} - \frac{V_s D T}{2L} \end{cases} \quad (II.15)$$

$$\begin{cases} (Lf)_{min} = \frac{D(1-D)^2}{2} \\ L_{min} = \frac{D(1-D)^2}{2f} \end{cases} \quad (II.16)$$

$$L = \frac{V_s D}{\Delta i_L f} \quad (II.17)$$

The output voltage ripple is expressed in equation II.18.

$$\begin{cases} Q = CV_o \rightarrow \Delta Q = C\Delta V_o \rightarrow \Delta V_o = \frac{\Delta Q}{C} \\ \frac{\Delta V_o}{V_o} = \frac{D}{R.C.f} \\ C = \frac{D}{R(\Delta V_o/V_o)f} \end{cases} \quad (II.18)$$

### II.3.1 The protection system of DC-DC Converters

Fuses are protective devices designed to interrupt the flow of current in a circuit when there is an excessive current or a fault condition as shown in Figure II.15. They help safeguard the converter and connected devices from damage caused by overcurrent or short circuits [64].

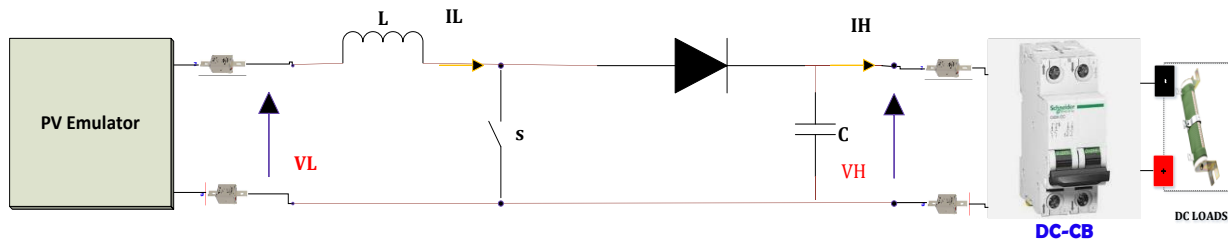


Figure II. 15: DC/DC Boost circuit using protective devices (Fuse and Circuit Breaker).

When sizing a fuse for a DC-DC boost converter, it is important to consider the maximum current and voltage ratings as well as the characteristics of the load it powers. While there are no standard rules for fuse sizing in boost converters, some general practices can be followed.

**Current Rating ( $I_{FUSE}$ ):** The fuse should have a current rating higher than the maximum expected current of the boost converter. One guideline is to select a fuse with a rating of approximately 1.56 times the short-circuit current ( $I_{SC}$ ) of the converter [65]. This ensures that the fuse can handle the current without blowing during normal operation.

$$I_{FUSE} \geq 1.56 * I_{SC} \quad (II.19)$$

**Voltage Rating ( $V_{FUSE}$ ):** The fuse should have a voltage rating higher than the maximum output voltage of the boost converter. One approach is to choose a fuse with a rating of around 1.2 times the open-circuit voltage ( $V_{OC}$ ) of the converter [65]. This provides a safety margin to handle voltage spikes or transients.

$$V_{FUSE} \geq 1.2 * V_{OC} \quad (II.20)$$

The results of our calculations are documented in the corresponding Table II-2.

**Table II. 2:** Sizing results: DC fuse.

	<b>BOOST-Input-</b>	<b>BOOST-Output-</b>	<b>Equation</b>
<b><math>I_{FUSE}</math> (A)</b>	13.15	7.80	For Equation (II.20)
<b><math>V_{FUSE}</math> (V)</b>	44.50	60	For Equation (II.21)

### II.3.2 Sizing of the standalone PV-System

To size a standalone PV system, several factors need to be taken into account. One important consideration is estimating the energy demand or load requirements of the system. This involves conducting an energy audit to determine the power requirements and load profile. By accumulating all the loads supplied by the PV system, you can establish the design load and energy requirements [66]. This title discusses specifics for sizing a DC/DC converter, current/voltage sensors, and gate drive components to system requirements and desired performance characteristics.

#### II.3.2.A Sizing of the DC Load

During our study, we conducted load variations around the  $R_{mpp}$  for the selected solar panel. We systematically adjusted the load in proximity to the  $R_{mpp}$  value to investigate its impact on the performance and characteristics of the solar panel adopted in our study.

### II.3.2.B Sizing of the PV source

The PV model for simulation tests has been selected regarding the available PV panels in the laboratory and the PV emulator. So, for experimental validation, these points have been considered.

Besides, the studied system aims to assess and evaluate the performance of the PV control using low power/voltage /current scales at the laboratory.

### II.3.2.C Sizing the DC/DC converters

We have employed two approaches in our sizing process to identify appropriate DC-DC converter components for our system, outlined as follows.

#### ✚ Power Stage Designer 5 (Texas instruments)

Power Stage Designer, developed by Texas Instruments (TI), is a Java-based software tool. It can calculate voltages and currents for 21 topologies as seen in Figure (II.16), assisting engineers in optimizing their power supply designs. It can be used to define scaling parameters for a DC-DC converter Boost topology [67].

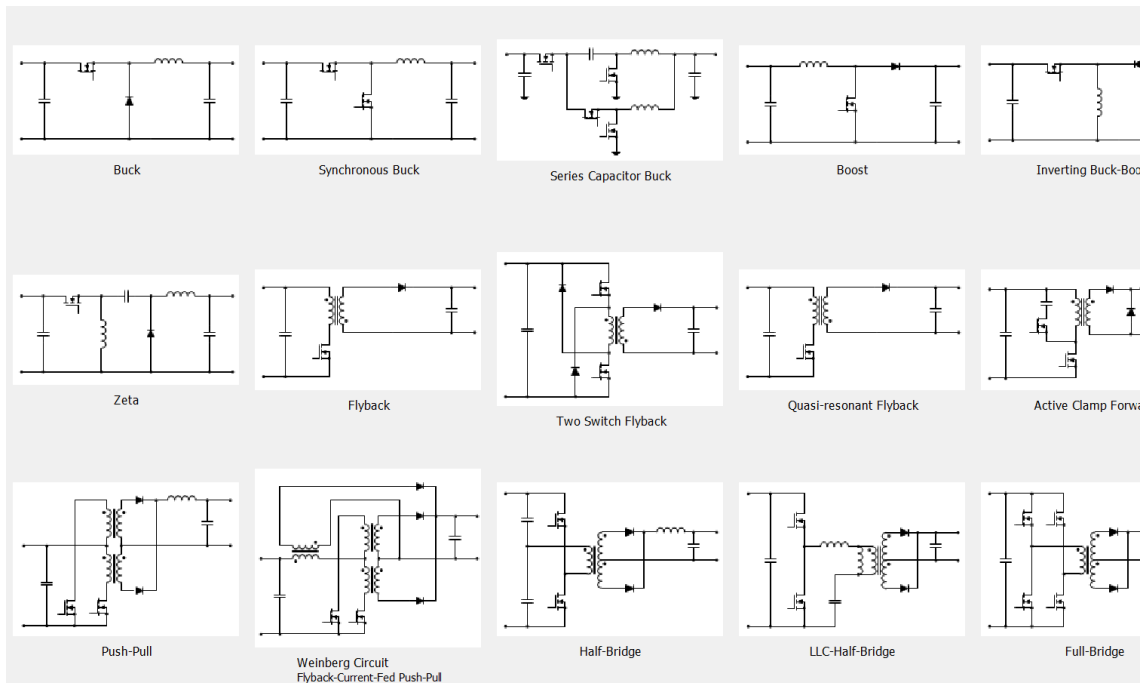


**Figure II. 16:** Main Window of Power Stage Designer Displaying Topologies.

To resize a DC-DC converter boost structure using Power Stage Designer, you'll typically need the following parameters:

- **Voltage Range ( $V_{IN(min)}$  &  $V_{IN(max)}$ ):** minimum and maximum input voltages of the converter.

- **Nominal Output Voltage ( $V_{Out}$ ):** The desired output voltage of the converter.
- **Maximum Output Current ( $I_{Out(max)}$ ):** maximum load current the converter needs to provide.
- **Integrated Circuit (IC) Selection:** the choice of IC to build the boost converter [68].

By providing these parameters as user inputs, Power Stage Designer can perform calculations to determine appropriate values for components such as inductors, capacitors, and resistors in a boost converter circuit. The software tool helps in sizing components for optimal performance and efficiency of the DC-DC converter topology [69]. We chose to use a DC-DC boost converter for Texas Instruments, as our primary focus is on ( step-up). For Sizing the converter, it is necessary to input the information mentioned above. It will be recognized in Table II.3.

**Table II. 3:**DC-DC Boost Converter Design Parameters.

Parameter	Value	Parameter	Value
Minimum input voltage	28.76	Switching frequency	20 kHz
Maximum input voltage	37.08V	Diode voltage drop	0.7 volts
Output voltage	50V	Inductor current ripple	27%~30%
Output current	5A	Inductor $L_{MIN}$	285 $\mu$ H ~257 $\mu$ H

Figures (II.17) and Figure (II.18) are presented to illustrate the results obtained after inputting the design parameters of the DC-DC Boost converter into Texas devices. These results provide valuable insights into the performance and behavior of the converter.

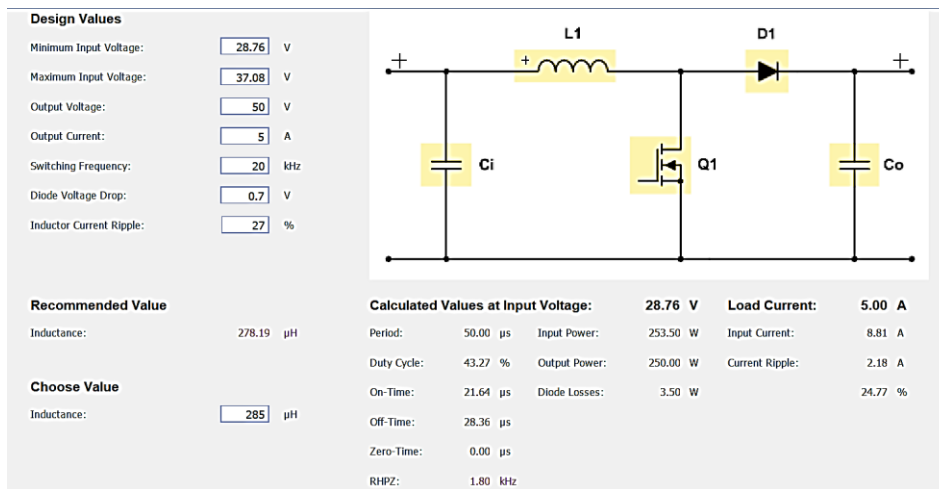


**Figure II. 17:** Topology Window for Boost ‘Inductor current ripple:  $\Delta_{iL}=27\%$ ’

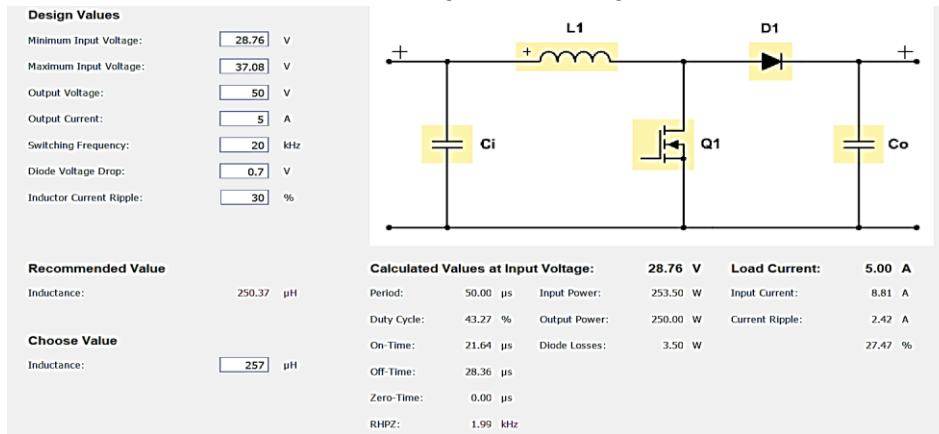


Figure II.18: Topology Window for Boost ‘Inductor current ripple:  $\Delta_iL=30\%$ ’



-a-



-b-



-c-



**Figure II.19:** Sizing results waveforms of the current and voltages: (a) for Inductor Input voltage=28.76 V / Load current = 0.05 (A), (b) for Inductor Input voltage=37.08 V / Load current = 5 (A), (c) for Mosfet Input voltage=28.76 V / Load current = 0.05 (A), and: (d) for Mosfet Input voltage=37.08 V / Load current = 5 (A).

Figure (II-19) displays the variations in input voltage and load current for the DC-DC Boost converter. In normal mode, it should maintain the shape (b) and (d). In position (a) and (c) limits we should not reach them. An observation is that when the Boost operates in a vacuum (a) and (c), the current curve drops to zero. From this, we can conclude that operating the Boost in a vacuum is not recommended for two reasons.

The first reason is related to the operating mode of the chopper, which has two modes: continuous conduction mode and discontinuous conduction mode. In this case, the Boost operates in DCM, causing the current to drop to zero and then rise again. This leads to a loss in efficiency.

The second reason is associated with the presence of an output capacitor in the Boost. While the capacitor is charging, the current continues to flow, resulting in an increase in voltage that exceeds the specified limit. This poses a danger as exceeding the capacitor's voltage rating can lead to undesirable consequences. Considering these factors, it is evident that operating the Boost in a vacuum is not advisable.

#### **Open-access (phone application) DC/DC Converter Designer**

The "DC-DC Converters Design Demo" app available on the Google Play Store offers design capabilities for the buck, boost as shown in Figure (II-12), and buck-boost converters. Users can design these converters by inputting the necessary passive components and specifying the desired duty cycle as a percentage. Furthermore, the app includes a dedicated help section to provide users with additional instructions and guidance [70].

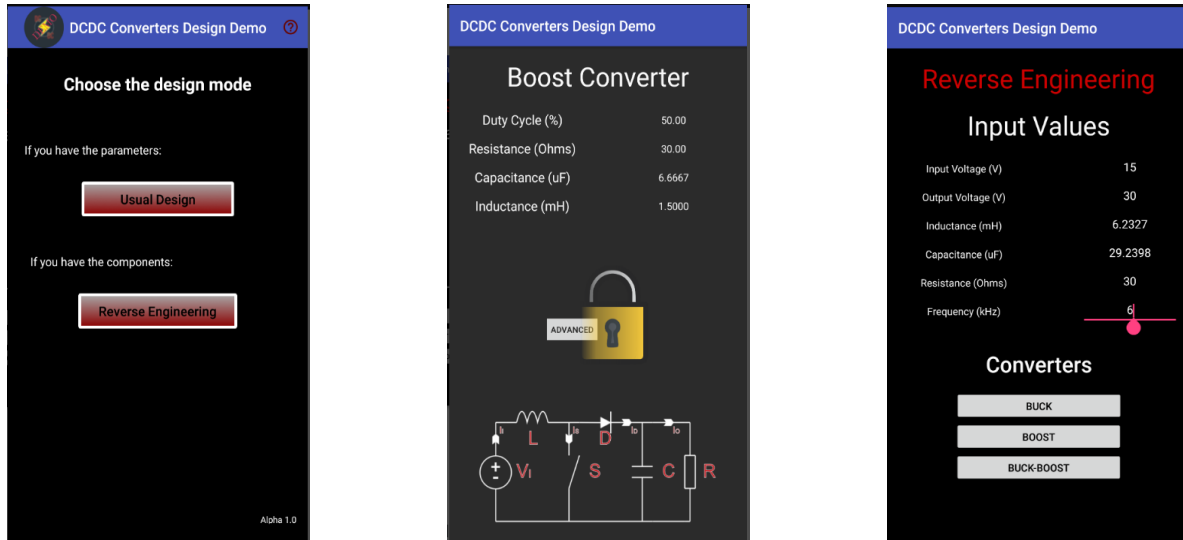


**Figure II. 17:** Topology Window for the DC-DC Converters Design Demo Application.

We used DC-DC converter experimental application design to calculate component values for conversion in DC-DC Circuit. The settings for the specified sizing have been inputted and recorded in Table II.4, besides the results of our calculations.

**Table II. 4:**DC-DC Boost Converter Sizing data and results.

Inputs				Output results	
Parameter	Value	Parameter	Value	Parameter	Value
$V_{in}$	28.76V	Efficiency	95%	$D$	44.72%
$V_{out}$	50V	$\Delta_v$	5%	$R_{load}$	10.20 $\Omega$
$P$	245W	$\Delta_{il}$	27%~30%	$C$	44 $\mu f$
$f$	20 kHz			$L$	268.69 $\mu H$ ~241 $\mu H$

### II.3.2.D Sizing the Current/Voltage Sensors

when sizing current and voltage sensors for a boost DC-DC converter, it is important to consider factors such as the desired measurement accuracy, the maximum expected current and voltage levels, and the power dissipation in the sensors. The selection of appropriate sensors depends on the specific requirements of the converter and the application [71].

#### ✚ Sizing the Voltage Sensor LEM-LV25

The LEM LV 25-P is a voltage transducer designed for voltage measurements. It operates by passing a current proportional to the measured voltage through an external resistor as Figure (II-21) shows, which is selected and installed by the user in series with the primary circuit of the transducer



[72]. Some additional technical information can be found in the datasheets [73](Appendice II-1) provided by LEM-LV25. For sizing LEM-LV, equation II.21 is used.

$$\begin{cases} R_1 = \frac{V_{FUSE}}{I_{PN}} \\ R_M = \frac{V_{out\ D-SPACE}}{I_S} \end{cases} \quad (II.21)$$

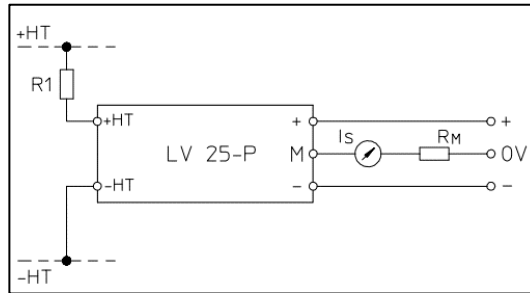


Figure II. 18: The LEM LV 25-P voltage transducer schematic[73].

The properties and settings for the LEM-LV25 are presented in the corresponding Table II-6.

Table II. 5: Specifications of LEM-LV25.

Voltage (V)	Current(mA)	$R_{M\ min}(\Omega)$	$R_{M\ max}(\Omega)$	Parameter	value
<b>±12</b>	±10	30	190	$I_{PN}$	[10 - 14] (Ma)
	±14	30	100	$I_S$	25 (mA)
<b>±15</b>	±10	100	350	$V_{OUT-DSPACE}$	5 (V)
	±14	100	190		

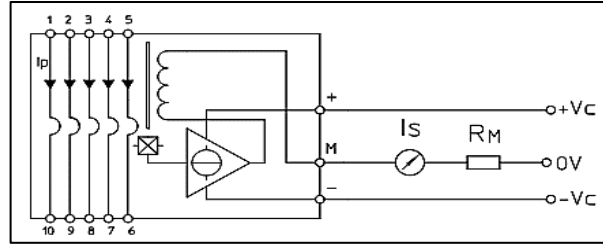
Upon seizing the LEM-LV25 from equations (II.21.a) and (II.21.b), the obtained results are presented in the accompanying Table II-7.

Table II. 6:Sizing results of the LV Voltage sensor.

	$R_1(\Omega)$	$R_M(\Omega)$	Terms ( $R_M$ )
<b>Boost input</b>	4450	200	[±15V - 10mA]
<b>Boost output</b>	6000	200	=
	From equation (II.21.a)	From equation (II.21.b)	[100Ω;350Ω]

### ✚ Sizing the Current Sensor LEM-LA25

The LEM LA25NP is a closed-loop Hall Effect current transducer designed for measuring DC as Figure II.22 shows. The datasheet [74] in (Appendice II-2) for the LA25-NP provides additional technical information. The calculation of  $R_M$  follows the same Equation (II.21.b).



**Figure II. 19:** The LEM-LA25 voltage transducer schematic[74].

The characteristics and parameters of the LEM-LA25 are shown in Tables (II.8) and (II.9).

**Table II. 7:** Specifications of LEM-LA25-NP.

Measuring resistance		$T_A = 70^\circ C$		$T_A = 85^\circ C$	
		$R_{M \min}(\Omega)$	$R_{M \max}(\Omega)$	$R_{M \min}(\Omega)$	$R_{M \max}(\Omega)$
<b>Witch <math>\pm 15 V</math></b>	$\pm 25 A$	100	320	100	315
	$\pm 36 A$	100	190	100	185

**Table II. 8:** Primary Turns, Nominal Output Current, and Recommended Connections.

Number of primary turns	Primary current		Nominal output current $I_S$ [mA]	Recommended connections
	Nominal $I_{PN}$ [A]	Maximum $I_{PN}$ [A]		
1	25	36	25	
2	12	18	24	
3	8	12	24	
4	6	9	24	
5	5	7	25	

The results of our calculations are documented in Table II.10.

**Table II. 9:**Sizing LA sensor.

	$R_M(\Omega)$ equation4	Terms ( $R_M$ )	$I_{FUSE}$ [A]	$I_{PN}$ [A]	Recommended connections
<b>Boost input</b>	200	$T_A = 70^\circ C ; \pm 15V$	13.15	12	
<b>Boost output</b>	200	$R = [100 ; 320]$	7.64	12	

### II.3.2.D Sizing of the Gate-drive (GD)

When sizing the gate drive for a DC-DC boost converter, several factors need to be considered. These include the desired switching frequency, the maximum current and voltage ratings of the gate driver, the gate capacitance of the power MOSFET, and the required drive strength. It is important to ensure that the gate driver is capable of providing sufficient voltage and current to drive the power MOSFET effectively. Also, considerations should be made for gate drive losses and heat dissipation to ensure the overall efficiency and reliability of the converter [75].

#### ✚ Simple gate-drive topology (Transistor 2N2222)

This topology Figure II.17 offers a simple GD circuit with no isolation and less secure control. This topology requires a supply  $V_{CC}$  adequate to the user switching device 15-30 (V)

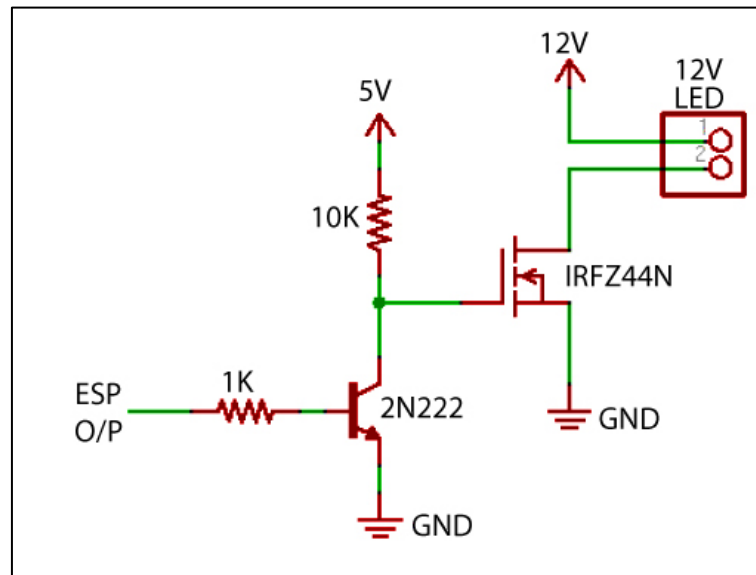
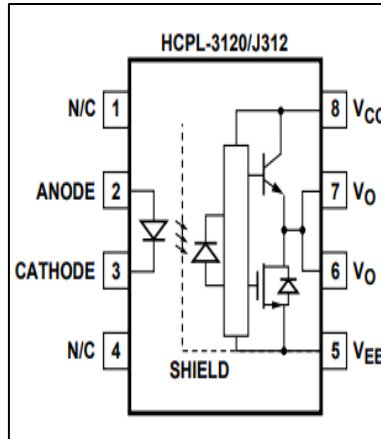


Figure II. 20: The LEM-LA25 voltage transducer schematic[74].

#### ✚ Simple gate drive topology (HCPL-3120)

Simple gate drive topology (HCPL-3120): The HCPL-3120 is an optocoupler that consists of a GaAsP LED optically coupled to an integrated circuit with a power output stage. It is specifically designed for driving power IGBTs / MOSFETs used in motor control and inverter applications as Figure (II-23) shows [76].

$$R_g = \frac{V_{CC} - V_{EE} - V_{OL}}{I_{OL}} \quad (\text{II.22})$$



**Figure II. 21:** Circuit Diagram of the optocoupler HCPL-3120

The HCPL-3120 optocoupler offers galvanic isolation, meaning that the logic input side and the gate drive side are completely isolated from each other [76]. This isolation provides electrical separation, which can enhance safety and security in certain applications by preventing unwanted electrical connections or disturbances. The datasheet (Appendice **II-3**) of the HCPL-3120 provides additional technical information.

The parameters in Table (**II.11**) showcase the scaling achieved using the equation (**II.23**).

**Table II. 10:** Sizing of the Gate-Driver (HCPL-3120)

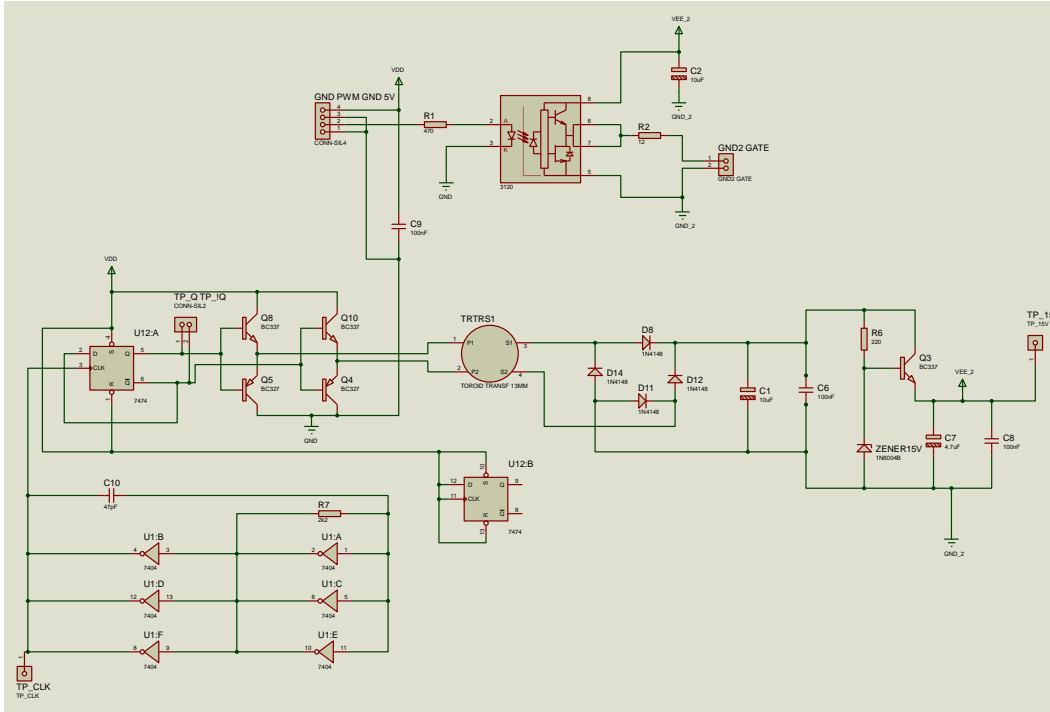
Parameter	Symbols	Values	Units
Power supply voltage	$V_{CC}$	15	V
Low-Level Output voltage	$V_{OL}$	2.2	V
Low-Level Output Current	$I_{OL}$	2	A
Gate Resistor - Equation II.22	$R_g$	6.4	$\Omega$

#### **Advanced gate drive topology (HCPL-3120).**

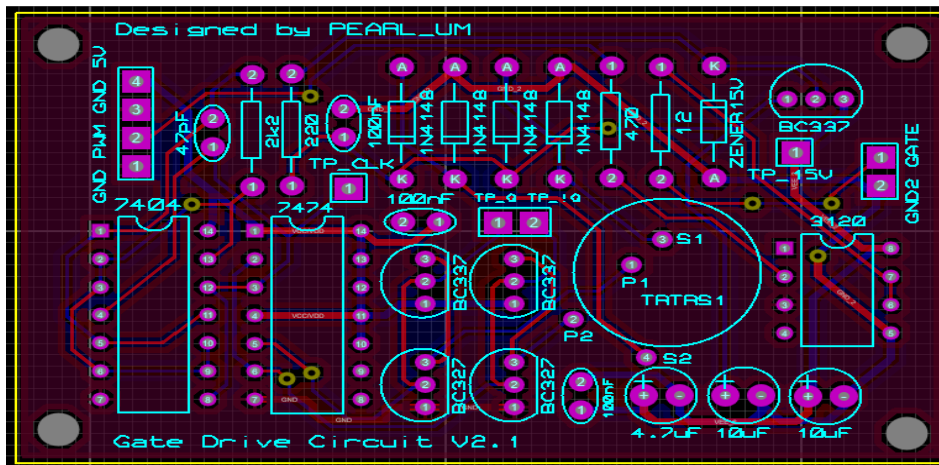
In this work, we used Proteus 8 Professional software to design an advanced gate drive topology (HCPL-3120). The design is illustrated in Figure **II.24**.

### **II.3.3 Description of realized acquisition boards**

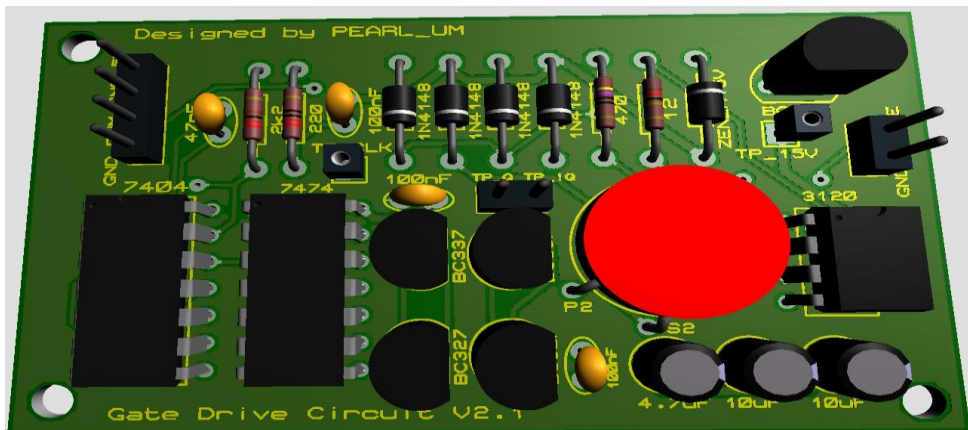
Designing and realizing a PCB board for real-time experimentations using Dspace acquisition boards can be a challenging process[77]. However, the following steps can help simplify the process and ensure a successful outcome.



-a-



-b-



-c-

Figure II. 22: Gate drive(HCPL-3120): a-Circuit Schematic PCB. b- PCB layout design diagram and c- 3D visualizer for HCPL-3120.

### II.3.3.A Start with a schematic capture

The first step is to create a schematic that defines the electrical level of the board's function and purpose. **In this work**, A chopper circuit with fusible protection was designed shown in Figure (II-26) to enable controlled power switching while ensuring safety and reliability.

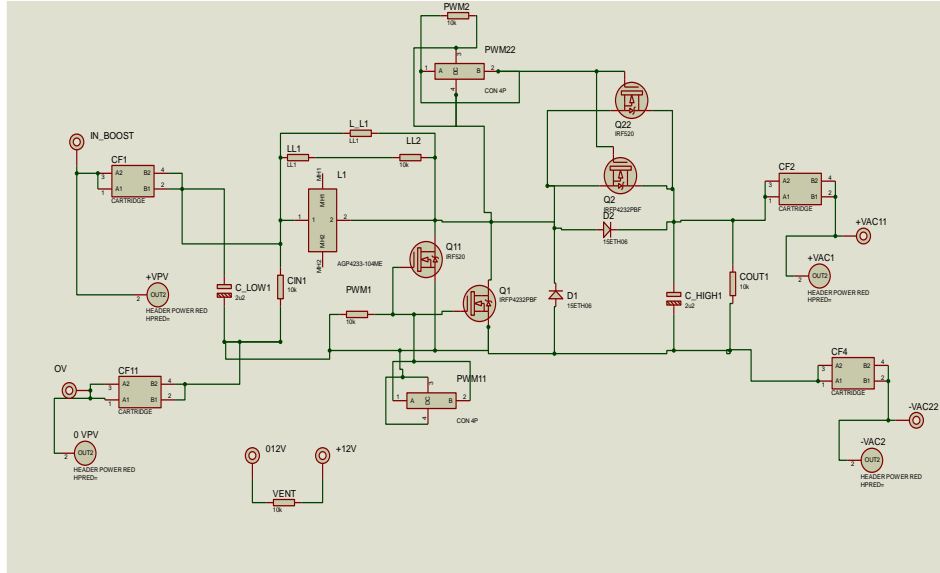


Figure II. 23: Chopper Circuit with Fusible Protection Schematic PCB.

### II.3.3.B Select a PCB layout tool

Use a PCB layout tool to create a blank PCB layout. There are various tools available, including ISIS Protuse, Altium Designer, and Eagle CAD, that can assist in PCB layout and design. **In this work**, We utilized *ISIS Proteus software* as our chosen tool for creating the PCB layout and design.

### II.3.3.C Design your PCB stackup

Your PCB stackup defines the layers, materials, and thickness of your board. It's essential to carefully consider the stackup based on the board's intended function and performance requirements.

**In this work**, Components in the diagram include:

- **MOSFET** ‘metal-oxide-semiconductor field-effect transistor’: a chopper switch controls the flow of current through the circuit by turning it on and off at a high frequency.
- **Hyperfast DIODE:** A hyperfast diode is a specialized diode that is designed to have fast switching characteristics and low reverse recovery time. used in chopper circuits to handle the current flow during switching transitions and to prevent voltage spikes or reverse currents.

- **Inductor:** an inductor is used to store and release energy in the form of a magnetic field. It helps smooth out the flow of current and control the rate of change of current in the circuit.
- **Capacitor:** a capacitor used for energy storage and filtering purposes. Helps maintain a constant voltage across a load by smoothing voltage ripples.
- **Fuse + Holders:** Fuses are protective devices that are used to interrupt the circuit in case of excessive current flow, preventing damage to the components. Fuse holders are the connectors or sockets that hold the fuses in place. They provide a convenient way to replace the fuse if it blows due to overcurrent conditions.
- **Power Connectors:** Power connectors are used to establish electrical connections between different parts of the circuit or to provide a means of connecting the chopper circuit to an external power source or load. These connectors are designed to handle high currents and ensure secure and reliable connections.

To account for situations where the values of certain components are unavailable, we have implemented a duplication strategy in the circuit. Thus, we have doubled the number of components. This redundancy ensures that if the value of a particular component is not known or obtainable, we have an alternative component in place as a solution. The PCB design is illustrated in Figure II.27.

#### II.3.3.D Add components to the board

Once you have the blank PCB layout, you can begin adding components to the board based on the schematic you created earlier. **In this work**, We have redesigned a fuse component and added it to the circuit. This modified fuse component serves as an addition to the existing circuit design.

#### II.3.3.E Route your traces

Routing refers to the process of creating electrical connections between the various components on your board. You will need to route your traces in a way that minimizes interference and maximizes performance. **In this work**, we did not rely on the features provided by Proteus ISIS for automatic linking. Instead, we opted for manual linking in our circuit design process.

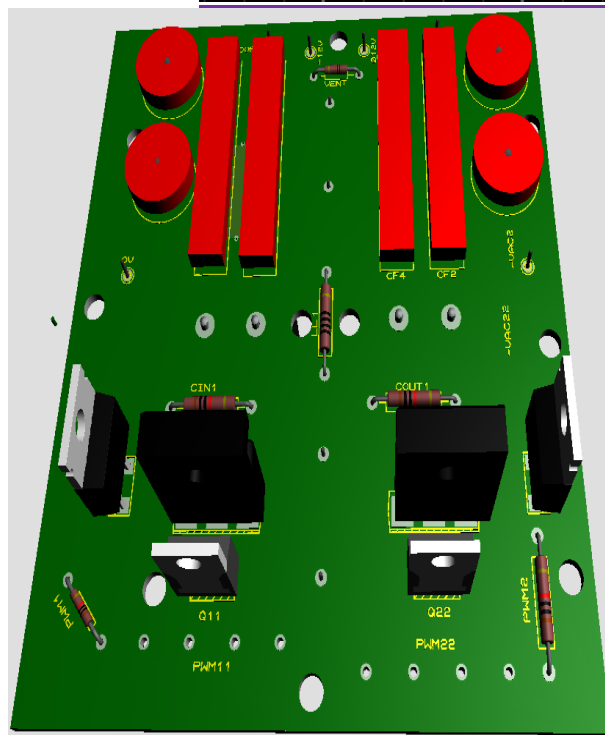
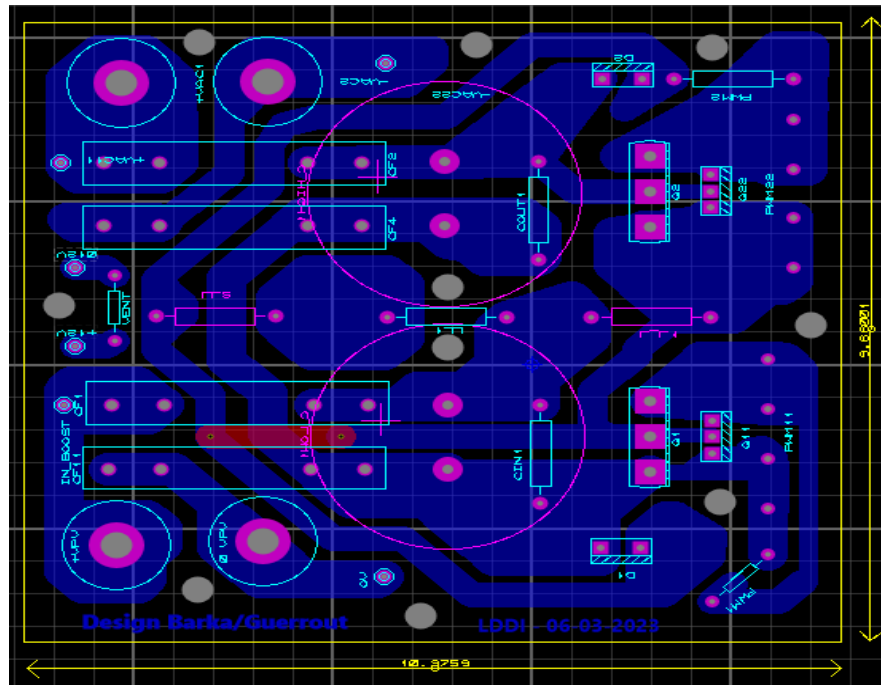


Figure II. 24:(a) PCB layout design diagram and (b) design 3D visualizer.

### II.3.3.F Perform design rule checks (DRC)

Use a DRC tool to check your design for any errors or rule violations. DRC tools can detect issues such as clearance violations and overlapping components. **In this work**, since we manually



routed our PCB, we utilized the DRC to check for any errors, rules, or route violations. This was done to ensure the connections between our components remained intact and free from any issues.

### II.3.3.F Generate Gerber file

Once you have completed your design, you will need to generate Gerber files. Gerber files contain the information needed to manufacture your board. **In this work**, We created a Gerber file but the print was traditional.

### II.3.3.G Fabricate your PCB

Once you have your Gerber files, you can send them to a PCB fabrication service to manufacture your board. **In this work**, Given in a table **II.12**.

**Table II. 11:** Steps for Manual PCB Fabrication Process.

Steps	Description
1	Print the PCB design onto paper using an inkjet printer
2	Transfer the PCB design onto a copper plate using an iron
3	Submerge the copper plate in acid for 120 minutes
4	Remove the copper plate from the acid and create the copper circuit
5	Drill holes for component connections in the copper circuit

### II.3.3.H Assemble your board

After fabrication, you can begin assembling your board by placing and soldering components in the correct locations. **In this work**, Once the copper is completed, we proceed to place measured components onto the circuit and perform soldering on the connection holes for secure connections.

### II.3.3.K Test and iterate

After assembly, you will need to test your board to ensure it performs as expected. If there are any issues, you will need to iterate and make modifications to your design. **In this work**, After successfully placing the components and soldering them onto the circuit, the next step is to proceed with testing the board's performance to ensure its functionality and proper operation.

## II.3.4 Description of the experimental setup

The experimental setup of a PV system often involves the use of various components such as a PV emulator, DC/DC converters, Current/Voltage sensors, Gate-drives, and DC loads:

The PV emulator is responsible for shaping the output I-V curves of the PV panel by taking input from a DC input source and converting it to a duty cycle command, which is amplified by the gate driver and used to drive the power transistor.

The sensors in the setup measure the output voltage and current of the PV system, which are used in the calculation of the duty cycle command. The closed-loop control system of a PV system typically includes voltage and current sensors to measure the system's parameters, a controller that compares the measured parameters to the desired values, and an actuator that adjusts the system's output to maintain the desired values.

The DC/DC converters are used for stepping up or down the voltage to match the voltage of the DC loads in the system.

Overall, the experimental setup of a PV system involves the use of several components that work together to ensure efficient energy conversion and utilization.

#### **II.3.4.A Objectives of the Experimental Validation**

Our goal is to validate a prototype that incorporates a PV emulator with multiple commands for Maximum PowerPoint Tracking (MPPT) under various weather conditions and load changes. The prototype includes essential components such as current and voltage sensors, as well as gate drives, to facilitate accurate testing and evaluation.

#### **II.3.4.B Description of PV-system structure**

Here, in our system structure, we have a PV emulator integrated with a boost converter DC-DC and connected to a load. To optimize the power extraction from the PV emulator, we employed two MPPT techniques, namely Perturb and Observe (P&O) and Incremental Conductance. These techniques enable efficient tracking of the maximum power point under varying environmental conditions, ensuring improved energy conversion.

#### **II.3.4.C Description of the implementation procedure**

In our system implementation, we opted for a hardware-based approach using a Digital Signal Processor (DSP). With the DSP, we were able to effectively control and manipulate the system parameters, enabling precise and real-time operations. This hardware implementation allowed us to achieve accurate and efficient performance in our system.

#### **II.3.4.D Description of the experimental methodology**

In this methodology, we first set up a boost converter DC-DC system with a solar panel, then transition to sensor(voltage/current) and DSP for control and data processing, and finally integrate Gate-Drives to regulate power flow while collecting data for analysis and evaluation.

### II.3.5 Selection of acquisition components

When selecting acquisition components for your experiment, it is important to consider the specific requirements of your application and the compatibility of the components with the used hardware and software.

#### II.3.5.A DSpace 1104

Dspace is a popular tool for real-time experimentation and control system development [78]. Here are some steps to consider when selecting the acquisition components using DSpace:

- 1) Identify the required signal conditioning and input/output (I/O) interface for your experiment.
- 2) Determine the sampling rate and bit resolution needed for your experiment.
- 3) Select the appropriate DSpace hardware based on the required I/O interface and sampling rate. DSpace offers different hardware options such as the Micro-LabBox and SCALEXIO LabBox.
- 4) Once you have selected the appropriate DSPACE hardware, choose the compatible I/O boards and signal conditioning modules for your experiment.
- 5) Use the DSpace Configuration-Desk software to configure and test your setup. Additionally, Simulink and MATLAB can be used to develop and test control models with DSpace [79].

#### II.3.5.B MicroLabBox

A development platform with high computing power and comprehensive functionalities. It offers more than 100 channels of high-performance I/O with easy access via an integrated connector panel and dedicated electric motor control features and interfaces for Ethernet and CAN buses [80].

To select acquisition components using MicroLabBox, it is important to consider the specific application requirements and select the appropriate I/O modules. The MicroLabBox can support various types of I/O, including analog input and output, digital input and output, PWM output, and encoder input. In addition, the MicroLabBox supports signal conditioning modules to interface with different sensors and actuators.

One possible approach for selecting the appropriate acquisition components using MicroLabBox is to consult the technical documentation provided by dSPACE, which includes datasheets, user guides, and technical reference manuals. In addition, there are several online forums and tutorials available that can guide how to use MicroLabBox with MATLAB and Simulink [79].

It is worth noting that there is an ongoing debate on the benefits of using MicroLabBox versus other DSpace products such as the DS1104, which also offers similar functionality. Some researchers argue that the MicroLabBox is more user-friendly and offers more I/O channels, while others argue that the DS1104 is more cost-effective and offers better real-time performance [81].

### **II.3.5.C DSP-TMS 28379D**

A 32-bit microcontroller from Texas Instruments that can be used in a variety of applications including motor control, power electronics, and industrial automation. To select the appropriate acquisition components for a project using this microcontroller, several factors need to be considered such as the type of signal being acquired, the required accuracy and resolution, and the available budget [82].

One possible approach to selecting acquisition components is to refer to the datasheet and technical reference manual of the **DSP-TMS 28379D**, which provide information on the features and capabilities of the microcontroller [83].

It is worth noting that Texas Instruments also offers development platforms and tools such as the **TMDXIDDK379D** and **Code Composer Studio** that can facilitate the selection and integration of acquisition components for projects using the DSP-TMS 28379D microcontroller [80].

## **II.4 Conclusion**

In conclusion, this chapter focused on the modeling and design of the PV-conversion chain in standalone PV systems. It highlighted the importance of accurately modeling the PV source and understanding PV curves in the PV emulator for closed-loop control. The chapter discussed MPPT control processes, and FPPT algorithms, and their advantages and limitations. The modeling of the DC-DC converter and its impact on system efficiency was explored. Sizing considerations for the DC load and various components were discussed, along with available tools for accurate sizing. The chapter concluded with a description of the experimental setup and validation objectives. Overall, the chapter provides valuable insights for optimizing system performance and reliability in standalone PV systems.



# **Chapter 3**

## **Simulation results and discussion**

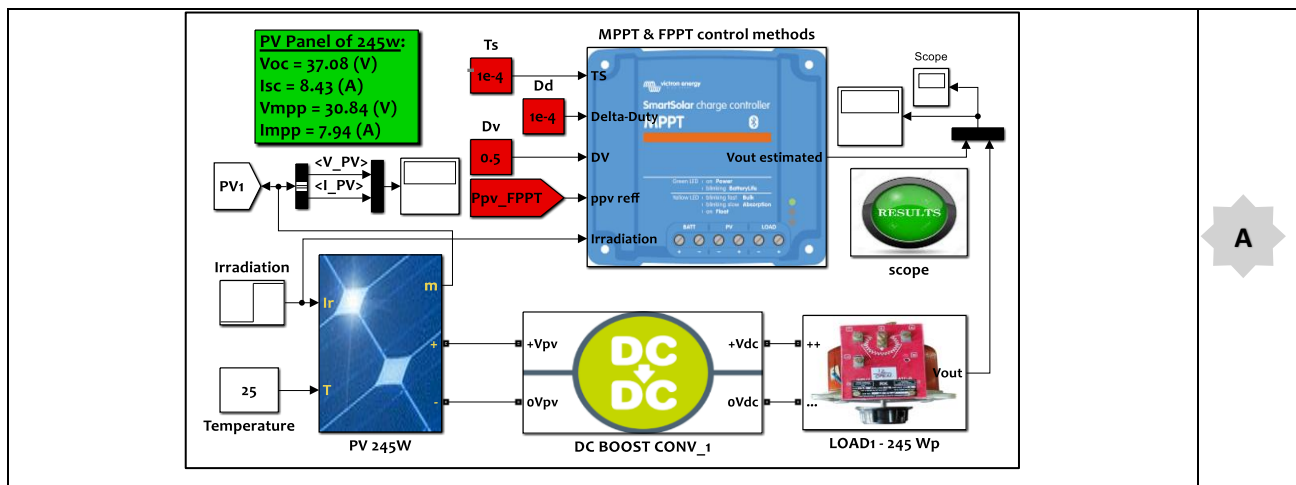
### III.1 Introduction

Chapter 3 of this thesis focuses on the simulation results and analysis of the standalone PV system under study. This chapter aims to investigate the various factors and parameters that impact the performance and behavior of the PV system. Through simulation studies, we will identify and analyze the PV diagram, which provides valuable insights into the system's characteristics and operation. Additionally, we will examine the effects of variable weather conditions, irradiation, and temperature, on the PV system. The impact of variable load demand, MPPT control time, duty cycle variation, and different PV control methods will also be explored. By studying and understanding these factors, we can gain a comprehensive understanding of the system's behavior and optimize its performance.

### III.2 Simulation results of the Standalone PV system- under study

To verify the performance of the proposed MPPT (Maximum Power Point Tracking) and FPPT (Fixed Power Point Tracking) algorithms in an independent PV system, the simulation of the PV system in Figure III.1 is developed in MATLAB/Simulink software. The different parts of the studied system are presented and described separately in Figure III.1.

The whole system structure is shown in Figure III.1.A, the DC-DC Boost circuit is displayed in Figure III.1.B, the variable DC Load with its control system is viewed in Figure III.1.C, and Figure III.1.D illustrates the direct P&O-MPPT control schema.



A

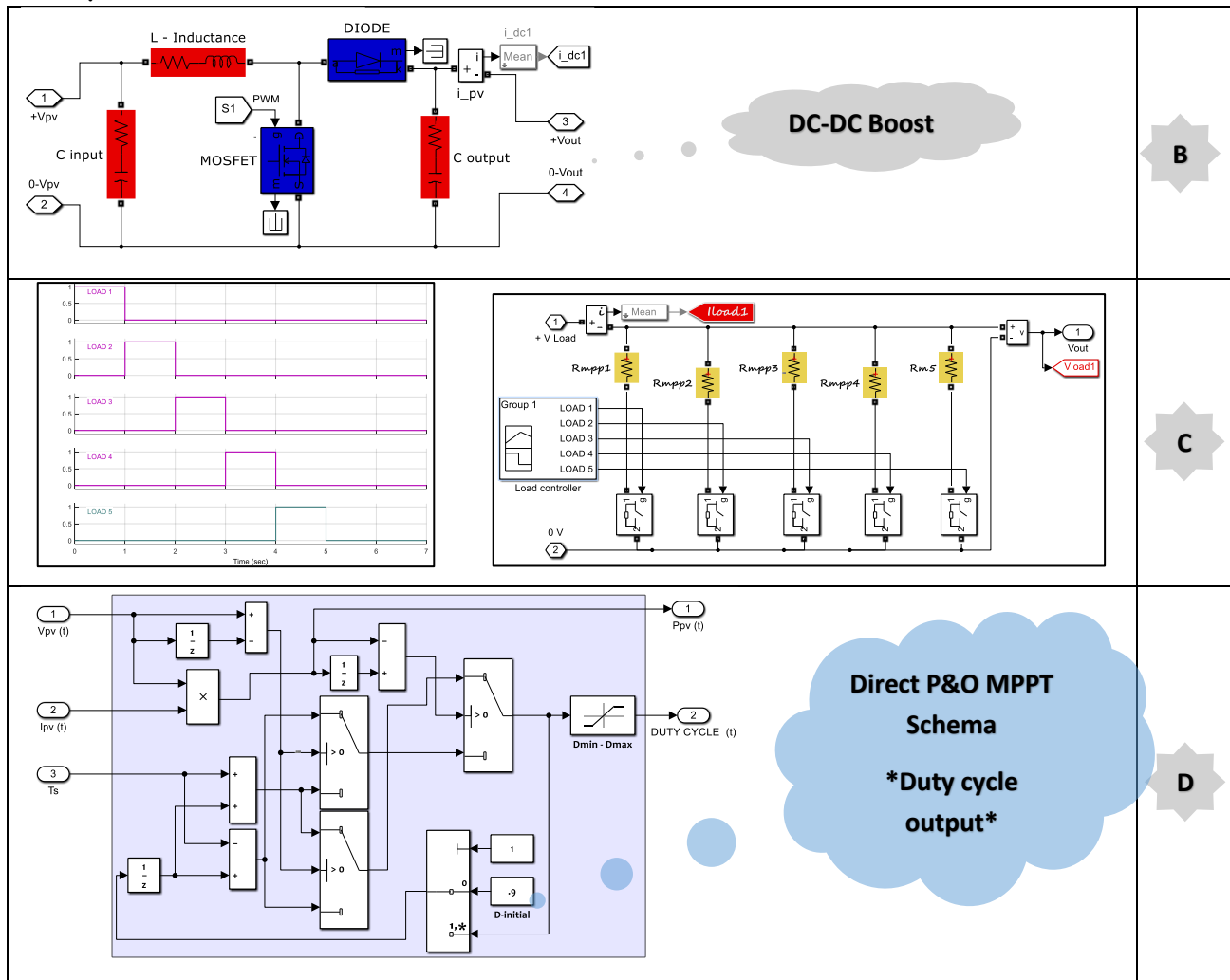


**Figure III. 1:** Presentation of the PV conversion chain components: A- Simulink model, B- DC/DC Boost, C-DC variable load with its control profile, and D-Direct P&O-MPPT schema. For the PV control, the Direct P&O-MPPT is viewed above in Figure III.1-D, while the algorithms of the Direct INC-MPPT and the indirect P&O-MPPT are presented in the pseudo-codes below.

```

function MPP = INC_MPPT (Vpv, Ipv, V0, I0, D, Delta_d)
d=0; du = Vpv - V0; di = Ipv - I0; ..... Initialization
if (du == 0)
    if di==0 ..... 1st condition
d=D; ..... 1st decision
else
    if di>0 ..... 2nd condition
d = D - Delta_d; ..... 2nd decision
    else
d = D + Delta_d; ..... 3rd decision
    end
end
elseif di/du == -(Ipv/Vpv) ..... 4th condition
    
```

**Direct INC MPPT algorithm**  
\*Duty cycle output\*

```

else
    if di/du == -(Ipv/Vpv)           ..... 5th condition
d = D - Delta_d;                   ..... 5th decision
    else
d = D + Delta_d;                   ..... 6th decision
    end
end
MPP = d;           end           ..... Final updated decision

```

---

```

function V_ref = V_ref(V, I, irrad, delta_V)
Voc=37.08; Vref_max=Voc;           ..... Initialization
Vref_min=28; Vref_init=37.08;     ..... Initialization
persistent Vold Pold Vref_old;
dataType = 'double';
    if isempty(Vold)
        Vold = 0; Pold = 0; Vref_old = Vref_init;
    end
P = V*I; dV = V - Vold; dP= P - Pold; ..... Initialization
if dP ~= 0           ..... 1st condition
    if dP<0           ..... 2nd condition
        if dV<0           ..... 3rd condition
            V_ref = Vref_old + delta_V; ..... 1st decision
        else
            V_ref = Vref_old - delta_V; ..... 2nd decision
        end
    else
        if dV<0           ..... 4th condition
            V_ref = Vref_old - delta_V; ..... 3rd decision
        else
            V_ref = Vref_old + delta_V; ..... 4th decision
        end
    end
end
    V_ref = Vref_old;           ..... 5th decision
end
if V_ref >= Vref_max || V_ref <= Vref_min ..... 5th condition
    V_ref = Vref_old;           ..... 6th decision
elseif irrad == 0           ..... 6th condition
    V_ref = 0;                 ..... 7th decision
end
Vref_old = V_ref; Vold = V; Pold = P; ... Final updated decision

```

---

```

function DUTY_CYCLE = MPPT_FPPT(Param, Ppv, Pref, Vin, Vout_estim,
D_mppt)
deltaD = Param(1); %Increment value to increase/decrease Vdc_ref
D1=0.9;           ..... Initial duty cycle value

```

Indirect – P&O  
MPPT algorithm  
\*Voltage output\*



```

dataType = 'double';
if Pref > 0 ..... 1st condition
    D1 = (Vout_estim/Vin); ..... 1st decision
    if Pref > Ppv % LACK DISCHARGE
        D1 = D1 + deltaD; ..... 2nd decision
    elseif Pref < Ppv ..... 2nd condition
        D1= D1 - deltaD; ..... 3rd decision
    end
else
    D1=D_mppt; Indirect – FPPT ..... 4th decision
    algorithm
end
DUTY_CYCLE= [D1]; end

```

**Figure III. 2:** Schema of the PV conversion chain using MATLAB Simulink.

### III.2.1 PV diagram identification

This test allows the identification of PV diagrams (VI and VP curves) using either a fixed load with a varying duty cycle [0-to-1] (p.u) or by varying the load values with a fixed duty cycle. These methods can be practically used to extract PV module parameters such as  $V_{OC}$  (Open-Circuit Voltage),  $I_{SC}$  (Short-Circuit Current),  $I_{MPP}$  (Maximum Power Point Current), and  $V_{MPP}$  (Maximum Power Point Voltage). Table III.1 provides the settings for which the VI and VP curves have been plotted.

**Table III. 1:** Settings for VI and VP Curve identification.

Parameters and criteria	Values	unit
Irradiation (Variable)	1000	(w/m <sup>2</sup> )
Temperature (Fixed)	25	(°C)
$R_{MPP}$ (Fixed)	24.45	$\Omega$
$T_s$ (Fixed) and $\Delta d$ (Fixed)	1e-4	(s) / (PU)

In the simulation, a ramp signal was used to define and characterize the VI and VP curves in the STC. By tracing the points (see parts A, B, and C of Figure III.3) associated with the characteristics of the solar panels, we chose three points which to plot the characteristics of the VI and VP curves.

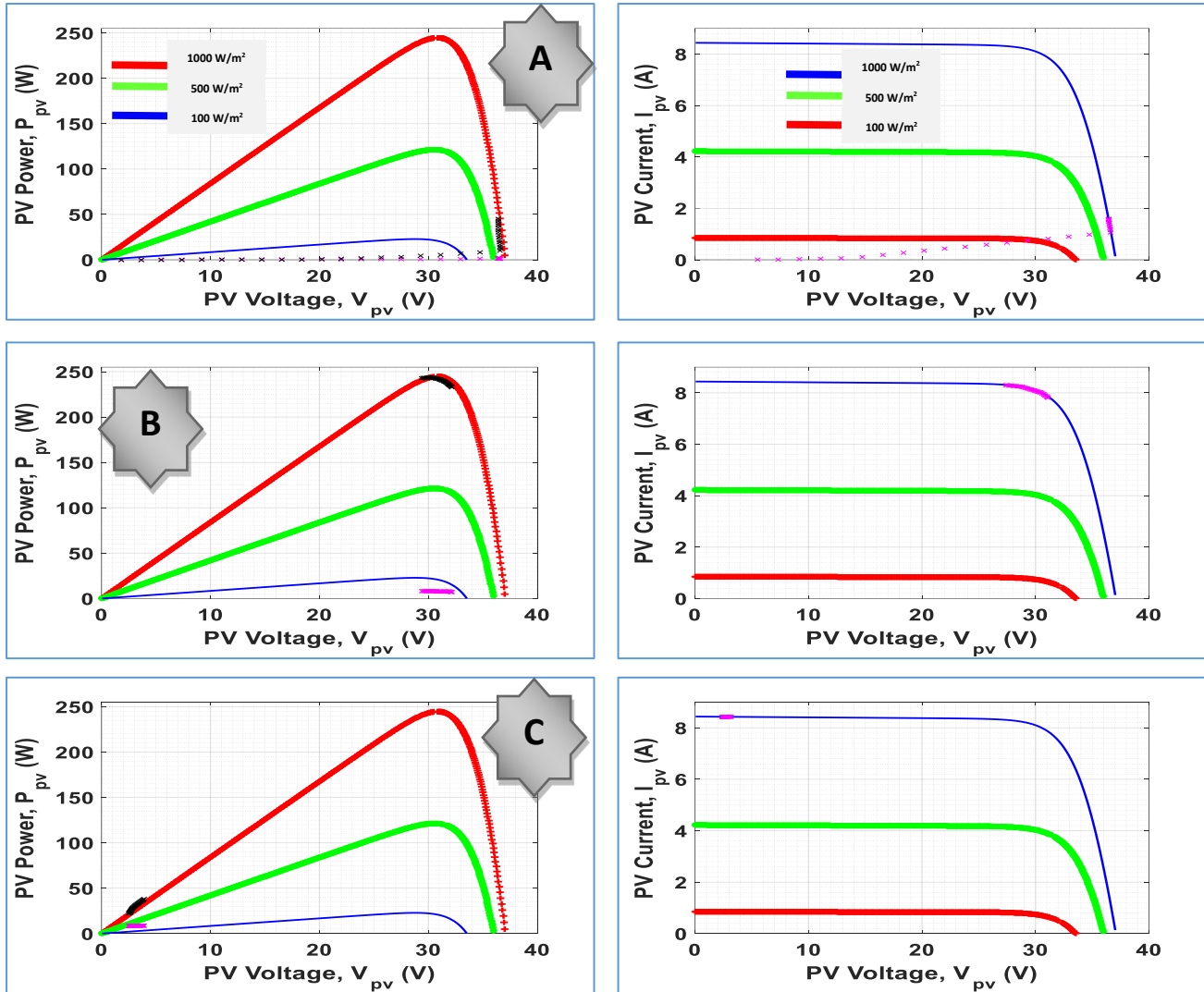


**Figure III. 3:** VI and VP characteristics of the PV Panel using Ramp Signal test.

As seen, the increment of the duty cycle command from 0 to 1 (p.u) tracked several operating MPPs of the PV source at the STC starting from the  $V_{oc}$  to the  $I_{sc}$ . The black moving points drew the VI curve, while the magenta moving points drew the VP curve.

### III.2.2 The impact of variable weather conditions on the PV system

This part includes two separate scenarios, the first aims to evaluate the PV outputs under variable solar irradiances and constant temperature, while the second assesses the PV outputs under fixed irradiation and variable temperature levels.

**III.2.2.A The impact of variable irradiation**

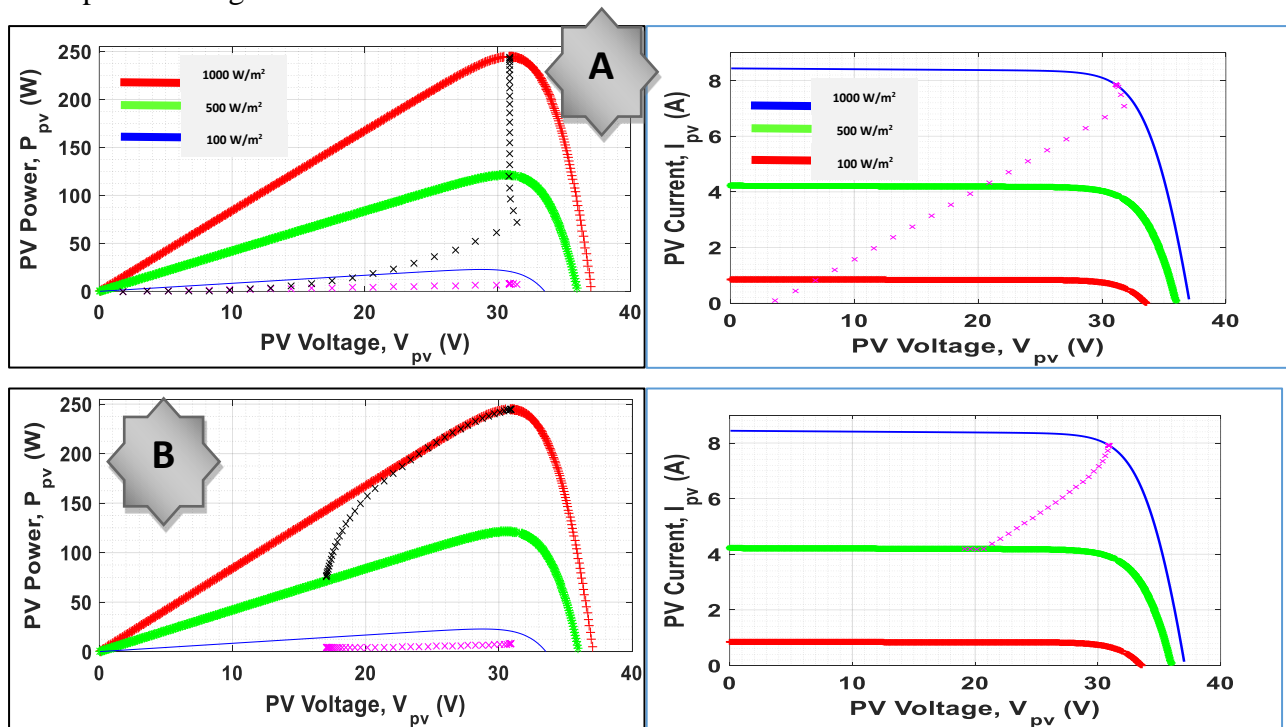
In this section, the focus is on assessing the impact of changing solar conditions on the performance of the PV system. Through simulation and experimental tests, the system's response to changes in solar radiation, We fix temperature, load,  $T_s$ , and  $D_d$ , as seen in Table (III.2).

**Table III. 2:** Experimental Parameters for Irradiation Variation Analysis.

Parameters and criteria	Values	unit
<b>Irradiation (Variable)</b>	1000 to 50 / 100 to 1000	(w/m <sup>2</sup> )
<b>Temperature (Fixed)</b>	25	(°C)
<b>R<sub>MPP</sub> (Fixed)</b>	4.89	Ω
<b>T<sub>s</sub> (Fixed) and Δd (Fixed)</b>	1e-4	(s) / (PU)

Our focus was on monitoring the movement of dots on I-V and P-V curves when exposed to variable radiation levels. We aimed to capture the significant differences in radiation to illustrate the transition process.

For this purpose, we divided the study into three phases. The first stage involved looking for Maximum Power Point Tracking (MPPT). In the second phase, there was a transition from 1000 to 500 W/m<sup>2</sup>. Finally, in the third phase, the transition was from 100 to 1000 W/m<sup>2</sup>. These transitions are depicted in Figure III.4.



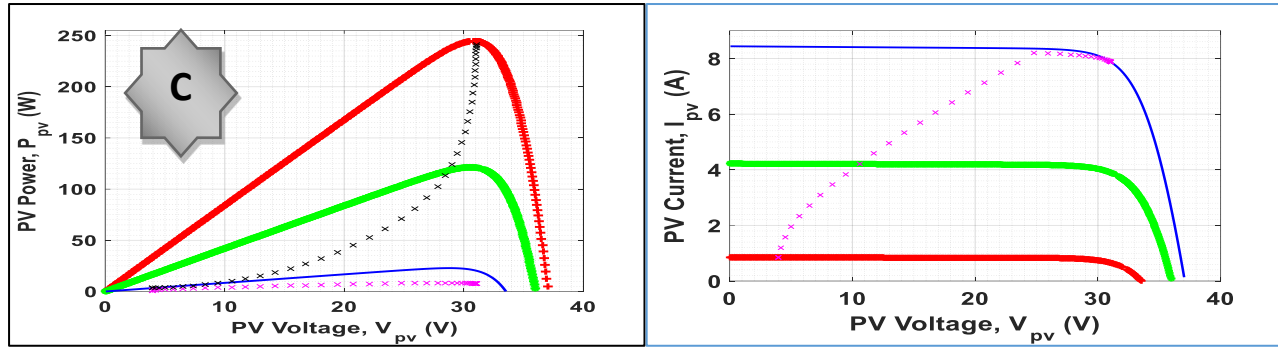


**Figure III. 4:** Variations of the PV outputs in the IV/VP curves: A- Initialization of MPPT search, B- Step change in solar irradiancies from 1000 to 500 (w/m<sup>2</sup>), and C- A step change in solar irradiancies from 100 to 1000 (w/m<sup>2</sup>).

Table III.3 presents the impact of varying radiation levels on the current, power, and efficiency of the PV system.

**Table III. 3:** Impact of irradiation variation on the PV outputs.

$I_{rad}$ (W/m <sup>2</sup> )	$I_{PV}$ (A)	$P_{Load}$ (W)	$P_{mpp}$ (W)	$\eta = \frac{P_{Load}}{P_{mpp}}$ (P. U)
1000	7.894	234	244.4	0.95
500	4.196	66.54	70.84	0.93
100	0.843	2.687	3.335	0.80

Solar radiation plays a crucial role in the performance of PV systems. The analysis of Figure III.4, obtained from the simulation, confirms the significance of solar radiation in influencing the behavior of the PV system. When the sunlight intensity decreases, there is a noticeable decrease in the system's current. This reduction in current can be attributed to the reduced availability of photons, which are the fundamental particles of light that generate the flow of electricity in PV cells. Consequently, a decrease in current leads to a decrease in energy production.

Furthermore, variations in solar radiation also impact the system's voltage. The voltage generated by a PV system is directly proportional to the intensity of solar radiation it receives. As solar radiation decreases, the voltage output of the system decreases as well. This voltage reduction affects the overall energy production and system efficiency. When the voltage decreases, the power generated by the system decreases, resulting in reduced energy output.

The interdependence of solar radiation, current, voltage, energy production, and efficiency highlights the direct impact of insufficient sunlight exposure on the performance of the PV system.

Inadequate solar radiation directly translates to a lack of energy generation, as evidenced by the decrease in current and voltage.

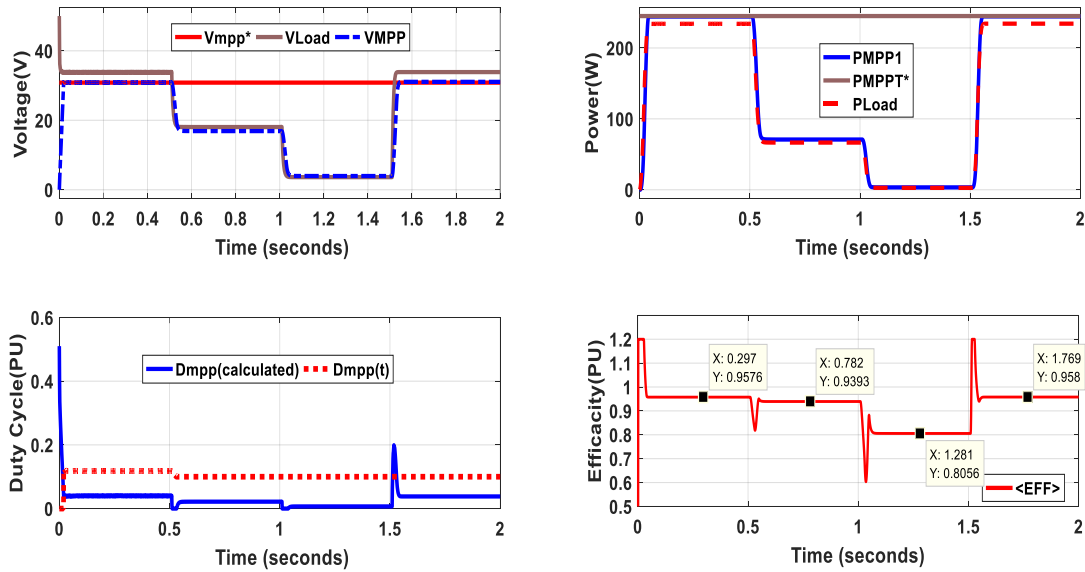


**Figure III. 5:** Simulation result of the impact of variable irradiation levels.

This reduced energy generation leads to diminished overall system efficiency. In conclusion, the analysis of the curves in Figure III.5 obtained from the simulation emphasizes the significant influence of solar radiation on the performance of the PV system. Insufficient sunlight exposure results in decreased current, reduced energy production, and diminished overall system efficiency. It is crucial to ensure optimal sunlight exposure to maximize energy generation and maintain high system performance.

**III.2.2.B The impact of variable temperature**

In this case, we explore the impact of varying temperatures while keeping the solar radiation, convection,  $T_s$  (sampling time), and  $D_d$  (Duty cycle increment) fixed, as specified in Table III.4.

**Table III. 4:** Experimental Parameters for Temperature Variation Analysis

Parameters and criteria	Values	unit
Irradiation (Fixed)	1000	(w/m <sup>2</sup> )
Temperature (Fixed)	60 /40/ 25	(°C)
R MPP (Fixed)	4.89	Ω
$T_s$ (Fixed) and $\Delta d$ (Fixed)	1e-4	(s) / (PU)

Figure III.6 shows the transition in the I-V and P-V curves when the temperature changes. The impact of various temperature levels on the current, and power, is shown in Table III.5.

**Table III. 5:** Impact of temperature variation on the PV outputs.

Temperature	$V_{PV}$ (A)	$P_{Load}$ (W)	$P_{mpp}$ (W)	$\eta = \frac{P_{Load}}{P_{mpp}}$ (P. U)
60	27.39	210.2	220.4	0.953
40	29.54	224.2	234.5	0.956
25	31.06	234.3	244.5	0.958

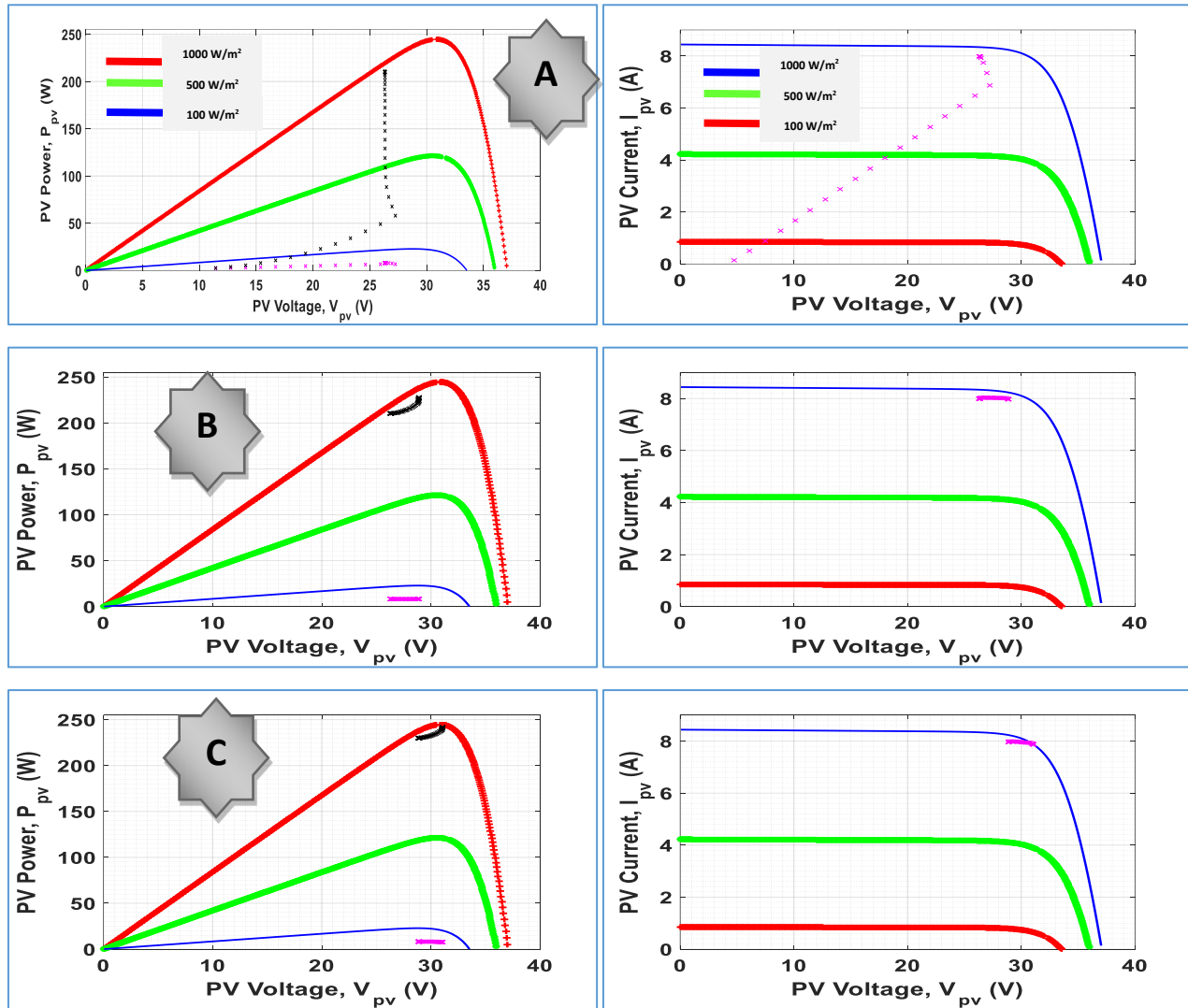


**Figure III. 6:** Variations of the PV outputs in the IV/VP curves: A- Initializing the search for the proposed point, B- A step change in temperature from 60 to 40 (°C), and C- A step change in temperature from 40 to 25 (°C).

Figure III.7 illustrates the variations in voltage, power, and efficiency that arise as a result of temperature fluctuations. Consequently, we can deduce that lower temperatures lead to higher load capacity and improved efficiency of the board.

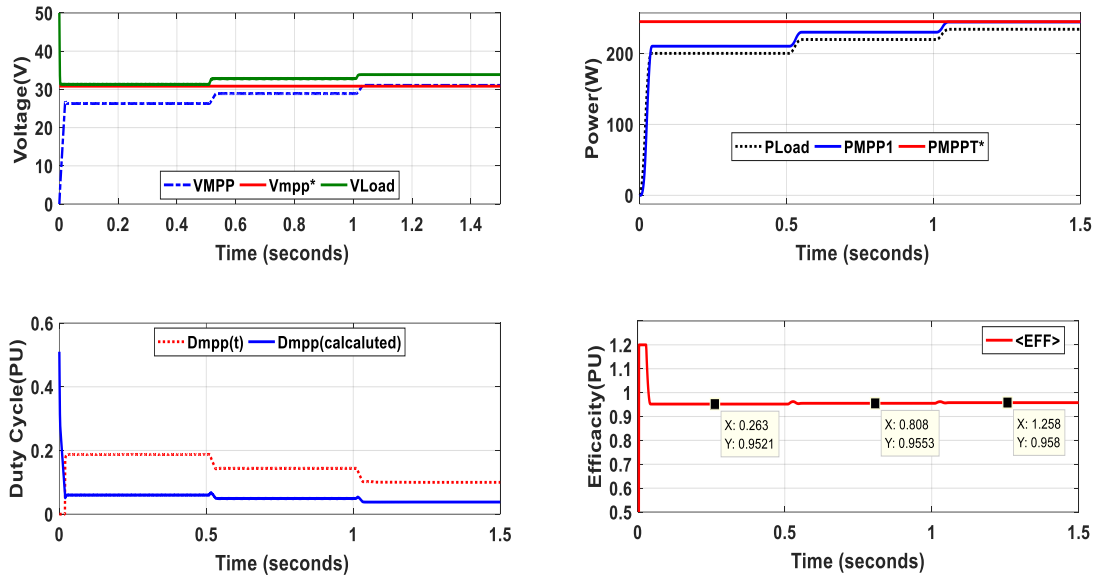


**Figure III. 7:** Simulation result of the impact of variable temperatures.

When examining the relationship between temperature fluctuations and voltage, power, and efficiency variations, several factors come into play. Variations in voltage can affect the performance of electronic circuits and devices.

**Voltage** fluctuations, which refer to rapid changes in the magnitude of the voltage, can also impact the performance of power systems and electrical devices. Voltage fluctuations can be caused by various factors, such as heavy loads, power quality disturbances, and variations in the power supply. These fluctuations can result in undesired effects on induction motors, including extra losses, overheating, and reduced efficiency. In terms of **power**, voltage fluctuations can lead to voltage variations along distribution feeders. Understanding the factors influencing voltage variations is essential for improving the operation and maintenance of distribution feeders.

Regarding **efficiency**, the relationship between temperature fluctuations and efficiency is influenced by various factors. For example, the efficiency of a motor-pump system can be affected by voltage and load variations. Power quality disturbances, such as voltage and frequency deviations, voltage unbalances, and voltage harmonics, can increase power losses and reduce the output power of induction motors, leading to decreased efficiency.

By optimizing the supply voltage, it is possible to improve the energy efficiency and temperature variation insensitivity of circuits. In summary, Figure III. 7 demonstrates the variations

III.2.3 Impact of variable load demand

In this section, we will explore the results of simulations investigating the impact of variable load demand on the PV system. By subjecting the system to different pulsing load requirements, we selected three load values that we can evaluate its ability to meet the load demand while maintaining stable operation. Table III.6 shows the Parameter that we relied on in this simulation.

Table III. 6: Experimental Parameters for Load Variations Analysis.

<b>Irradiation and Temperature (Fixed)</b>	1000 / 25	(w/m <sup>2</sup> ) / (°C)
<b>R MPP (Variable)</b>	9.78 / 4.89 / 3.42	(Ω)
<b>Ts (Fixed) and Δd (Fixed)</b>	2 / 1 / 0.7	(P.U)
	1e-4	(s) / (PU)

Figure III.8 examines the boost converter to determine its behavior under different loads.

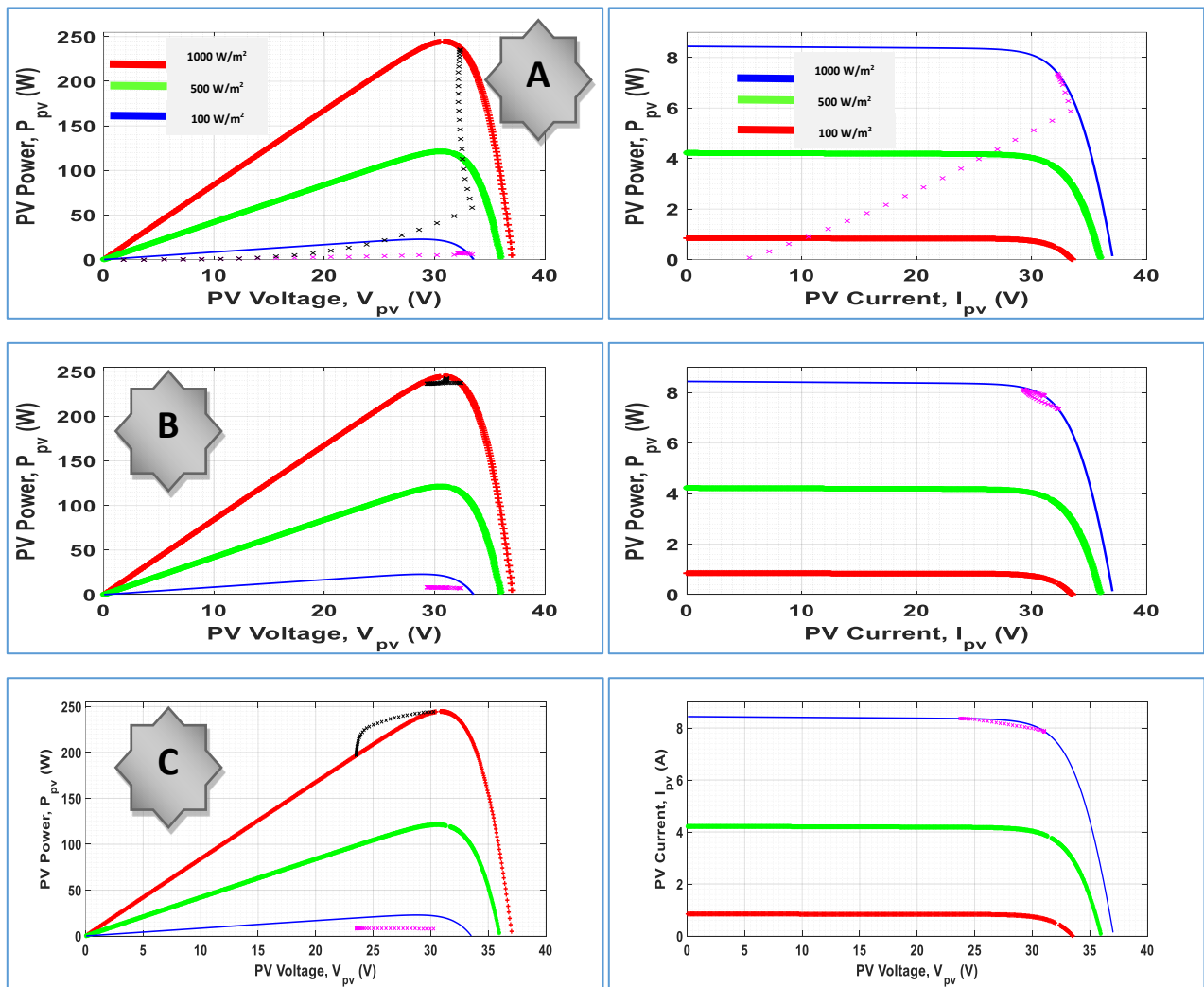


Figure III. 8: Variations of SPV outputs in the IV/VP curves: A- Initializing the search for MPPs, B- A step change in load: 9.78 to 4.89 (Ω), and C- A step change in load: 4.89 to 3.423(Ω).



We selected three distinct loads for analysis: the first load with  $R_{MPP} = 4.89 \text{ } (\Omega)$ , the second load greater than  $R_{mpp}$ , and the third load smaller than  $R_{mpp}$ . By monitoring the performance of the Boost at each load, we aim to evaluate the effect of load differences on its operation.

In this section, we focused on three values of load:  $4.89 \text{ } (\Omega)$  ( $R_{mpp}$ ),  $9.78 \text{ } (\Omega)$  ( $R_{mpp} * 2$ ), and  $2.445 \text{ } (\Omega)$  ( $0.5 * R_{mpp}$ ). We observed that in Figure III.9,  $R_{mpp} * 2$  had the same value as  $R_{mpp}$  in terms of power, efficiency, duty cycle, and voltage. On the other hand, the value of  $0.5 * R_{mpp}$  was lower but a small proportion.

If we refer back to Figure II.7, we find that the value of  $0.5 * R_{mpp}$  falls within the operating range of the Boost converter DC-DC, while the value of  $R_{mpp} * 2$  is outside that range. However, in our Matlab simulation, we found that  $R_{mpp} * 2$  performed better than  $0.5 * R_{mpp}$ . This is because the Boost converter DC-DC should be modeled accurately, considering its components such as an inductor, capacitor, diode, and MOSFET, which have internal resistance or parasitic resistance.

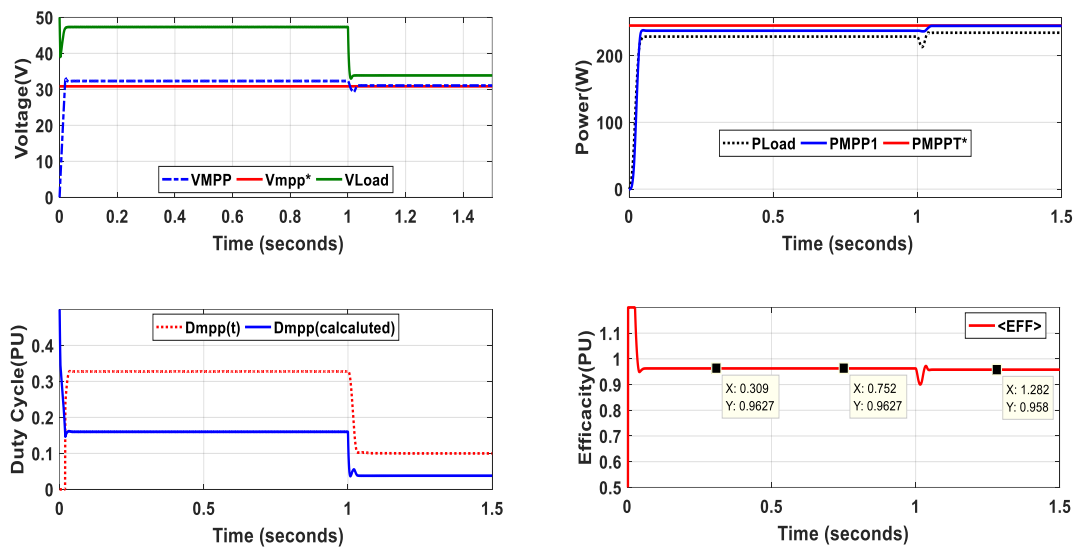


Figure III. 9: Simulation result of the impact of variable Load resistance.

### III.2.4 Impact of variable MPPT simple time ( $T_s$ )

Variable MPPT sampling time ( $T_s$ ) refers to the interval between consecutive measurements of the PV system's operating parameters during maximum power point tracking. We selected two times to compare them, as shown in Table III.7.

**Table III. 7:** Parameters for simple time Variation Analysis.

<b>Irradiation and Temperature (Fixed)</b>	1000 / 25	(w/m <sup>2</sup> ) / (°C)
<b>R MPP (Variable)</b>	4.89 / 1	(Ω) / (P.U)
<b>Ts (Variable)</b>	1/10 - 10	(ms)
<b>Δd (Fixed)</b>	1e-4	(PU)

Upon analyzing Figure III.10, we observe a distinct behavior. When  $T_s=1e-4$  (s), the point converges to the maximum power point (MPP), whereas for  $T_s =1e-2$  (s), the point deviates from the MPP. This leads us to the conclusion that a slower value of  $T_s$  results in higher resolution, enabling the system to accurately track and reach the MPP. Conversely, a faster  $t_s$  value compromises the resolution, impeding the system's ability to achieve precise MPP tracking.

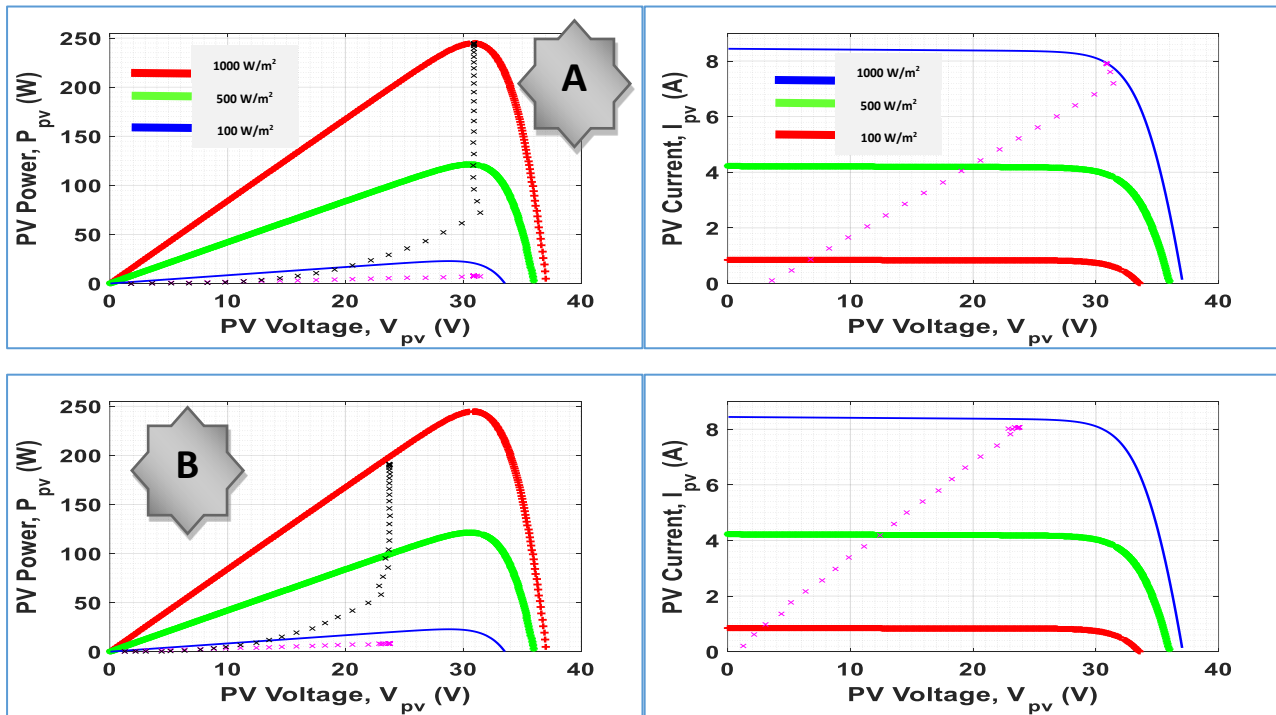


**Figure III. 10:** Variations of PV outputs in IV/VP curves: A-  $T_s=1e-4$  (s) and B-  $T_s=1e-2$  (s).

It can be seen that the MPPT has reached the MPP with  $P = 245$  (W) adopting a  $T_s=1e^{-4}$  (s), while the tracked power was lower and dropped to 200 (W) using a higher sample time  $T_s = 1e^{-2}$  (s).

Table III.8 provides a comparative analysis of power and efficiency between two different values of  $T_s$ :  $T_s=1e^{-4}$  and  $T_s=1e^{-2}$ .

**Table III. 8:** Comparison of Power and Efficiency for  $T_s = 1e-4$  and  $T_s = 1e-2$ .

Dd (PU)	Ppv (W)	Pload (W)	$\eta = \frac{P_{ch}}{P_{pv}}$ (PU)
1e-4	244.4	234	0.95
1e-2	174.7	191.15	0.91

To conclude, the impact of variable MPPT sampling time ( $T_s$ ) on MPPT performance includes its influence on tracking speed, tracking accuracy, and system stability. The optimal choice of  $T_s$  depends on factors of the specific MPPT algorithm, the characteristics of the PV system, and the desired trade-off between accuracy, speed, and stability.

### III.2.5 Impact of Duty cycle variation or Delta-duty ( $\Delta d$ )

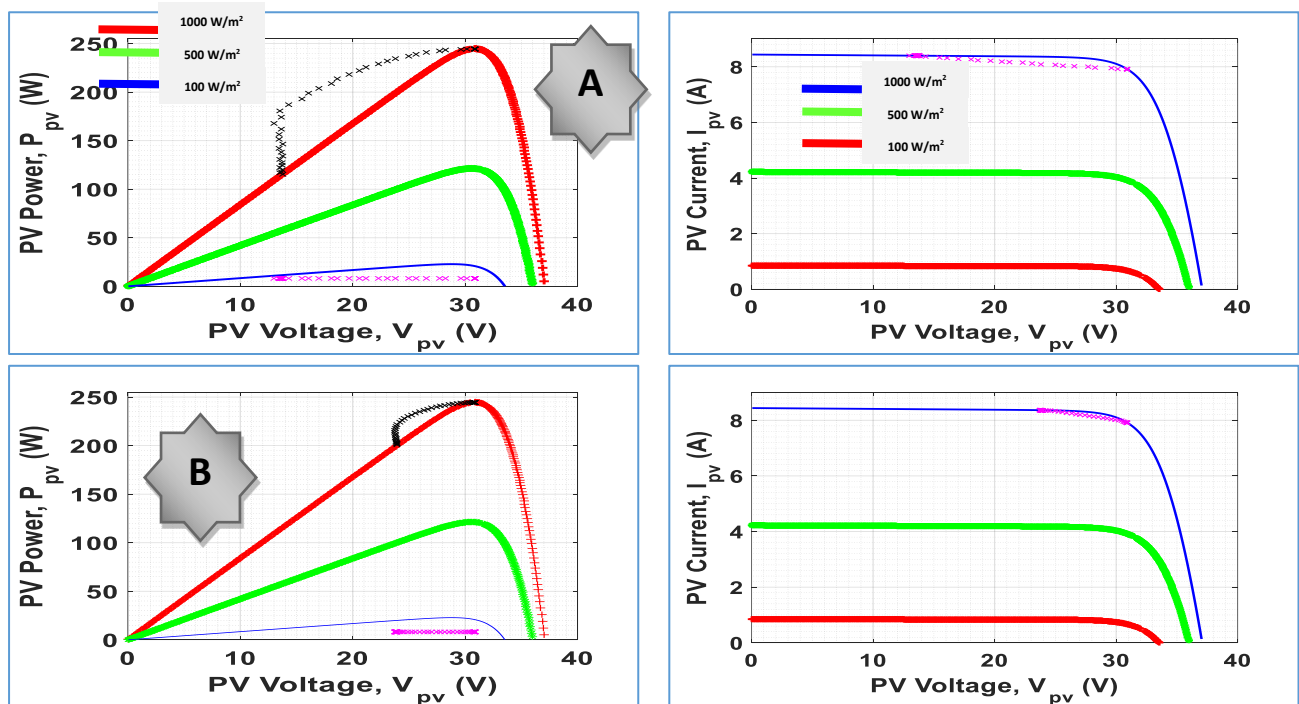
In this section, we analyzed by varying the values of  $\Delta d$  in the FPPT method. We selected three specific values for  $\Delta d$  and examined their impact on the performance of the algorithm.

Table III. 10 presented below outlines the parameters that were chosen for this investigation.

Figure III.11 illustrates the movement along the VI and VP curves in the FPPT algorithm for two different values of Delta-duty:  $\Delta d = 1e-4$  and  $\Delta d = 1e-2$ .

**Table III. 9:** Impact of Delta-duty ( $\Delta d$ ) Variations using the FPPT control.

Irradiation and Temperature (Fixed)	$1000 / 25$	$(w/m^2) / (^\circ C)$
R MPP (Variable)	4.89 / 1	$(\Omega) / (P.U)$
$T_s$ (Fixed)	$1e-4$	(s)
$\Delta d$ (Variable)	$1e-2 / 1e-4$	(PU)
Setpoint FPPT power	200	(W)



**Figure III. 11:** Variations of PV outputs in IV/VP curves: A-  $\Delta d=1e-2$  (PU) and B-  $d =1e-4$  (PU).

The FPPT algorithm was utilized with a power value of 200 W within 0.5 to 1.5 seconds. Simulations were conducted using 03 values of Dd as mentioned in Table III.10 earlier. The outcomes exhibited significant variations in the energy values for each Dd setting, as illustrated in Figure III.12.

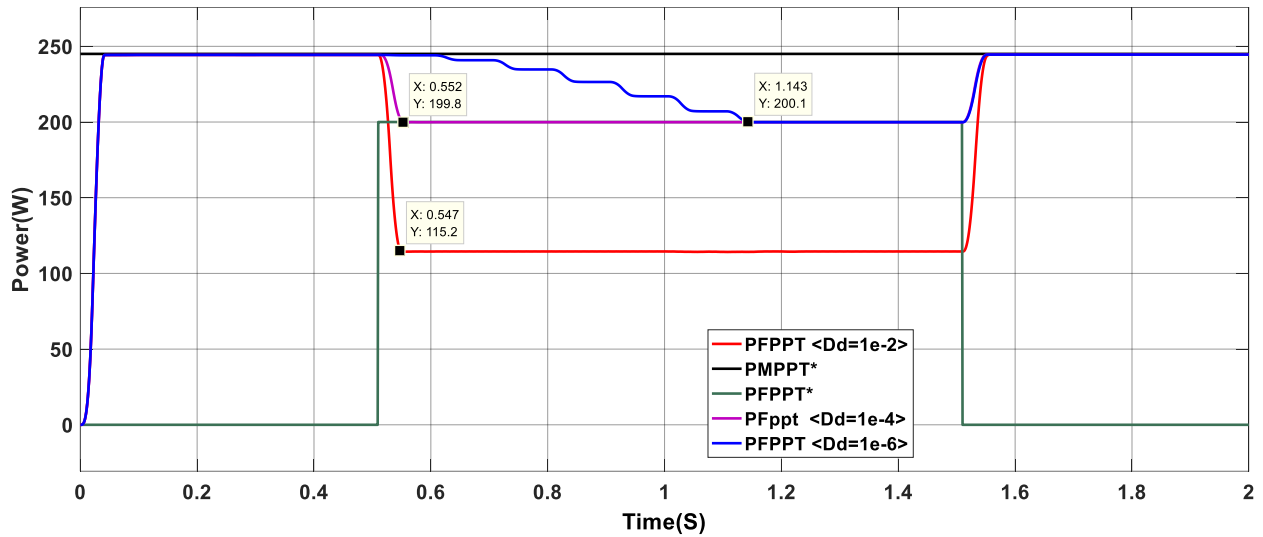


Figure III. 12: Impact of Variable Delta-duty cycle on the PV output power.

When Dd was set to  $1e^{-6}$  (PU), it took a considerable amount of time to reach the desired output, but it demonstrated the highest level of precision. On the other hand, when Dd was set to  $1e^{-4}$ , the speed and accuracy were moderate, similar to the first case. Finally, when Dd was set to  $1e^{-2}$ , the algorithm achieved the highest speed, but the accuracy was relatively poor.

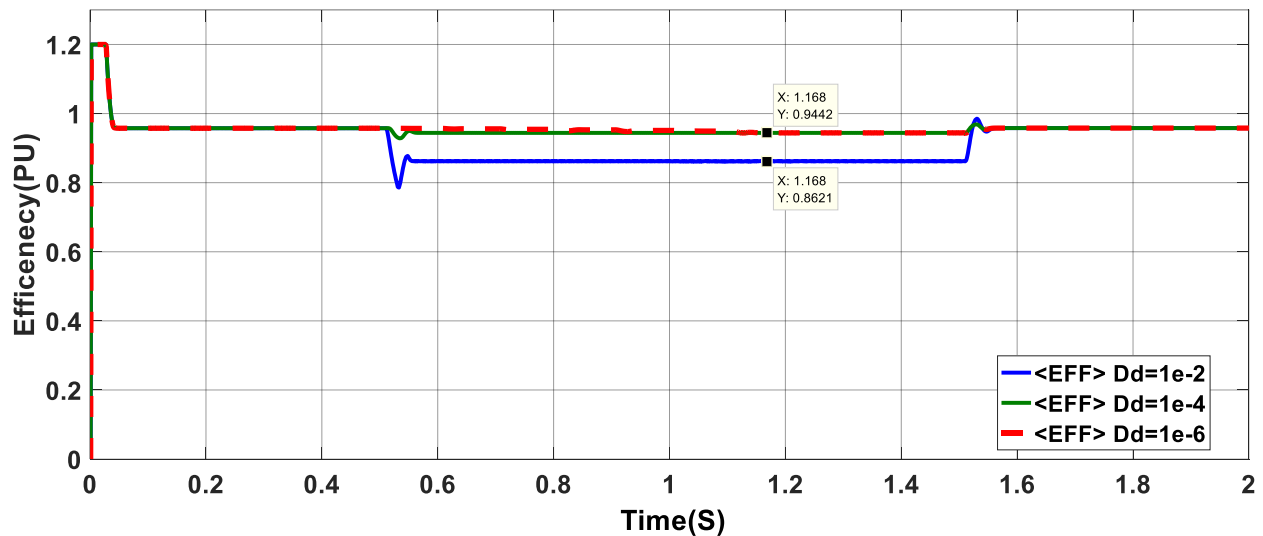


Figure III. 13: Impact of Variable Delta-duty on the DC-DC converter efficiency.

Table III.11 provides a comparative analysis of power and efficiency between Dd values.

**Table III. 10:** Comparison of Power and Efficiency for  $Dd = 1e^{-2}, 1e^{-4},$  and  $1e^{-6}$  (PU).

Dd (PU)	$P_{pv-FPPT}$ (W)	$P_{PV}$ (W)	Pload (W)	$\eta = \frac{P_{ch}}{P_{pv}}$
$1e^{-6}$	200(W)	199.9	188.7	0.944
$1e^{-4}$		199.9	188.7	0.944
$1e^{-2}$		114.5	98.71	0.86

In conclusion, variable FPPT Delta-duty (Dd) plays a crucial role in optimizing power extraction and efficiency in PV systems. By adjusting the duty cycle, the FPPT algorithm can enhance power tracking accuracy, and increase system efficiency.

### III.2.6 Impact of Variable PV control methods

#### III.2.6. A Impact of switching between MPPT and FPPT control methods

In this section, our objective was to compare the P&O algorithm for direct MPPT and FPPT. with the impact of load changes on the performance of these algorithms. Table III.12 presents the specific settings and parameters we utilized for our comparison.

**Table III. 11:** Impact of MPPT/FPPT switching under proposed variations.

Irradiation and Temperature (Fixed)	1000 / 25	( $w/m^2$ ) / ( $^{\circ}C$ )
<b>R MPP (Variable)</b>	3.91/4.40/4.64/4.89/5.37	( $\Omega$ )
<b>Ts (Fixed)</b>	0.8 / 0.9 / 0.95 / 1 / 1.1	(P.U)
<b><math>\Delta d</math> (Variable)</b>	$1e^{-2} / 1e^{-4}$	(PU)
<b>Setpoint FPPT power</b>	200 / 160 / 120 / 80 / 40	(W)

The proposed load profile and setpoint FPPT power variations are viewed in Figure III.15.

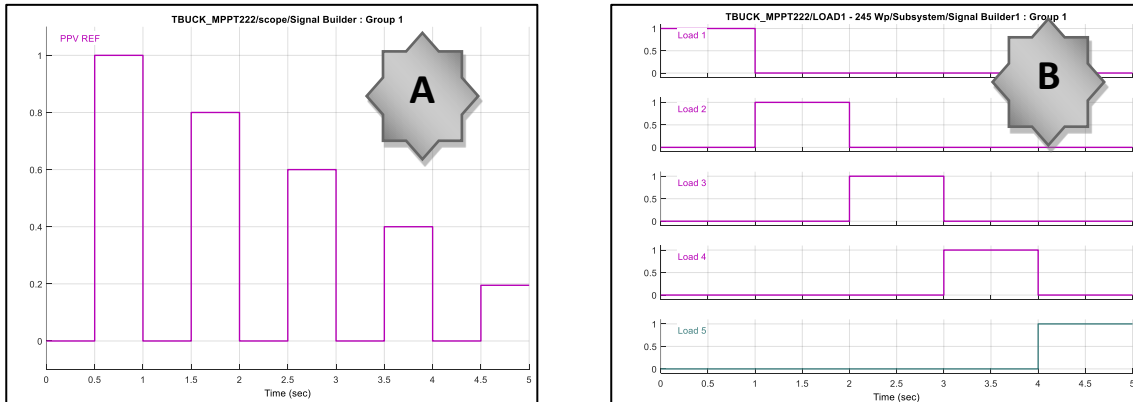


**Figure III. 14:** (A) Variable profiles of the FPT setpoint, (B) power and load schedule

The figure above illustrates the changes in the I-V and P-V curves when a load change is applied, as well as the transition from the MPPT algorithm to the FPPT algorithm. It demonstrates the trajectory and adjustments made during the load variation, highlighting the shift in operating points and power outputs between the two algorithms.

In Figure III.16. B, the PV control switched from the MPPT to the FPPT to track the setpoint power of 200 (W) during [0.5-1](s). Instead, in Figure III.16. C, the PV control tracked the PV MPP during [1-1.5](s) after switching back from the FPPT to the MPPT mode using a load resistance of 3.91( $\Omega$ ) equivalent to 0.8 (PU).

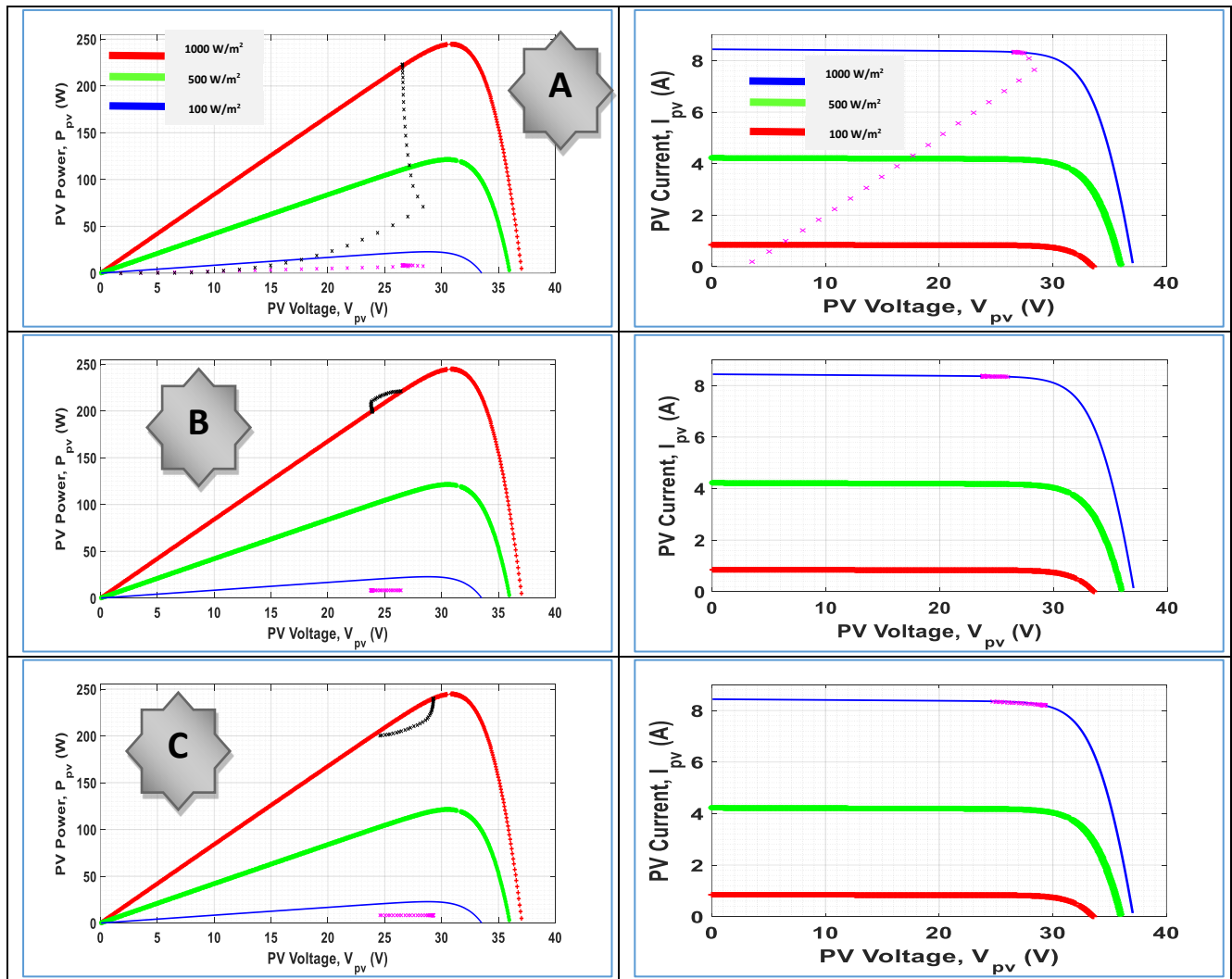


**Figure III. 15:** Variations of PV outputs in IV/VP curves: **A-** Initializing the search for MPPs, **B-** switching from MPPT to FPPT: [0.5-1](s), and **C-** switching from FPPT to MPPT: [0.5-1](s).

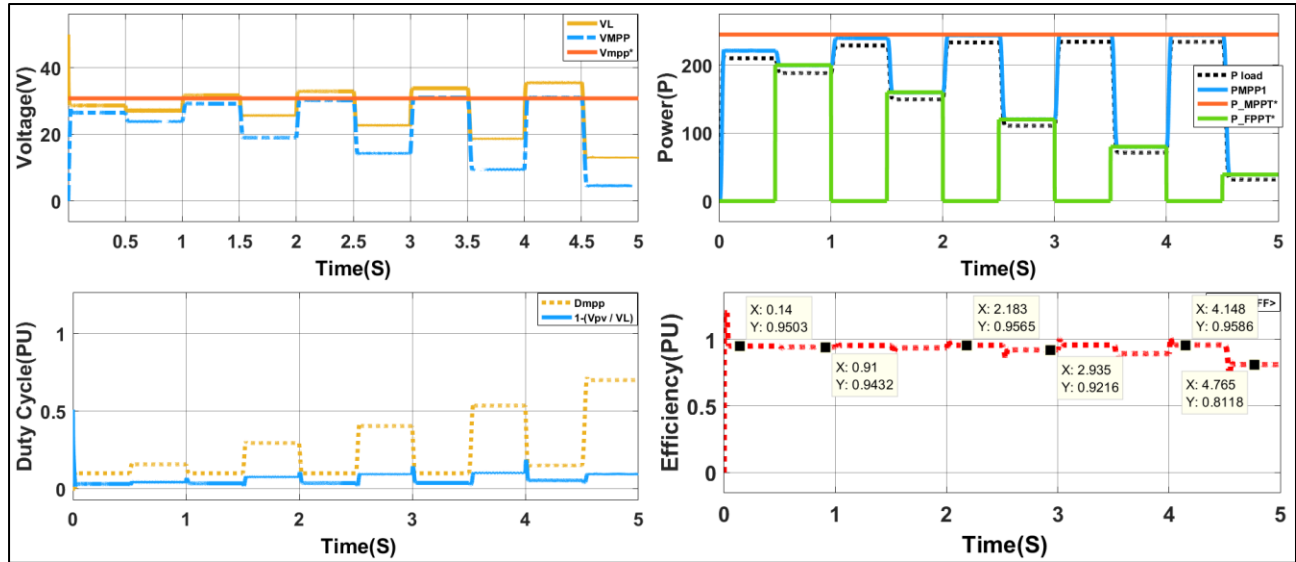


**Figure III. 16:** Impact of switching control between MPPT and FPPT modes.

Figure III.16 presented the robust and accurate transitions between the MPPT and FPPT modes regarding the setpoint powers and the variable load demand schedule, as proposed in Table III.11 and Figure III.11 above. The MPPT algorithm is highly efficient when dealing with load changes. It rapidly tracks and adapts to new load conditions, maximizing the power output of the solar panels. This allows the system to efficiently utilize the available solar energy and deliver the optimal power to the load. Table III.12 resumes the statistical results of the switching control between MPPT and FPPT modes.

**Table III. 12:** Statistical results of the switching control between MPPT and FPPT modes.

$P_{FPPT}$ (W)	$R_{Load}$ ( $\Omega$ )	MPPT			FPPT		
		$P_{PV}$ (W)	$P_{Load}$ (W)	$\eta$ (PU)	$P_{PV}$ (W)	$P_{Load}$ (W)	$\eta$ (PU)
200	3.912	221.4	210	<b>0.949</b>	199.5	188.2	<b>0.943</b>
160	4.4	239.7	228.8	0.954	159.7	149.6	0.936
120	4.64	243.9	233.3	0.956	120.3	110.7	0.921
80	4.89	244.5	234.3	0.958	79.68	71.2	0.893
40	5.37	244.3	234.2	<b>0.958</b>	38.93	31.62	<b>0.812</b>

The efficiency of the FPPT algorithm in handling load changes is lower compared to MPPT. Since it operates at a fixed point, it may not fully utilize the available power from the solar panels when the load changes. If the load increases, the PV may not generate enough power to meet the new demand. Conversely, if the load decreases, excess power may be generated and not efficiently utilized.

**III.3 Conclusion**

This chapter presents the simulation results and analysis of the standalone PV system under study. Through extensive simulations, we have examined the PV diagram, which provides valuable insights into the system's characteristics and operation. The analysis of variable weather conditions, including irradiation and temperature, has shed light on their impact on the PV system's performance. We have also explored the effects of variable load demand, MPPT control time, duty cycle variation, and different PV control methods. These investigations have contributed to a deeper understanding of the system's behavior and its response to various conditions. The findings from this chapter provide important insights for optimizing the system's design, operation, and control strategies.





**General**

**Conclusion**

## *Conclusion generale*

### **GENERAL CONCLUSION**

In conclusion, this research has provided valuable insights into the study and simulation of standalone solar photovoltaic (PV) systems. By analyzing the impact of variable weather conditions, load fluctuations, and the implementation of different control algorithms, such as MPPT and FPPT, this study has contributed to understanding the performance and efficiency of PV systems.

The use of PV emulators has been highlighted as essential for ensuring the efficient operation and performance of PV systems, enabling testing, research, development, and training. The research has shed light on the significance and diverse applications of PV emulators, emphasizing their role in advancing the field of PV systems.

The focus on maximum power point tracking (MPPT) systems has shown their prominence in optimizing solar panel efficiency, regardless of environmental conditions. This technology has the potential to enhance the overall performance and cost-effectiveness of solar installations, leading to ongoing research efforts in developing advanced and intelligent MPPT algorithms and control systems.

By conducting thorough modeling and design analyses, this research has provided valuable insights into accurately capturing the electrical characteristics and behavior of PV arrays. The discussions on the DC-DC Boost Converter, sensor sizing, and acquisition board realization have contributed to the knowledge surrounding the design aspects of standalone PV systems.

Through simulation and evaluation using MATLAB Simulink software, the research has assessed the impact of variable weather conditions, load demand, and control method switching on PV system performance. These findings offer practical implications for optimizing the performance of standalone PV systems and maximizing energy harvested from renewable sources.

In conclusion, this research contributes to the body of knowledge surrounding PV systems and emulators, offering new perspectives, solutions, and avenues for future research. It is hoped that the insights gained from this work will further advance the field, leading to more efficient and sustainable solar power generation.

## References

### REFERENCES

1. Ram, J.P., et al., *Analysis on solar PV emulators: A review*. Renewable and Sustainable Energy Reviews, 2018. **81**: p. 149-160.
2. Paul, S., K.P. Jacob, and J. Jacob, *Solar photovoltaic system with high gain DC to DC converter and maximum power point tracking controller*. Journal of Green Engineering, 2020. **10**: p. 2956-2972.
3. Nwaigwe, K., P. Mutabilwa, and E. Dintwa, *An overview of solar power (PV systems) integration into electricity grids*. Materials Science for Energy Technologies, 2019. **2**(3): p. 629-633.
4. Hao, D., et al., *Solar energy harvesting technologies for PV self-powered applications: A comprehensive review*. Renewable Energy, 2022.
5. *How solar power works - on-grid, off-grid and Hybrid Systems*. 04 May 2023 05/04/2023 2:39 PM]; Available from: <https://www.cleanenergyreviews.info/blog/2014/5/4/how-solar-works>.
6. Studer, T. and C. Kremer, *Solar PV Emulator*. 2021.
7. Imam, A.A. and Y.A. Al-Turki, *Techno-economic feasibility assessment of grid-connected PV systems for residential buildings in Saudi Arabia—A Case Study*. Sustainability, 2019. **12**(1): p. 262.
8. Chtouki, I., et al., *Design, implementation and comparison of several neural perturb and observe MPPT methods for photovoltaic systems*. International Journal of Renewable Energy Research (IJRER), 2019. **9**(2): p. 757-770.
9. Fang, J., et al., *Thermodynamic evaluation of a concentrated photochemical–photovoltaic–thermochemical (CP-PV-T) system in the full-spectrum solar energy utilization*. Applied Energy, 2020. **279**: p. 115778.
10. El Hammoumi, A., et al., *Design and construction of a test bench to investigate the potential of floating PV systems*. Journal of Cleaner Production, 2021. **278**: p. 123917.
11. Baouche, F.Z., et al., *Design and Simulation of a Solar Tracking System for PV*. Applied Sciences, 2022. **12**(19): p. 9682.
12. Mahjoubi, A., R.F. Mechlouch, and A.B. Brahim, *Fast and low-cost prototype of data logger for photovoltaic water pumping system*. International Journal of Sustainable Energy, 2012. **31**(3): p. 189-202.
13. Sitompul, E., A. Febian, and A. Suhartono, *Portable Solar Charger System with Energy Measurement and Access Control*. Jetri: Jurnal Ilmiah Teknik Elektro, 2022: p. 45-67.
14. Azab, M., *A finite control set model predictive control scheme for single-phase grid-connected inverters*. Renewable and Sustainable Energy Reviews, 2021. **135**: p. 110131.
15. Sidek, A. and M.M. Som, *A Review of FPGA-based Implementation related to Electrical Engineering and Contribution to MPPT, Converter and Motor Drive Control*. Multidisciplinary Applied Research and Innovation, 2021. **2**(1): p. 357-365.
16. Ahmed, O.A., et al., *Design and implementation of an indoor solar emulator based low-cost autonomous data logger for PV system monitoring*. International Journal of Power Electronics and Drive Systems, 2019. **10**(3): p. 1645.
17. Ma, C.-T., et al., *Design and Implementation of a Flexible Photovoltaic Emulator Using a GaN-Based Synchronous Buck Converter*. Micromachines, 2021. **12**(12): p. 1587.
18. Pankaj, L.M., R.S. Kasibhatla, and R. Vijaya Santhi, *FPGA-based statechart controller for MPPT of a photovoltaic system*. IETE Journal of Research, 2022: p. 1-11.
19. Jayawardana, I., C.N.M. Ho, and M. Pokharel. *Design and implementation of switch-mode solar photovoltaic emulator using power-hardware-in-the-loop simulations for grid*

## References

- integration studies*. in *2019 IEEE Energy Conversion Congress and Exposition (ECCE)*. 2019. IEEE.
20. Mallal, Y., L. El Bahir, and T. Hassboun, *High-performance emulator for fixed photovoltaic panels*. *International Journal of Photoenergy*, 2019. **2019**: p. 1-11.
  21. Alaoui, M., et al., *Real-time emulation of photovoltaic energy using adaptive state feedback control*. *SN Applied Sciences*, 2020. **2**(3): p. 492.
  22. Korasiak, P. and J. Jaglarz, *A New Photovoltaic Emulator Designed for Testing Low-Power Inverters Connected to the LV Grid*. *Energies*, 2022. **15**(7): p. 2646.
  23. Ayop, R. and C.W. Tan, *A comprehensive review on photovoltaic emulator*. *Renewable and Sustainable Energy Reviews*, 2017. **80**: p. 430-452.
  24. Di Piazza, M.C. and G. Vitale, *Photovoltaic sources: modeling and emulation*. 2013: Springer.
  25. Bressan, M., et al., *Development of a real-time hot-spot prevention using an emulator of partially shaded PV systems*. *Renewable energy*, 2018. **127**: p. 334-343.
  26. Moussa, I., A. Khedher, and A. Bouallegue, *Design of a low-cost PV emulator applied for PVECS*. *Electronics*, 2019. **8**(2): p. 232.
  27. Chalh, A., et al., *Study of a low-cost PV emulator for testing MPPT algorithm under fast irradiation and temperature change*. *Technology and Economics of Smart Grids and Sustainable Energy*, 2018. **3**(1): p. 11.
  28. Callegaro, L., et al., *Testing evidence and analysis of rooftop PV inverters response to grid disturbances*. *IEEE Journal of Photovoltaics*, 2020. **10**(6): p. 1882-1891.
  29. <https://www.chromausa.com/applications/pv-inverter/>. 5/28/2023 2:14 PM].
  30. García, M.P., et al., *Photovoltaic Microgrid Emulator for Educational Purposes*. 2019.
  31. <https://edquip.co/en/dikoin/photovoltaic-installation-demonstrator---stand-alone-and-network-connected>. 5/28/2023 2:44PM].
  32. Montoya, J., et al., *Advanced laboratory testing methods using real-time simulation and hardware-in-the-loop techniques: A survey of smart grid international research facility network activities*. *Energies*, 2020. **13**(12): p. 3267.
  33. Jayawardana, I.D., et al., *A fast-dynamic control scheme for a power-electronics-based PV emulator*. *IEEE Journal of Photovoltaics*, 2020. **11**(2): p. 485-495.
  34. Ickilli, D., H. Can, and K.S. Parlak. *Development of a FPGA-based photovoltaic panel emulator based on a DC/DC converter*. in *2012 38th IEEE photovoltaic specialists conference*. 2012. IEEE.
  35. Moussa, I. and A. Khedher, *Photovoltaic emulator based on PV simulator RT implementation using XSG tools for an FPGA control: Theory and experimentation*. *International Transactions on Electrical Energy Systems*, 2019. **29**(8): p. e12024.
  36. *Solar Array Simulator DC Power Supply*. Chroma Systems Solutions, Inc. June 10, 2023].
  37. Li, X., et al., *A comparative study on photovoltaic MPPT algorithms under EN50530 dynamic test procedure*. *IEEE Transactions on Power Electronics*, 2020. **36**(4): p. 4153-4168.
  38. Samano-Ortega, V., et al., *Hardware in the loop platform for testing photovoltaic system control*. *Applied Sciences*, 2020. **10**(23): p. 8690.
  39. *E4360 Series Modular Solar Array Simulators*. June 11, 2023]; Available from: <https://www.keysight.com/us/en/products/dc-power-supplies/dc-power-solutions/e4360-series-modular-solar-array-simulators.html>.
  40. Michaelson, D., J. Jiang, and P. Eng. *A Hardware-in-the-Loop Test Platform for a Vehicular Auxiliary Power System with Onboard PV*. in *2019 IEEE Transportation Electrification Conference and Expo (ITEC)*. 2019. IEEE.
  41. *Regenerative AC Load Model 9430 - NH Research (NHR)*. June 01, 2023].

## References

42. Onwe, C.A., et al. *Smart Hubs I-A Demonstration of Electric Vehicle's Lithium-Ion Battery Charging Characteristic and Efficient Demand Side Energy Management with Solar Photovoltaic System*. in *2021 12th International Renewable Engineering Conference (IREC)*. 2021. IEEE.
43. *1500V Photovoltaic System Simulation Solution*. June 12, 2023].
44. Aghenta, L.O. and M.T. Iqbal. *Development of an IoT based open source SCADA system for PV system monitoring*. in *2019 IEEE Canadian Conference of Electrical and Computer Engineering (CCECE)*. 2019. IEEE.
45. Patel, A., et al., *A practical approach for predicting power in a small-scale off-grid photovoltaic system using machine learning algorithms*. *International Journal of Photoenergy*, 2022. **2022**: p. 1-21.
46. Rehman, A.U., *Design of a photovoltaic system for a house in Pakistan and its open source ultra-low power data logger*. 2020, Memorial University of Newfoundland.
47. Janaki, N., *STUDY OF SOLAR PHOTOVOLTAIC SYSTEM USING DATA ACQUISITION*. *PalArch's Journal of Archaeology of Egypt/Egyptology*, 2020. **17**(9): p. 5006-5012.
48. *DAQ Basics* <https://daqifi.com/daq-basics/> DAQiFi May 11, 2023].
49. Ansari, S., et al., *A review of monitoring technologies for solar PV systems using data processing modules and transmission protocols: Progress, challenges and prospects*. *Sustainability*, 2021. **13**(15): p. 8120.
50. Vargas-Salgado, C., et al., *Low-cost web-based Supervisory Control and Data Acquisition system for a microgrid testbed: A case study in design and implementation for academic and research applications*. *Heliyon*, 2019. **5**(9): p. e02474.
51. Garg, V.K. and S. Sharma, *Performance evaluation of solar module with emulator and DC microgrid*. *International Journal of Renewable Energy Research (IJRER)*, 2021. **11**(4): p. 1552-1560.
52. Boucharef, A., et al., *Solar module emulator based on a low-cost microcontroller*. *Measurement*, 2022. **187**: p. 110275.
53. [https://energyeducation.ca/encyclopedia/Photovoltaic\\_cell#cite\\_note-4](https://energyeducation.ca/encyclopedia/Photovoltaic_cell#cite_note-4). [cited 12/5/2023
54. Sharma, A.K., et al., *Role of Metaheuristic Approaches for Implementation of Integrated MPPT-PV Systems: A Comprehensive Study*. *Mathematics*, 2023. **11**(2): p. 269.
55. Bentayeb, K., I. Hala, and S. MAKHLOUFI, *Étude et réalisation d'un hacheur SEPIC commandé par DSP en vue d'implémenter des commandes MPPT*. 2022, UNIVERSITE AHMED DRAIA-ADRAR.
56. *What is a closed loop control system and how does it work?* 15/5/2023].
57. Nkambule, M., A. Hasan, and A. Ali. *Proportional study of Perturb & Observe and Fuzzy Logic Control MPPT Algorithm for a PV system under different weather conditions*. in *2019 IEEE 10th GCC Conference & Exhibition (GCC)*. 2019. IEEE.
58. Reddy, D.C.K., S. Satyanarayana, and V. Ganesh, *Design of hybrid solar wind energy system in a microgrid with MPPT techniques*. *International Journal of Electrical and Computer Engineering*, 2018. **8**(2): p. 730-740.
59. Bouksaim, M., M. Mekhfioui, and M.N. Srifi, *Design and Implementation of Modified INC, Conventional INC, and Fuzzy Logic Controllers Applied to a PV System under Variable Weather Conditions*. *Designs*, 2021. **5**(4): p. 71.
60. Paduani, V.D., et al., *A unified power-setpoint tracking algorithm for utility-scale PV systems with power reserves and fast frequency response capabilities*. *IEEE Transactions on Sustainable Energy*, 2021. **13**(1): p. 479-490.
61. Mumtaz, F., et al., *Review on non-isolated DC-DC converters and their control techniques for renewable energy applications*. *Ain Shams Engineering Journal*, 2021. **12**(4): p. 3747-

## References

- 3763.
62. Gogolou, V., et al. *Design considerations for a DC-DC Boost Converter in standard CMOS technology*. in *2021 10th International Conference on Modern Circuits and Systems Technologies (MOCASST)*. 2021. IEEE.
  63. *Analysis of Four DC-DC Converters in Equilibrium - Technical Articles*. All About Circuits [15/5/2023].
  64. Vardhan, B.S., M. Khedkar, and N.K. Kulkarni, *Impact on Fuse Settings and Size of Photovoltaic Distributed Generation Source Due to Fault Current*.
  65. *Nick*. [18/5/2023].
  66. Spea, S.R. and H.A. Khattab. *Design sizing and performance analysis of stand-alone PV system using PVSyst software for a location in Egypt*. in *2019 21st International Middle East Power Systems Conference (MEPCON)*. 2019. IEEE.
  67. *POWERSTAGE-DESIGNER*. [15/5/2023].
  68. <https://www.ti.com/lit/pdf/slva372>. Available from: <https://www.ti.com/lit/pdf/slva372>.
  69. *Understanding the I2C Bus - Texas Instruments India*. [15/5/2023]; Available from: <https://www.ti.com/lit/pdf/SLVUBB4B>.
  70. [https://play.google.com/store/apps/details?id=com.dcdconvertersdesigndemo&hl=en\\_US](https://play.google.com/store/apps/details?id=com.dcdconvertersdesigndemo&hl=en_US). [24/05/2023 12:58 AM].
  71. Martí-Arbona, E., et al., *A high-voltage-compliant current-to-digital sensor for DC-DC converters in standard CMOS technology*. *IEEE Transactions on Power Electronics*, 2016. **32**(3): p. 2180-2188.
  72. <https://www.lem.com/en/product-list/lv-25p>. [19/05/2023 10:30PM].
  73. <https://pdf1.alldatasheet.com/datasheet-pdf/view/87952/LEM/LV25-P.html>. [19/05/2023 10:59PM].
  74. [https://www.lem.com/sites/default/files/products\\_datasheets/la%2025-np.pdf](https://www.lem.com/sites/default/files/products_datasheets/la%2025-np.pdf). [18/05/2023 10:27 AM].
  75. Hu, J., et al., *High-density current-transformer-based gate-drive power supply with reinforced isolation for 10-kV SiC MOSFET modules*. *IEEE Journal of Emerging and Selected Topics in Power Electronics*, 2019. **8**(3): p. 2217-2226.
  76. *HCNW3120*. [20/5/2023].
  77. Hmidet, A., et al., *Design of efficient off-grid solar photovoltaic water pumping system based on improved fractional open circuit voltage MPPT technique*. *International Journal of Photoenergy*, 2021. **2021**: p. 1-18.
  78. Yahiaoui, F., et al., *An Experimental Testing of Optimized Fuzzy Logic-Based MPPT for a Standalone PV System Using Genetic Algorithms*. *Mathematical Problems in Engineering*, 2023. **2023**.
  79. *dSPACE Hardware-in-the-Loop Test Systems*. [20/5/2023].
  80. *International Journal of Computer Sciences and ... - ijcsenline.org*. [20/5/2023].
  81. A. Alturki, F., A.A. Al-Shamma'a, and H. MH Farh, *Simulations and dSPACE Real-Time Implementation of Photovoltaic Global Maximum Power Extraction under Partial Shading*. *Sustainability*, 2020. **12**(9): p. 3652.
  82. [https://www.ti.com/lit/ds/symlink/tms320f280038c-q1.pdf?HQS=dis-mous-null-mousermode-dsf-pf-null-ww&ts=1685923279157&ref\\_url=https%253A%252F%252Fwww.ti.com%252F](https://www.ti.com/lit/ds/symlink/tms320f280038c-q1.pdf?HQS=dis-mous-null-mousermode-dsf-pf-null-ww&ts=1685923279157&ref_url=https%253A%252F%252Fwww.ti.com%252F). [cited 2023 25/04/2023].
  83. Ainah, P., A. Muhammad, and G. Biowei, *DSP TMS320F28335 Implementation of dq-PI Vector Controller for Voltage Source Inverter using SPWM Technique*. *Nigerian Journal of Engineering*, 2020. **27**: p. 106-112.

# APPENDIXS

## APPENDIX



# Appendix II-1: The voltage sensor LEM-LV25.

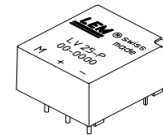


## Voltage Transducer LV 25-P

For the electronic measurement of voltages : DC, AC, pulsed..., with a galvanic isolation between the primary circuit (high voltage) and the secondary circuit (electronic circuit).

$$I_{PN} = 10 \text{ mA}$$

$$V_{PN} = 10 \dots 500 \text{ V}$$



### Electrical data

$I_{PN}$	Primary nominal r.m.s. current	10	mA		
$I_P$	Primary current, measuring range	0 .. $\pm 14$	mA		
$R_M$	Measuring resistance	$R_{Mmin}$	$R_{Mmax}$		
		with $\pm 12 \text{ V}$	@ $\pm 10 \text{ mA}_{max}$	30	190
		@ $\pm 14 \text{ mA}_{max}$	30	100	$\Omega$
	with $\pm 15 \text{ V}$	@ $\pm 10 \text{ mA}_{max}$	100	350	$\Omega$
	@ $\pm 14 \text{ mA}_{max}$	100	190	$\Omega$	
$I_{SN}$	Secondary nominal r.m.s. current	25	mA		
$K_N$	Conversion ratio	2500 : 1000			
$V_C$	Supply voltage ( $\pm 5 \%$ )	$\pm 12 \dots 15$	V		
$I_C$	Current consumption	10 (@ $\pm 15 \text{ V}$ ) + $I_S$	mA		
$V_d$	R.m.s. voltage for AC isolation test <sup>1)</sup> , 50 Hz, 1 mn	2.5	kV		

### Features

- Closed loop (compensated) voltage transducer using the Hall effect
- Insulated plastic case recognized according to UL 94-V0.

### Principle of use

- For voltage measurements, a current proportional to the measured voltage must be passed through an external resistor  $R_1$  which is selected by the user and installed in series with the primary circuit of the transducer.

### Accuracy - Dynamic performance data

$X_G$	Overall Accuracy @ $I_{PN}, T_A = 25^\circ\text{C}$	@ $\pm 12 \dots 15 \text{ V}$	$\pm 0.9$	%	
		@ $\pm 15 \text{ V} (\pm 5 \%)$	$\pm 0.8$	%	
$\epsilon_L$	Linearity		< 0.2	%	
$I_O$	Offset current @ $I_P = 0, T_A = 25^\circ\text{C}$		Typ	Max	
$I_{OT}$	Thermal drift of $I_O$	0°C .. + 25°C	$\pm 0.06$	$\pm 0.25$	mA
		+ 25°C .. + 70°C	$\pm 0.10$	$\pm 0.35$	mA
$t_r$	Response time <sup>2)</sup> @ 90 % of $V_{Pmax}$		40	$\mu\text{s}$	

### Advantages

- Excellent accuracy
- Very good linearity
- Low thermal drift
- Low response time
- High bandwidth
- High immunity to external interference
- Low disturbance in common mode.

### General data

$T_A$	Ambient operating temperature	0 .. + 70	$^\circ\text{C}$
$T_S$	Ambient storage temperature	- 25 .. + 85	$^\circ\text{C}$
$R_P$	Primary coil resistance @ $T_A = 70^\circ\text{C}$	250	$\Omega$
$R_S$	Secondary coil resistance @ $T_A = 70^\circ\text{C}$	110	$\Omega$
$m$	Mass	22	g
	Standards <sup>3)</sup>	EN 50178	

### Applications

- AC variable speed drives and servo motor drives
- Static converters for DC motor drives
- Battery supplied applications
- Uninterruptible Power Supplies (UPS)
- Power supplies for welding applications.

Notes : <sup>1)</sup> Between primary and secondary  
<sup>2)</sup>  $R_1 = 25 \text{ k}\Omega$  (L/R constant, produced by the resistance and inductance of the primary circuit)  
<sup>3)</sup> A list of corresponding tests is available

981125/14

LEM Components

www.lem.com

Tope Co., Ltd. Tel: (02) 8228-0658 Fax: (02) 8228-0659 http://www.sensor.com.tw e-mail: tope@ms1.hinet.net

## APPENDIXS



# Appendix II-2: The Current Sensor LEM-LA25.



## Current Transducer LA 25-NP

For the electronic measurement of currents: DC, AC, pulsed..., with galvanic isolation between the primary circuit and the secondary circuit.

$I_{PN} = 5-6-8-12-25 \text{ At}$



### Electrical data

$I_{PN}$	Primary nominal current rms	25	At
$I_{PM}$	Primary current, measuring range	0 .. ± 36	At
$R_M$	Measuring resistance @ with ± 15 V	$T_A = 70^\circ\text{C}$	
		$R_{M \min}$	$R_{M \max}$
		100	320
		$T_A = 85^\circ\text{C}$	
	@ ± 25 At <sub>max</sub>	$R_{M \min}$	$R_{M \max}$
	@ ± 36 At <sub>max</sub>	100	190
		$R_{M \min}$	$R_{M \max}$
		100	185
$I_{SN}$	Secondary nominal current rms	25	mA
$K_N$	Conversion ratio	1-2-3-4-5	: 1000
$V_C$	Supply voltage (± 5 %)	± 15	V
$I_C$	Current consumption	10 + $I_S$	mA

### Accuracy - Dynamic performance data

$X$	Accuracy @ $I_{PN}$ , $T_A = 25^\circ\text{C}$	± 0.5	%
$\epsilon_L$	Linearity error	< 0.2	%
$I_O$	Offset current <sup>1)</sup> @ $I_p = 0$ , $T_A = 25^\circ\text{C}$	Typ	Max
		± 0.05	± 0.15
$I_{OM}$	Magnetic offset current <sup>2)</sup> @ $I_p = 0$ and specified $R_M$ , after an overload of $3 \times I_{PN}$	± 0.05	± 0.15
		± 0.06	± 0.25
		± 0.10	± 0.35
		± 0.5	mA
		± 1.2	mA
$I_{OT}$	Temperature variation of $I_O$	0°C .. + 25°C	± 0.06 ± 0.25
		+ 25°C .. + 70°C	± 0.10 ± 0.35
		- 25°C .. + 85°C	± 0.5
		- 40°C .. + 85°C	± 1.2
$t_r$	Response time <sup>3)</sup> to 90 % of $I_{PN}$ step	< 1	µs
$di/dt$	di/dt accurately followed	> 50	A/µs
$BW$	Frequency bandwidth (- 1 dB)	DC .. 150	kHz

### General data

$T_A$	Ambient operating temperature	- 40 .. + 85	°C
$T_S$	Ambient storage temperature	- 45 .. + 90	°C
$R_p$	Primary coil resistance per turn @ $T_A = 25^\circ\text{C}$	< 1.25	mΩ
$R_S$	Secondary coil resistance @ $T_A = 70^\circ\text{C}$	110	Ω
		115	Ω
		@ $T_A = 85^\circ\text{C}$	
$R_{IS}$	Isolation resistance @ 500 V, $T_A = 25^\circ\text{C}$	> 1500	MΩ
$m$	Mass	22	g
	Standards	EN 50178: 1997	

- Notes:**
- Measurement carried out after 15 mn functioning
  - The result of the coercive field of the magnetic circuit
  - With a di/dt of 100 A/µs.

### Features

- Closed loop (compensated) current transducer using the Hall effect
- Isolated plastic case recognized according to UL 94-V0.

### Advantages

- Excellent accuracy
- Very good linearity
- Low temperature drift
- Optimized response time
- Wide frequency bandwidth
- No insertion losses
- High immunity to external interference
- Current overload capability.

### Applications

- AC variable speed drives and servo motor drives
- Static converters for DC motor drives
- Battery supplied applications
- Uninterruptible Power Supplies (UPS)
- Switched Mode Power Supplies (SMPS)
- Power supplies for welding applications.

### Application domain

- Industrial.





## Appendix II-3: Gate drive (HCPL-3120).



### 2.0 Amp Output Current IGBT Gate Drive Optocoupler

#### Technical Data

#### HCPL-3120

##### Features

- 2.0 A Minimum Peak Output Current
- 15 kV/μs Minimum Common Mode Rejection (CMR) at  $V_{CM} = 1500\text{ V}$
- 0.5 V Maximum Low Level Output Voltage ( $V_{OL}$ ) Eliminates Need for Negative Gate Drive
- $I_{CC} = 5\text{ mA}$  Maximum Supply Current
- Under Voltage Lock-Out Protection (UVLO) with Hysteresis
- Wide Operating  $V_{CC}$  Range: 15 to 30 Volts
- 500 ns Maximum Switching Speeds
- Industrial Temperature Range:  $-40^{\circ}\text{C}$  to  $100^{\circ}\text{C}$
- Safety Approval  
UL Recognized - 2500 V rms for 1 minute per UL1577  
CSA Approval  
VDE 0884 Approved with  $V_{ORM} = 630\text{ V peak}$  (Option 060 only)

##### Applications

- Isolated IGBT/MOSFET Gate Drive
- AC and Brushless DC Motor Drives

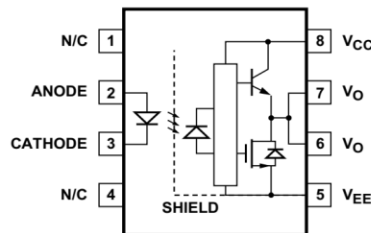
- Industrial Inverters
- Switch Mode Power Supplies (SMPS)

##### Description

The HCPL-3120 consists of a GaAsP LED optically coupled to an integrated circuit with a power output stage. This optocoupler is ideally suited for driving power IGBTs and MOSFETs used in

motor control inverter applications. The high operating voltage range of the output stage provides the drive voltages required by gate controlled devices. The voltage and current supplied by this optocoupler makes it ideally suited for directly driving IGBTs with ratings up to 1200 V/100 A. For IGBTs with higher ratings, the HCPL-3120 can be used to drive a discrete power stage which drives the IGBT gate.

##### Functional Diagram



##### TRUTH TABLE

LED	$V_{CC} - V_{EE}$ "POSITIVE GOING" (i.e., TURN-ON)	$V_{CC} - V_{EE}$ "NEGATIVE GOING" (i.e., TURN-OFF)	$V_O$
OFF	0 - 30 V	0 - 30 V	LOW
ON	0 - 11 V	0 - 9.5 V	LOW
ON	11 - 13.5 V	9.5 - 12 V	TRANSITION
ON	13.5 - 30 V	12 - 30 V	HIGH

A 0.1 μF bypass capacitor must be connected between pins 5 and 8.

CAUTION: It is advised that normal static precautions be taken in handling and assembly of this component to prevent damage and/or degradation which may be induced by ESD.